172238

LOWER-MIDDLE CARBONIFEROUS BOUNDARY IN CENTRAL TAURIDES, TURKEY (HADİM AREA): PALEONTOLOGICAL AND SEQUENCE STRATIGRAPHIC APPROACH

A THESIS SUBMITTED TO
THE GRADUATE SCHOOL OF NATURAL AND APPLIED SCIENCES
OF
MIDDLE EAST TECHNICAL UNIVERSITY

BY

AYŞE ATAKUL

IN PARTIAL FULFILLMENT OF THE REQUIREMENTS
FOR
THE DEGREE OF MASTER OF SCIENCE
IN
GEOLOGICAL ENGINEERING

JANUARY 2006

Approval of the Graduate School of Natural and Applied Sciences.

Prof. Dr. Canan Özgen
Director

I certify that this thesis satisfies all the requirements as a thesis for the degree of Master of Science.

Prof. Dr. Vedat Doyuran
Head of Department

This is to certify that we have read this thesis and that in our opinion it is fully adequate, in scope and quality, as a thesis for the degree of Master of Science.

Prof. Dr. Demir Altıner
Supervisor

Examining Committee Members

Prof. Dr. Cemal Göncüoğlu	(METU, GEOE)	
Prof. Dr. Demir Altıner	(METU, GEOE)	
Assoc. Prof. Dr. Sevinç Özkan Altıner	(METU, GEOE)	
Assist. Prof. Dr. İsmail Ömer Yılmaz	(METU, GEOE)	
Dr. Zühtü Batı	(TPAO)	

I hereby declare that all information in this document has been obtained and presented in accordance with academic rules and ethical conduct. I also declare that, as required by these rules and conduct, I have fully cited and referenced all material and results that are not original to this work.

Name, Last Name: Ayşe ATAKUL

Signature : 

ABSTRACT

LOWER-MIDDLE CARBONIFEROUS BOUNDARY IN CENTRAL TAURIDES, TURKEY (HADİM AREA): PALEONTOLOGICAL AND SEQUENCE STRATIGRAPHIC APPROACH

Atakul, Ayşe

M. Sc., Department of Geological Engineering

Supervisor: Prof. Dr. Demir Altıner

January 2006, 202 pages

The aim is to delineate the effective boundary between Lower and Middle Carboniferous (mid-Carboniferous boundary) and to study the meter-scale cyclicity and foraminiferal evolution across a stratigraphic section comprising this boundary. In order to perform such a study, a 25,64 m stratigraphic section, which is mainly composed of carbonates has been measured in the Hadim region of the Central Taurides.

In this study, calcareous foraminifers have been studied in the measured section. These foraminiferal assemblages contain 62 species. Based on these foraminifers, four biostratigraphic zones have been defined covering the interval from Upper Serpukhovian to Lower Bashkirian. These zones comprise in ascending order, the *Eostaffella* ex gr. *ikensis* – *E. postmosquensis* Zone (Zapaltyubinsky Horizon – Upper Serpukhovian), the *Plectostaffella jakhensis* – *P. bogdanovkensis* Zone and the *Millerella marblensis* Zone (Bogdanovsky Horizon – Lower Bashkirian) and the *Semistaffella* sp. Zone (Syuransky Horizon – Lower Bashkirian).

In order to construct the sequence stratigraphic framework, detailed microfacies studies were carried out and eleven different microfacies types were identified. Based on the stacking patterns of these microfacies, six main types of cycles, A-F, and ten subcycles are recognized. Twenty-three shallowing upward

meter-scale cycles and three sequence boundaries have been determined in the studied section. The duration of cycles has been calculated as 2 my and cycle periodicities correspond to the Milankovitch eccentricity bant.

Results of quantitative analysis of benthic foraminifera have been used to demonstrate the biological response to cyclicity. Eostaffellids, archaediscids, unilocular forms and irregularly coiled bilocular forms are the calcareous foraminiferal groups responding the meter-scale cycles.

Keywords: Mid-Carboniferous boundary, Foraminifera, Meter-scale cycles, Central Taurides

ÖZ

ORTA TOROSLARDA ALT ORTA KARBONİFER SINIRI :
PALEONTOLOJİK VE SEKANS STRATİGRAFİK YAKLAŞIM

Atakul, Ayşe
Yüksek Lisans, Jeoloji Mühendisliği Bölümü
Tez Yöneticisi: Prof. Dr. Demir Altıner
Ocak 2006, 202 sayfa

Orta Toroslarda gerçekleştirilen bu çalışmanın amacı Alt ve Orta Karbonifer arasındaki sınırını tespit etmek ve kesit boyunca metre-ölçekli devirleri ve foraminiferlerin evrimini çalışmaktır. Bu çalışmayı gerçekleştirebilmek için Orta Torosların Hadim bölgesinde, çoğunlukla karbonat kayalarından oluşan bir stratigrafik kesit ölçülmüştür.

Bu çalışmada, Fusulin ve küçük foraminiferler çalışılmıştır. Bu foraminifer toplulukları 62 tür içermektedir. Foraminifer topluluklarına dayanarak, Üst Serpukhoviyen – Alt Başkiriyen aralığında dört biostratigrafik zon ayrılmıştır. Donets Havzası'ndaki foraminifer zonlarıyla karşılaştırılabilen biyozonasyon, *Eostaffela* ex gr. *ikensis* – *E. postmosquensis* Zone (Zapaltyubinsky – Üst Serpukhoviyen), *Plectostaffella jakhensis* – *P. bogdanovkenis* Zonu and *Millerella marblensis* (Bogdanovsky – Alt Başkiriyen) Zonu and *Semistaffella* sp. Zonu'ndan (Syuransky – Alt Başkiriyen) oluşmaktadır.

Sekans stratigrafisi çatısını oluşturabilmek için, detaylı mikrofasiyes çalışmaları yapılmış ve onbir değişik mikrofasiyes tipi ayıklanmıştır. Mikrofasiyeslerin üstüste depolanmalarına göre, altı tane temel, A-F, ve on tane as devir tanımlanmıştır. Bu çalışmada, yirmi üç metre ölçekli devir ve üç sekans sınırı belirlenmiştir. Sekans sınırlarını Donets Havzası'ndakilerle karşılaştırarak, sekansların depolanma süresinin iki my olduğu hesaplanmış ve metre ölçekli

devirlerin "Milankovich eccentricity" devirlerine karşılık geldiği ortaya koyulmuştur.

Bu çalışmada ayrıca, bentik foraminifer sayısal analiz sonuçları devirselliğin foraminiferler üzerine etkilerini ortaya koymak için kullanılmıştır. Eostaffellidler, archaediscidler, tek localı formlar ve düzensiz sarılımlı iki localı formlar, metre bazında üste doğru sığlaşan devirlere yanıt veren kalkerli foraminifer gruplarıdır.

Anahtar Kelimeler: Orta Karbonifer sınırı, Foraminifer, Metre-ölçekli devirsellik, Orta Toroslar

To my parents and my sister...

ACKNOWLEDGEMENTS

I am greatly indebted to my supervisor Prof. Dr. Demir ALTINER for his valuable guidance advice, encouragement and constructive criticism during the preparation of this thesis. I would like to thank to my co-supervisor Assoc. Prof. Dr. Sevinç ÖZKAN-ALTINER for her attention, and I am grateful to her for valuable recommendations and encouragements during my studies.

I would like to express my gratitude to Assistant Prof. Dr. İ. Ömer YILMAZ for his help during the field and laboratory studies, for his scientific support and encouragements during this study.

I express my gratefulnes to Zühtü BATI for his valuable recommendations and detailed examination of the thesis.

I am most grateful to all my friends for their friendships and endless encouragements. Especially, I would like to thank Fatma GENELİ, Müge AKIN, Şule DEVECİ, Yavuz ÖZDEMİR, Harun AYDIN and my roommate Selin SÜER for their encouragements.

I would like to thank to Mr. Orhan KARAMAN for the preparation of thin sections.

Finally (at last but does not mean the least), I would like to express my grateful appreciation to my sister and my parents for their support and encouragements during my studies.

TABLE OF CONTENTS

PLAGIARISM..... iii
ABSTRACT iv
ÖZ vi
ACKNOWLEDGEMENTS ix
TABLE OF CONTENTS x
LIST OF TABLES xiii
LIST OF FIGURES xiv

CHAPTERS

I. INTRODUCTION 1
1.1. Purpose and Scope 1
1.2. Geographic Setting 2
1.3. Methods of Study 4
1.4. Previous Works 5
1.5. Regional Geological Setting 10

II. LITHOSTRATIGRAPHY AND BIOSTRATIGRAPHY 17
2.1 Lithostratigraphy 17
2.1.1. Yarıcak Formation 20
2.2 Biostratigraphy 23
2.2.1. *Eostaffella* ex. gr. *ikensis – E. postmosquensis* Zone 26
2.2.2. *Plectostaffella bogdanovkensis – P. jakhensis* Zone 27
2.2.3. *Millerella marblensis* Zone 28
2.2.4. *Semistaffella* sp. Zone 29
2.3. Mid-Carboniferous Boundary 30
2.3.1. Calcareous foraminifers across the mid- Carboniferous boundary . 31

III. SEQUENCE STRATIGRAPHY 34

3.1. Historical Background **34**
3.2. Microfacies Types and Depositional Environments **35**
3.2.1. Coated crinoidal packstone (CP) 41
3.2.2. Bioclastic grainstone with abundant foraminifers (BG) 41
3.2.3. Coated bioclastic grainstone (CG) 41
3.2.4. Oolitic grainstone (O1, O2, O3) 45
3.2.5. Oolitic packstone-grainstone (OPG) 45
3.2.6. Oolitic packstone (OP) 48
3.2.7. Aggregate-grain grainstone (AG) 48
3.2.8. Mudstone-wackestone (M) 51
3.2.9. Sandy oolitic grainstone (SO) 51
3.2.10. Sandy pelloidal packstone (SP) 51
3.2.11. Quartz arenitic sandstone (S) 54
3.3. Meter-scale shallowing upward cycles (Parasequences) **56**
3.3.1 Types of shallowing upward cycles (Parasequences) 59
3.3.1.1. A type cycles 59
3.3.1.2. B type cycles 59
3.3.1.3. C type cycles 61
3.3.1.4. D type cycles 61
3.3.1.5. E type cycles 66
3.3.1.6. F type cycles 66
3.3.2. Origin and Duration of Cycles 66
3.4. Sequence stratigraphic interpretation **569**

IV. RESPONSE OF FORAMINIFERS TO CARBONATE CYCLICITY . 72
4.1. Response of foraminifers to carbonate cyclicity **72**
4.1.1. General descriptions of the counted forms 72
4.1.2. Interpretation of response of calcareous foraminifers 74

V. SYSTEMATIC PALEONTOLOGY **85**

VI. DISCUSSIONS AND CONCLUSIONS **142**

REFERENCES **146**

APPENDIX A **171**

PLATE I **171**

PLATE II **173**

PLATE III **175**

PLATE IV **177**

PLATE V **179**

PLATE VI **181**

PLATE VII **183**

PLATE VIII **185**

PLATE IX **187**

PLATE X **189**

PLATE XI **191**

PLATE XII **193**

PLATE XIII **195**

PLATE XIV **197**

PLATE XV **199**

APPENDIX – B **201**

LIST OF TABLES

Table 1. Upper Serpukhovian – Lower Bashkirian horizons in different regions.....24

Table 2. Foraminiferal zones in different studies 25

Table 3. Foraminiferal distribution chart..... ...33

Table 4. Carbonate and siliciclastic facies and their depositional environments in the studied section.....39

Table 5. Correlation of occurrence of glacial ice based on different studies....71

LIST OF FIGURES

Figure 1. Geographic setting of the study area and the location of the measured section. 3

Figure 2. A. Location of the measured section (the red line shows the measured section), B – C. Close-up view of the measured section (the red bullets indicate the sampling points)..... 6

Figure 3. Stratigraphic sections of Bozkır, Bolkar Dağı, Antalya, Alanya and Geyik Dağı Units (simplified from Özgül, 1976).....12

Figure 4. Tectonic map of the study area (Özgül, 1984).....13

Figure 5. Autochthonous and Allochthonous units in the Hadim –Taşkent area (Altıner and Özgül, 2001)..... 14

Figure 6. Geologic map of the study area (Altıner and Özgül, 2001)..... ...18

Figure 7. Generalized columnar section of the Aladağ Unit in the Hadim-Taşkent area (simplified from Özgül, 1997). 19

Figure 8. The Carboniferous biostratigraphy (Yarıcak Formation) of the Aladağ Unit in the Hadim-Taşkent area (Altiner and Özgül, 2001).....21

Figure 9. Lithostratigraphy of the measured section with biozones.....22

Figure 10. Distribution of SMF types in the Facies Zones (FZ) of the rimmed carbonate platform model (Flügel, 2004)..... 37

Figure 11. Generalized distribution of microfacies types in different parts of a homoclinal carbonate ramp (Flügel, 2004).....38

Figure 12. Photomicrographs of coated crinoidal packstone lithofacies, (c: coated grain, cr: crinoid fragment, f: foraminifer, g: gastropod and i: intraclast), (A-B-C: HB04-33 and D: HB04)..... ...42

Figure 13. Photomicrographs of bioclastic grainstone with abundant foraminifers lithofacies, (b: brachiopod fragment, c: crinoid fragment, f: foraminifer, i: intraclast and o: oolite) (A-B: HB04-05 and C-D-E-F: HB04-11)..... ...43

Figure 14. Photomicrographs of coated bioclastic grainstone lithofacies, (c: coated grain, cr: crinoid fragment, f: foraminifer, i: intraclast), (A-B-C: HB04-33 and D: HB04-47)..... ...44

Figure 15. Photomicrographs of oolitic grainstone lithofacies. A-B: oolitic grainstone with bioclasts (O1 type), C-D: oolitic grainstone with lumps and aggregate grains (O2 type), E-F: oolitic grainstone with quartz sands (O3 type), (b: bioclast, f: foraminifer, i: intraclast, l: lump, o: ooid, q: quartz grain) (A-B: HB04-41, C-D: HB04-28, E-F: HB04-20)..... ...46

Figure 16. Photomicrographs of oolitic packstone-grainstone (A-B) and oolitic packstone lithofacies (C-D), (b: bioclast, f: foraminifer, o: oolite), (A-B: HB04-21, C-D: HB04-40)..... ...47

Figure 17. Photomicrographs of aggregate grain grainstone lithofacies (cg: coated grains, i: intraclasts, f: foraminifera), (A: HB04-50; B: HB04-52; C: HB04-51; D: HB04-49)..... ...49

Figure 18. Photomicrographs showing mudstone-wackestone lithofacies (f: fossil fragments, p: pellet, v: vug), (A-B: HB04-03 and C-D: HB04-34)..... ...50

Figure 19. Photomicrographs of sandy oolitic grainstone lithofacies, (f: foraminifer, o: ooid, q: quartz grain, p: pellet), (A: HB04-59; B-C: HB04-63; D: HB04-60)..... ...52

Figure 20. Photomicrographs of sandy pelloidal packstone lithofacies (f: foraminifer, o: ooid, p: pellet, q: quartz grain), (A-B: HB04-62; C-D: HB04-61; E: HB04-60 and F: HB04-53).....53

Figure 21. Photomicrographs of the quartz arenitic sandstone lithofacies, o: opaque mineral, q: quartz grain (A, B: HB04-12; C,D: HB04-64)..... ...55

Figure 22. Close-up view of quartz arenite displaying herringbone cross-bedding..... ...56

Figure 23. Composite model illustrating the microfacies distribution of Serpukhovian – Bashkirian boundary beds in the studied section 57

Figure 24. Columnar section of the studied section showing meter scale cycles..... ...58

Figure 25. A type cycle (Cycle 2), B type cycle (Cycle 6) and photomicrographs of microfacies deposited within these cycles..... ...60

Figure 26. C1 type cycle (Cycle 21); C2 type cycle (Cycle 23) and photomicrographs of microfacies deposited within these cycles..... ...62

Figure 27. D1 type cycle (Cycle 10); D2 type cycle (Cycle 11) and photomicrographs of microfacies deposited within these cycles..... ...63

Figure 28. D3 type cycle (Cycle 12) D4 type cycle (Cycle 15) and photomicrographs of microfacies deposited within these cycles..... ...64

Figure 29. D5 type cycle (Cycle 20); E type cycle (Cycle 13) and photomicrographs of microfacies deposited within these cycles..... ...65

Figure 30. F1 type cycle (Cycle 18); F2 type cycle (Cycle 22) and photomicrographs of microfacies deposited within these cycles..... ...67

Figure 31. Point counting results of total abundance for determining the response of foraminifers to cyclicity..... ...75

Figure 32. Point counting results of archaediscids for determining the response of foraminifers to cyclicity..... ...77

Figure 33. Point counting results of eostaffellids for determining the response of foraminifers to cyclicity..... ...78

Figure 34. Point counting results of unilocular forms for determining the response of foraminifers to cyclicity..... ...79

Figure 35. Point counting results of paleotextularids for determining the response of foraminifers to cyclicity..... ...80

Figure 36. Point counting results of irregularly coiled bilocular forms for determining the response of foraminifers to cyclicity..... ...81

Figure 37. Point counting results of biseriamminids for determining the response of foraminifers to cyclicity..... ...82

Figure 38. Point counting results of pseudoendothyrids for determining the response of foraminifers to cyclicity..... ...83

Figure 39. Point counting results of endothyrids for determining the response of foraminifers to cyclicity..... ...84

CHAPTER I

INTRODUCTION

1.1. Purpose and Scope

The main objective of this study is to delineate the mid-Carboniferous boundary based on calcareous foraminifera and to define the shallowing upward meter-scale cycles across this boundary in the allochthonous Aladağ Unit in the Hadim region (Central Taurides). Since the Aladağ Unit includes a continuous Paleozoic carbonate sequence and the best preserved mid-Carboniferous boundary succession is exposed in the Hadim region, a 25,64 m thick stratigraphic section has been measured across the Mantar Tepe Member of the Yarıcak Formation, widely exposed in the region.

The mid-Carboniferous boundary has been recently modified (Vachard and Maslo, 1996; Shcherbakov, 1997; Groves, 1999). Previously the boundary was placed at the top of the Voznesensky Horizon of the Russian Platform. However, recently the boundary is defined at the base of the Voznesensky Horizon and at top of the Zapaltyubinsky Horizon in the Russian Platform and at the base of the Bogdanovsky Horizon in Urals. In this study, the mid-Carboniferous boundary is placed at the limit of Bogdanovsky and Zapaltyubinsky Horizons of the Russian Platform based on the calcareous benthic foraminifera because significant variations occur in the foraminiferal assemblages across this boundary. The measured section has been divided into four biozones which are comparable with the Donets Basin (Vachard and Maslo, 1996). The mid-Carboniferous boundary beds are mainly composed of continuous carbonate deposition including quartz arenitic sandstone intercalations at the bottom.

Shallow marine peritidal carbonates are mainly composed of shallowing upward cycles. Meter scale shallowing upward cycles have been determined based on the detailed microfacies analysis. The discrimination of the facies-types is based on the petrographic analysis. The microfacies have been determined by using standard microfacies models of Flügel (2004) and Wilson (1975). By using stacking pattern of these microfacies, several types of cycles have been determined. These higher order cyclic patterns can be identified as climate induced sea-level changes (Milankovitch cycles). These cycles in the studied section were deposited during the glacial (icehouse) period (Late Serpukhovian – Early Bashkirian). Therefore, the amplitude of sea-level changes are likely associated with the glaciation and have durations similar to the Milankovitch eccentricity cycles.

Recently, there has been a growing amount of interest in biotic responses to cyclicity (Weber et al., 2001). This study also presents an account on response of calcareous foraminifers to sedimentary cyclicity. Biostratigraphy and micropaleontological studies are very important for understanding the shallowing upward cycles since fossils are very sensitive to sea level changes. For this reason, the responses of benthic foraminiferal groups have been studied and documented in this study.

Furthermore, in this study a broad taxonomic work is also presented giving an account of morphological descriptions, distributions and occurrences of foraminiferal fauna.

1.2. Geographic Setting

The study area is located at approximately 10 km southwest of the town of Hadim (Figure 1). It is situated in the topographic map of Alanya – O 28 – b2 of 1:25.000 scales. The section starts at coordinates 36445144 E – 4085730 N and finishes at 36445160 E – 4085675 N. The section measured at the west of Hadim-Alanya road (Figure 1) is easily accessible from the town of Hadim. The study area can be reached along the stabilized road from Hadim to Alanya. The accessibility to the town of Hadim provided by the Konya-Hadim highway.

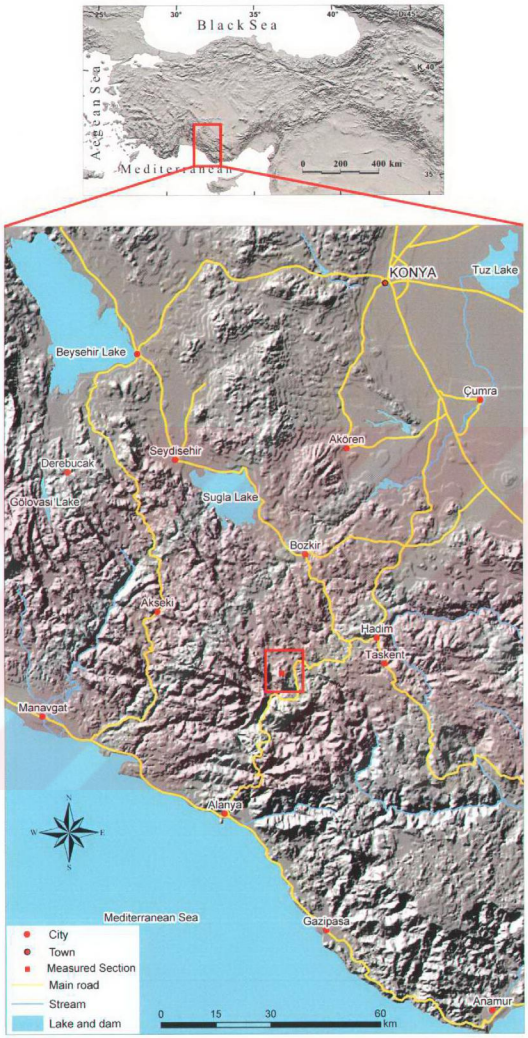


Figure 1. Geographic setting of the study area and the location of the measured section.

1.3. Methods of Study

This study consisted of field and laboratory works. In the field, a stratigraphic section, which is 25,64 m in thickness, was measured on a regularly bedded succession mainly composed of carbonates (Figure 2). 64 samples were collected from nearly each bed and also, thicker beds were sampled both from their bottom and top. During the fieldwork, the microfacies and faunal content of each sample were described by a hand-lense in order to detect and to control facies changes.

Detailed microfacies and micropaleontological studies were carried out in the laboratory. Thin sections were prepared from each sample for petrographic and paleontological analysis.

Calcareous foraminifera have been used to construct the biostratigraphy and delineate the identification of the mid-Carboniferous boundary because significant changes occur in the composition of calcareous foraminiferal assemblages across this boundary and calcareous foraminifera are sufficiently abundant throughout the section. Paleontological and taxonomical studies were carried out by taking the photographs of every well-oriented individuals and making morphological analyses on populations.

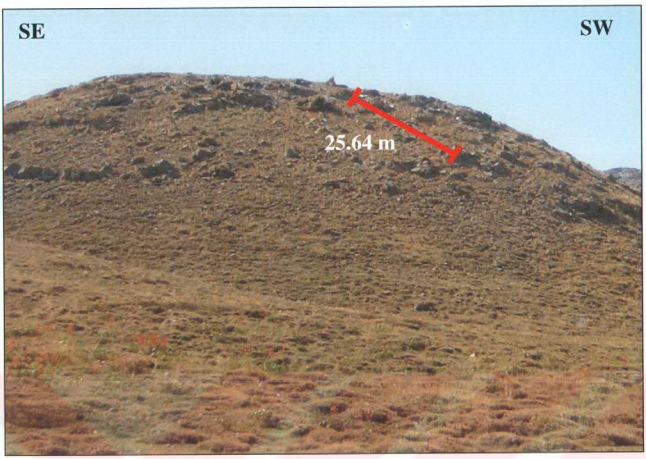
It is not easy to detect the shallowing upward cycles in the field because cycles are subtidal in character and the sea level fluctuations were hardly recorded. Therefore, detailed microscopic and micropaleontologic studies were carried out in order to identify cyclic repetitions due to sea level oscillations.

The point counting studies were also carried out in order to understand fossil (especially calcareous foraminifera) responses to environmental variations caused by sea-level oscillations and reflected in the anatomy of shallowing upward cycles. In order to perform numerical analysis, the foraminiferal assemblages are categorized into eight different groups, namely archaediscids, eostafellids, unilocular forms, paleotextularids, irregularly coiled bilocular forms, biseriamminids, pseudoendothyrids and endothyrids. Quantitative analysis of calcareous foraminifera were carried out in 4 cm^2 area of each thin section to find out the abundance and diversitification of these foraminiferal groups. For numerical analysis, all individual calcareous foraminifera of these

groups were counted in each sample with a point counter attached to the microscope. Approximately 200 to 300 specimens were counted in most thin sections. Total and relative abundances of each group have been used to understand the biotic response to sedimentary cyclicity.

1.4. Previous Works

In Taurides, various geological studies have been carried out for different purposes by many researchers over the last century. Related to the topic of this thesis, the earliest and important studies were carried out by Blumenthal (1944, 1947, 1951 and 1956) concerning the geology of the Tauride Belt. The studies of Blumenthal had been guide to other researchers for later studies in the Tauride region. In these studies, Blumenthal studied the general geologic and geomorphologic features of Seydişehir – Beyşehir region and the exposures of the Aladağ Unit around Beyşehir – Bozkır and northern Alanya region in western Taurides. Upper Paleozoic and Mesozoic to Neogene successions, their distributions within the region and fossil contents were defined and maps illustrating general tectonic structures of the Tauride were presented in these studies. Following studies of Blumenthal, Monod (1967, 1977) and Monod and Akay (1984) described the evolution of Tauride Carbonate Platform, including stratigraphy, structural geology and evolution of Aladağ Unit in Western Taurides. Among these studies, Monod (1977) described the Paleozoic units of Bademli. In Monod (1977), the Carboniferous is represented by carbonates and intercalated quartz arenitic sandstones and dolomites. The Aladağ and Bozkır Units are named as "Beyşehir-Horan Nappes" by Monod (1977) and the rock units belonging to the Aladağ Unit are defined as the "Bademli-Cevizli Unit" in context of these nappes (Monod, 1977). Gutnic et al. (1979) studied the geology and stratigraphy of Tauride Belt. Like Monod (1977), this study also described Carboniferous Units of Bademli. According to this study, Carboniferous units are composed of shales with brachiopods at the base and neritic carbonate deposits rich in macrofossils. Visean and Namurian are composed of alternations



A



B C

Figure 2. A. Location of the measured section (the red line shows the measured section), B-C. Close-up view of the measured section (the red bullets indicate the sampling point).

of carbonates and quartz arenitic sandstone-dolomites. Özgül (1971, 1976, 1984, and 1997), Özgül and Gedik (1973), Özgül et al. (1973, 1991) and Özgül and Turşucu (1984) are among the authors who have carried out detailed and more precise studies on the geodynamic evolution, geology and stratigraphy of Taurides. Özgül and Gedik (1973) studied the Lower Paleozoic Çaltepe Formation (Lower – Middle Cambrian) and Seydişehir Formation (Upper Cambrian – Lower Ordovician) in Seydişehir region and the Hadim area. Özgül (1976) divided Taurides into several tectonostratigraphic units and described the main tectonic units of the Tauride Belt. This study has become principle guide for other researchers. He described the Aladağ Unit comprising the Upper Devonian – Upper Cretaceous shelf type clastics and carbonates. He has mentioned that this unit is equivalent to the "Hadim Nappe" of Blumenthal (1944). Özgül (1984) defined the Carboniferous of the Aladağ Unit represented by shale, biostromal limestone and quartz arenitic sandstone. Demirtaşlı (1984) studied the Paleozoic stratigraphy and tectonics of the Hadim Nappe (Aladağ Unit), exposed between Silifke and Anamur regions in Central Taurus Mountains. Tekeli et al. (1984) studied the Paleozoic and Mesozoic sequences of Aladağ Mountains cropping out Eastern Taurides. They described the Upper Paleozoic rocks composed of shallow marine platform carbonates and terrigenous clastic interbeds. Özgül (1997) presented the main tectonic units of Hadim-Taşkent region in the Central Taurides and divided the Aladağ Unit into six different formations, Gölboğazı Formation (Devonian), Yarıcak Formation (Carboniferous), Çekiç Dağı Formation (Permian), Gevne Formation (Triassic), Çambaşı Formation (Jurassic – Cretaceous) and Zekeriya Formation (Maastricthian). The Yarıcak Formation has been divided into two members, Çityayla Member and Mantar Tepe Member. The latter is the main interest in this study because the stratigraphic section analyzed in this study has been measured within the carbonates of this member. Göncüoğlu (1997) studied the Lower Paleozoic, especially infra-Cambrian, Cambrian, Ordovician and Silurian stratigraphy and paleogeographic constrains of the Tauride belt. Göncüoğlu et al. (1997) stated that the complete Paleozoic sequence was correletable with the Southeast Anatolian Paleozoic sequence. Şenel (1999) introduced new

definitions of autochthonous-paraautochthonous and allochthonous rock units of the Taurus Belt. In this study, the autochthonous rock units, from west to east, are called the Beydağları autochthon, Anamas-Akseki autochthon and Southeast Anatolian autochthon; the allochthonous units are called the Lycian Nappes, Antalya Nappes, Alanya Nappe, Beyşehir-Hoyran-Hadim-Bolkar Nappes, Yahyalı-Munzur Nappes and Bitlis-Pötürge-Malatya Nappes.

Biostratigraphic studies were also carried out in the study region. Late Paleozoic (Carboniferous and Permian) and Triassic biostratigraphic studies were carried out in the Tauride Belt by Altıner (1981, 1984), Altıner and Zaninetti (1980), Altıner et al. (2000) and Altıner and Özgül (2001). Late Paleozoic stratigraphy and biostratigraphy of the Kayseri Pınarbaşı area was studied by Altıner (1981) in his Ph.D. thesis. In addition to these studies, Okuyucu (1999) carried out a biostratigraphic study in the Hadim Nappe of Central Taurides in order to delineate the Carboniferous – Permian boundary. Altıner et al. (2000) analyzed the Late Permian biofacies belts of the Tethyian carbonate platform. Moreover, the Southern Biofacies Belt including the Aladağ Unit, also the study area, was recognized by Altıner et al. (2000). Altıner and Özgül, (2001) provided most detailed data on the Carboniferous and Permian foraminiferal associations. In their study, several biozones were described in the Carboniferous and Permian deposits of the Hadim region. The Serpukhovian – Bashkirian boundary is defined by the foraminiferal biostratigraphic zones. Serpukhovian stage was divided into three zones, namely ST1, ST2 and ST3 and the Bashkirian stage was divided into four zones, namely BT1, BT2, BT3 and BT4. The mid-Carboniferous boundary (Serpukhovian – Bashkirian) boundary was placed between ST3, *Eostaffella postmosquensis – Plectostaffella* ex gr. *bogdanovkensis,* and BT1, *Semistaffella – Plectostaffella jakhensis,* zones. Okan and Hoşgör (2005) described the Bivalve species in the Bashkirian sequence of Nohutluk Tepe located in the eastern Taurides and commented on the paleobiogeographic value of the studied fauna. This study also presented the Serpukhovian and Bashkirian stratigraphy which consists mainly of limestones with the intercalations of quartz arenitic sandstones.

Sequence stratigraphical studies in the carbonate platform of the Taurides began in the Central Taurides with the studies of Marine Micropaleontology Research Unit, directed by Prof. Dr. Demir Altıner. The first sequence stratigraphical study was carried out by Yılmaz (1997) who described the meter-scale cyclicity and the sequence stratigraphic framework of the Upper Jurassic – Upper Cretaceous peritidal carbonates of the Polat Formation around the Fele area. This study has been followed by the study of Akçar (1998) who studied the Lower Cretaceous peritidal carbonates of the Üzümlü area. In addition to these studies, Bayazıtoğlu (1998) and Gaziulusoy (1999) also carried out sequence stratigraphic studies in the Fele and Seydişehir areas. The high resolution sequence stratigraphic study in Turkey was first published by Altıner et al. (1999). In this study, the cyclicity and its hierarchy within the Late Jurassic-Late Cretaceous sequences in the Western Taurides were defined and correlation between measured sections was presented. Moreover, Yılmaz and Altıner (2001) defined the use of sedimentary structures in the recognition of sequence boundaries in the Upper Jurassic – Upper Cretaceous peritidal carbonates of the Central Taurides. Following these sequence stratigraphic studies in the Jurassic and Cretaceous of the Taurides, Pütürgeli (2002) described the meter-scale shallowing upward cycles in the Midian (Upper Permian) strata. Ünal (2002) and Ünal et al. (2003) defined the cyclic sedimentation across the Permian-Triassic boundary in the Central Taurides and presented a global correlation of Permian-Triassic boundary beds with known sections in the world and some quantitative studies were carried out in order to test responses of organisms to cyclicity. Şen (2002) studied the nature of meter scale cycles in subtidal carbonates of the Middle Carboniferous (Moscovian) age. Biofacies, lithofacies and responses of fusulinacean foraminifers to sedimentary cyclicity were also examined in this work.

Outside of Turkey, there are studies carried out on meter-scale cyclicity and the delineation of the mid-Carboniferous (Serpukhovian – Bashkirian) boundary. Brenckle et al. (1977) discussed the reference section for this boundary as an intercontinental biostratigraphic datum. Brenckle et al. (1982) defined this boundary in North America based on calcareous foraminifera.

Moreover, Lane and Manger (1985) described the delineation of the mid-Carboniferous boundary by using fossils. Skipp et al. (1985) proposed a reference area for the mid-Carboniferous boundary in East Central Idaho, USA. Nemirovskaya et al. (1990) made the first proposal for a mid-Carboniferous boundary stratotype in the U.S.S.R. Gibshman and Akhmetshina (1990) described the micropaleontological basis for determination of the mid-Carboniferous boundary in the North Caspian Syneclise, U.S.S.R based on conodonts and foraminifers. Additional information was given by Brenckle et al. (1997) and Lane et al. (1999) for the determination of the mid-Carboniferous boundary by using conodonts, ammonoids and calcareous foraminifera in the Arrow Canyon of Nevada GSSP. Lane et al. (1999) also defined the sequence stratigraphy of the boundary interval. Geochemical studies were also carried out across the boundary successions by Bruckschen et al. (1999), Brand & Brenckle (2001) and Brand & Bruckschen (2002). Brucksen et al. (1999) carried out isotope studies of the European Carboniferous deposits and isotopic changes across the boundary. Brand & Brenckle (2001) established, compared and contrasted chemostratigraphic trends about the boundary in the Arrow Canyon GSSP. Brand & Bruckschen (2002) correlated sections in the Southeastern Russia with the mid-Carboniferous GSSP in Nevada.

Under the light of all these previous studies, this study has been undertaken in order to delineate the Serpukhovian – Bashkirian boundary in the Carboniferous based on calcareous foraminifera. Sedimentary cyclicity and sequence stratigraphic studies have also been performed in order to test the biotic response to cyclicity.

1.5. Regional Geological Setting

Özgül (1984) indicated that the Central Taurides show most of the characteristic features of the Tauride Belt. Because of this importance, it has been intensely studied during the last years. The Central Taurides consist of several tectono-stratigraphic units which have distinct stratigraphical, structural and metamorphic features (Blumenthal, 1947; 1951, Özgül, 1976, 1984, 1997). These units are, in fact, characterized by an autochthonous-paraautochthonous

unit (Geyik Dağı Unit) and several allochthonous units (Aladağ, Bolkar Dağı, Bozkır, Antalya and Alanya Units) (Özgül, 1984) (Figure 3). In the studied region, Geyik Dağı, Aladağ, Bolkar Dağı and Bozkır Units are widely exposed (Özgül, 1976; 1984; 1997, Altıner and Özgül, 2001) (Figure 4-5). Beyşehir-Hoyran nappes of Monod (1977) are the equivalent tectonic unit to the Bozkır and Aladağ Units of Özgül (1976).

The Geyik Dağı Unit which is the autochthonous-paraautochthonous unit of the Central Taurides is called as the "relative autochthon" and lies at the base of other units (Özgül, 1976; 1984; 1997). It is composed of platform type sediments starting with a Paleozoic basement comprising Cambrian and Ordovician rocks and a transgressive Upper Mesozoic – Lower Tertiary rocks (Özgül, 1984) (Figure 5). Lower Paleozoic units consist of the Hamzalar Formation with dark colored shales, the Çaltepe Formation including neritic and nodular limestone and the Seydişehir Formation consisting of micaceous turbiditic clastics (Dean and Monod, 1970; Özgül, 1984). The Mesozoic sequence of the Geyik Dağı Unit which lies with an unconformity over the Lower Paleozoic basement includes the Polat Limestone, the Çataloluk Formation and Çobanağacı Formation (Özgül, 1997).

The Bolkar Dağı Unit consists of Devonian – Upper Cretaceous shelf type carbonates and clastics (Özgül, 1984) (Figure 5). This unit shows the regional metamorphism unlike the Geyik Dağı and the Aladağ Units (Özgül, 1997). The grade of the metamorphism changes from place to place and the unit is composed at its base of the Hocalar Formation (Devonian) which includes low-grade metamorphosed schists. The overlying Lower-Middle Carboniferous Kongul Formation comprises mainly limestones intercalated with dark colored and fine grained clastics. The Taşkent Formation of Late Permian age consists mainly of algal and foraminiferal limestones and quartz arenitic sandstone intercalations at the top. The Mesozoic starts with the Ekinlik Formation of Triassic age containing neritic limestones and clastics and continued with the Morbayır Formation of Liassic age which is basically composed of conglomerates and sandstones. The Jurassic – Lower Cretaceous Sinat Dağı

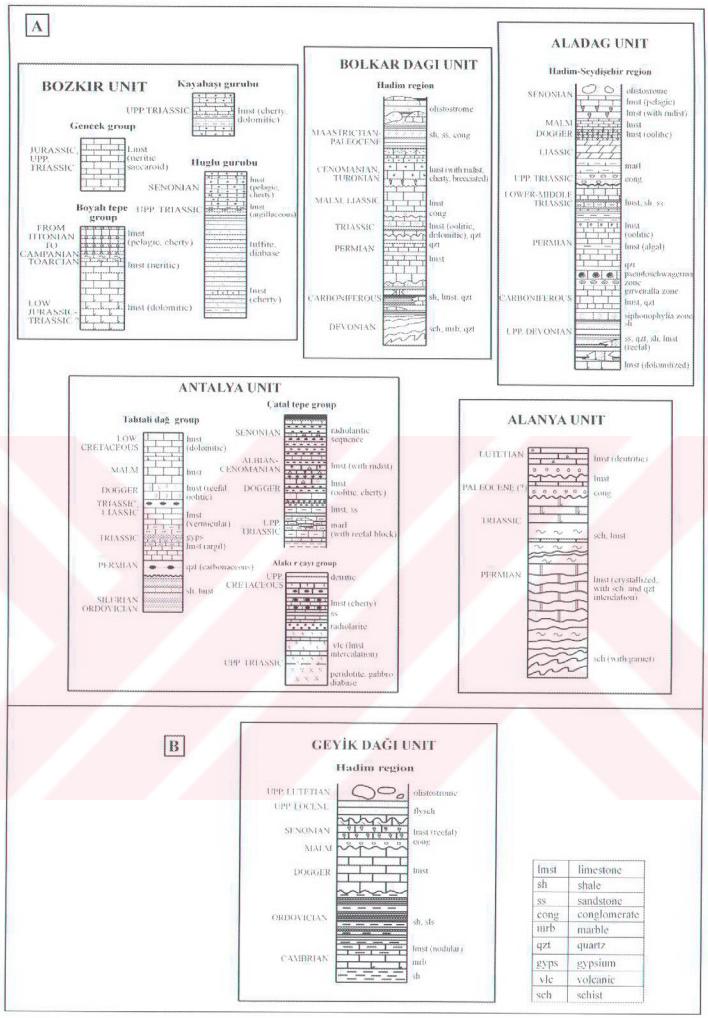


Figure 3. Stratigraphic sections of Bozkır, Bolkar Dağı, Antalya, Alanya and Geyik Dağı Units (simplified from Özgül, 1976).

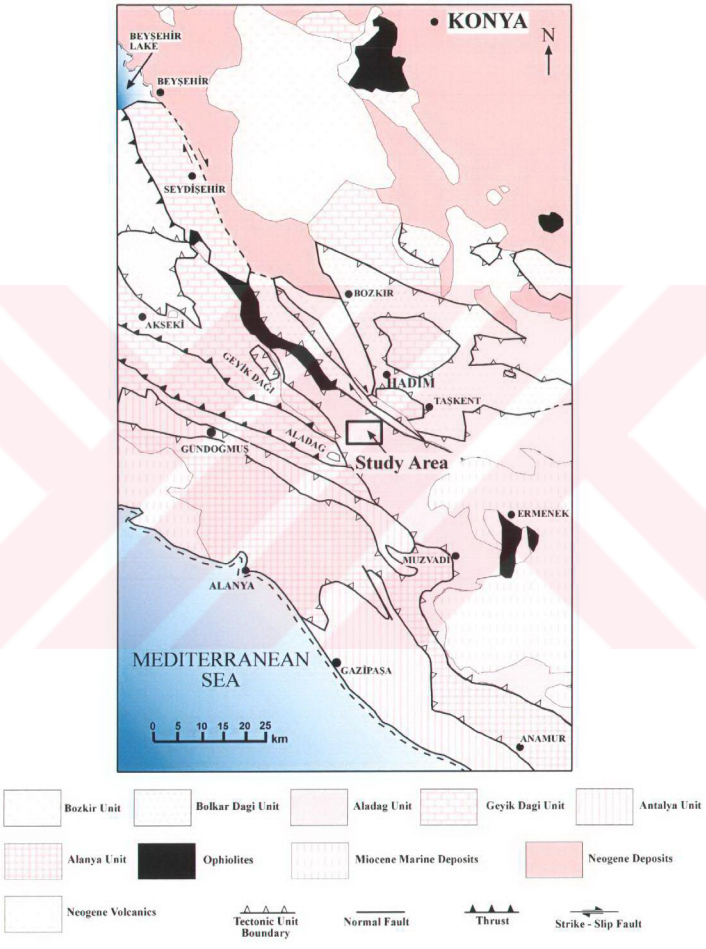


Figure 4. Tectonic map of the study area (Özgül, 1984).

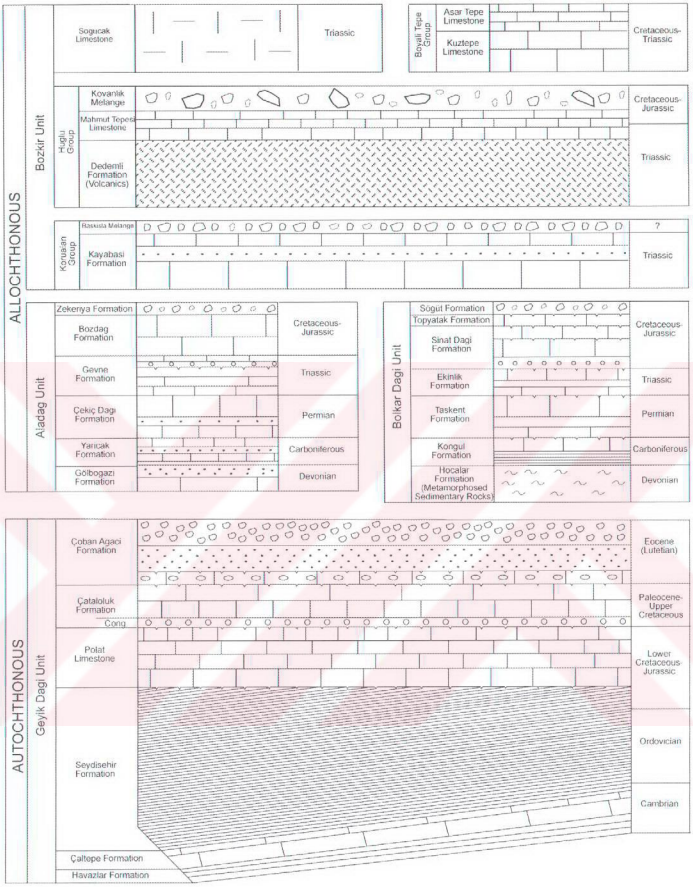


Figure 5. Autochthonous and Allochthonous units in the Hadim–Taşkent area (Altıner and Özgül, 2001).

Limestone is characterized by neritic limestones and the Liassic – Upper Cretaceous Pusula Group consists of pelagic limestones.

The Cenomanian Topyatak Limestone comprises mainly rudist limestones and finally the Söğüt Formation of Senonian age is composed pelagic limestones, olistoliths and olistrostroms (Özgül, 1997).

The Bozkır Unit is composed of pelagic and neritic limestones deposited during Triassic – Cretaceous and a variety of rocks of oceanic and upper mantle origin consisting of radiolarites, spilite, submarine volcanics, tuffs, diabase, ultramafic blocks and serpentinites (Özgül, 1984) (Figure 5). The general appearance of this unit is like a "mélange" due to tectonic mixing by nappes (Özgül, 1997). The Bozkır Unit consists of the Korualan, Huğlu, and Boyalı Tepe Groups, and the Soğucak Limestone. The Korualan Group comprises pelagic and neritic limestones, radiolarites, clastics, submarine volcanics. The Huğlu Group is characterized by shale and pelagic limestone alternations, green tuffs and basic volcanics, cherty limestones and olistostroms. The Boyalı Tepe Group includes thick neritic carbonates and the overlying pelagic limestones and chert and the Soğucak Limestone made up of neritic limestones.

The Aladağ Unit, one of the allochthonous units of the Central Tauride Belt, is composed of shelf type carbonates and clastic rocks of Late Devonian – Late Cretaceous age (Figure 5). This unit shows a continuous sedimentation from Upper Devonian to Upper Cretaceous. It includes the Gölboğazı Formation, the Yarıcak Formation, the Çekiç Dağı Formation, the Gevne Formation, the Çambaşı Formation, and the Zekeriya Formation. The Gölboğazı Formation of Devonian age consists mainly of quartz arenitic sandstone, shale intercalation, and reefal limestone. The Carboniferous Yarıcak Formation of the Aladağ Unit comprises basically quartzite shelf type limestone intercalations and dark colored shale at bottom part of the unit. The overlying Permian Çekiç Dağı Formation includes foraminiferal, algal limestone. The Gevne Formation of Triassic age comprises mainly shallow marine carbonates and clastic rocks. The Çambaşı Formation of Jurassic – Cretaceous age is composed of thick carbonate succession including dolomite and shallow marine limestone and the

Maastrichtian Zekeriya Formation consisting of olistoliths and olistrostroms (Özgül, 1997).

Within the geological frame, our study area is located in the exposures of the Aladağ unit near the town of Hadim and the studied section was measured in the continuous Carboniferous deposits of the Mantar Tepe Member of the Yarıcak Formation (Figure 1-2). Lithostratigraphic and biostratigraphic details of this unit will be given in the following chapter.

CHAPTER II

LITHOSTRATIGRAPHY AND BIOSTRATIGRAPHY

2.1 Lithostratigraphy

In the study area, Devonian – Triassic carbonate deposits of the Aladağ Unit are widely exposed with a nearly complete Upper Paleozoic succession (Figure 6). This Paleozoic succession starts at its base with the Gölboğazı Formation of Devonian age consisting of quartz arenitic sandstones, shales, sandy limestones and reefal limestones (Figure 7). The overlying Yarıcak Formation of Carboniferous age consists of shales and siltstones at the base and quartz arenitic sandstones and limestones above (Figure 7). The Permian Çekiç Dağı Formation is composed of quartz arenitic sandstones and limestones at the base, mainly carbonates in the upper part and is paraconformably overlain by the Gevne Formation of Triassic age (Figure 7). Gevne Formation starts with stromatolitic and oolitic limestones and continues with sandstones and sandy limestones (Figure 7). Following a well-defined unconformity surface within the formation, conglomerates, sandstones, lacustrine limestones and clayey limestones constitute the upper part of the formation (Figure 7). The rest of the Mesozoic deposits of Aladağ Unit, the Çambaşı Formation (Jurassic – Cretaceous) and the Zekeriya Formation (Maastricthian) are exposed outside of the study area. Among these formations of the Aladağ Unit, this study has been focused on the Yarıcak Formation in which a section has been measured in the continuous Carboniferous deposits in order to delineate the mid-Carboniferous boundary.

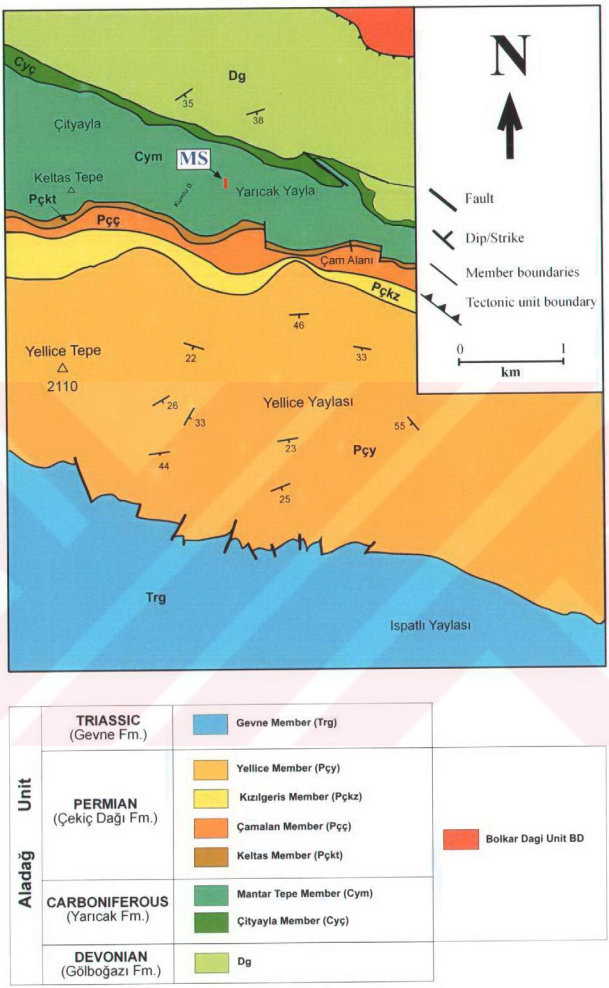


Figure 6. Geologic map of the study area (Altıner and Özgül, 2001) and MS indicates the measured section.

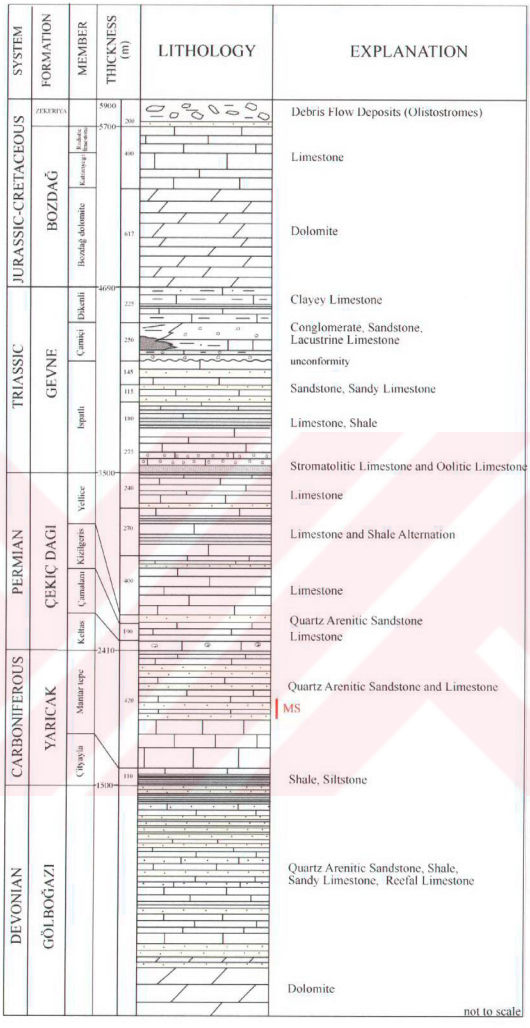


Figure 7. Generalized columnar section of the Aladağ Unit in the Hadim-Taşkent area (simplified from Özgül, 1997). The measured section (MS) is shown by the red line.

2.1.1. Yarıcak Formation

The Carboniferous succession in the Aladağ Unit is named as the Yarıcak Formation and the type section of the unit is nearly at 9-10 km southwest of the town of Hadim and lies within the study area (Özgül, 1997). In the type section, the formation consists of shelf type limestones with quartz arenitic sandstone intercalations and dark colored shales (Figure 7). The thickness measures 860 m. The formation conformably overlies the Gölboğazı Formation (Devonian) and is overlain by the Çekiç Dağı Formation (Permian) (Figure 7). The Yarıcak Formation is divided into two members, the Çityayla Member and the Mantar Tepe Member (Özgül, 1997).

The Çityayla Member is characterized by dark colored shales interbedded with thin limestone beds with abundant macrofossils. It contains Tournasian brachiopods, crinoids, bryozoa and rarely trilobites and lesser amount of microfossils (Özgül, 1997). This member was probably deposited in low energy shelf conditions below the wave base level.

The Mantar Tepe Member is mainly composed of bioclastic, oolitic and micritic limestones in the lower part and quartz arenitic sandstones intercalated with fusuline-rich limestone levels in the upper part (Altıner and Özgül, 2001). It also includes siliceous-iron cemented conglomerate lenses with quartz and flintstone fragments (Özgül, 1997). Based on foraminiferal and algal zones, Özgül (1997) recognized Visean, Serpukhovian, Bashkirian, Moscovian stages in the succession. More recently, Altıner and Özgül (2001) have divided the Carboniferous into several foraminiferal biozones (Figure 8). The Mantar Tepe Member with its sandy, pelloidal, oolitic, crossed bedded, bioturbated grainstones and packstones with abundant microfossils and macrofossils was deposited in a relatively high energy environment of a shallow shelf receiving high amount of sediment influx from the land.

The measured section within the Yarıcak Formation starts with the quartz arenitic sandstones at the base and then continues with the sandy oolitic grainstone facies intercalated with quartz arenitic sandstones (Figure 9). It passes upward into bioclastic, oolitic limestone facies with abundant microfossils and ooids. The section also includes mudstone intercalations (Figure 9). Towards the

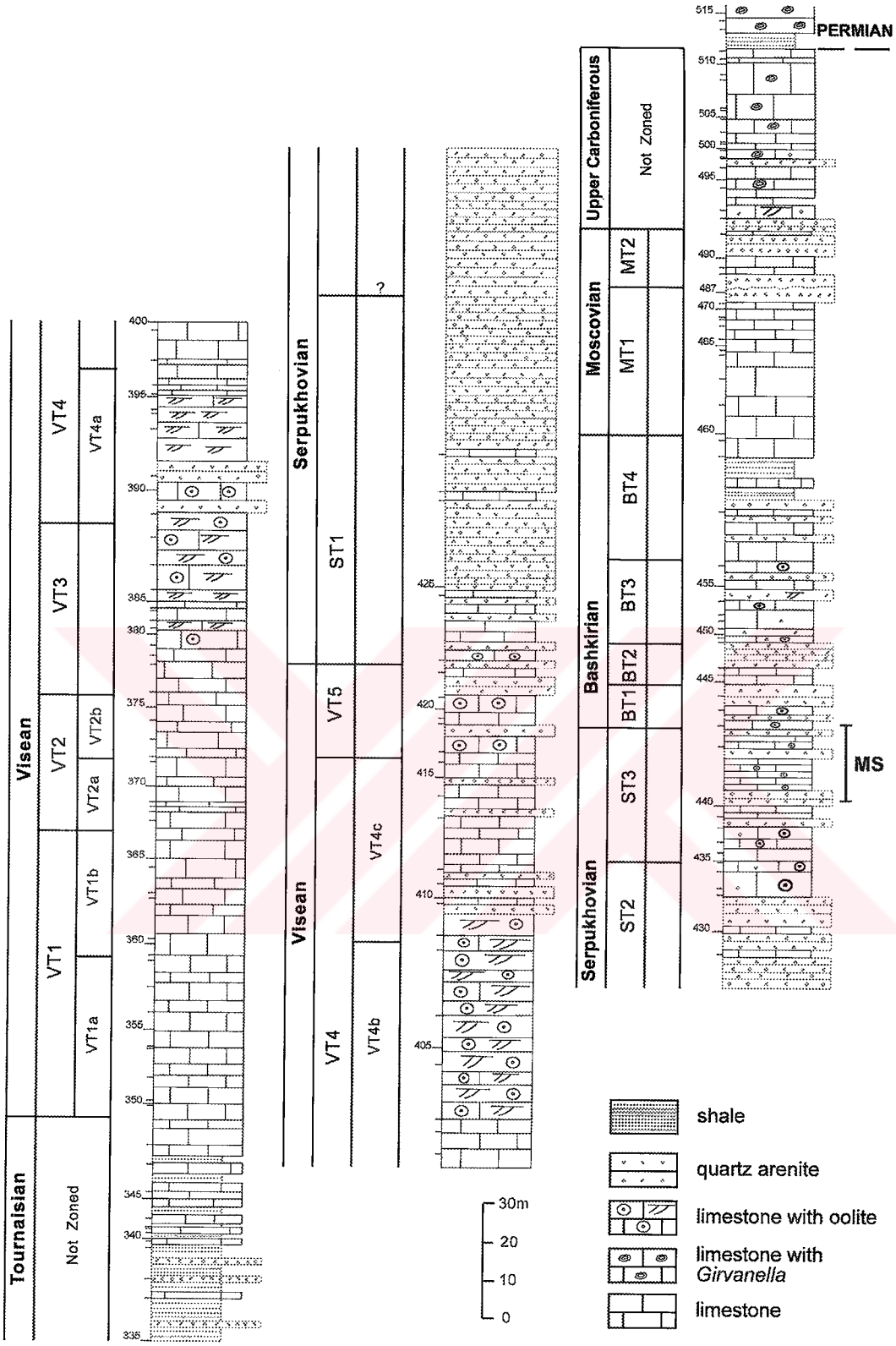


Figure 8. The Carboniferous biostratigraphy (Yarıcak Formation) of the Aladağ Unit in the Hadim-Taşkent area (Altıner and Özgül, 2001) (MS indicates the measured section).

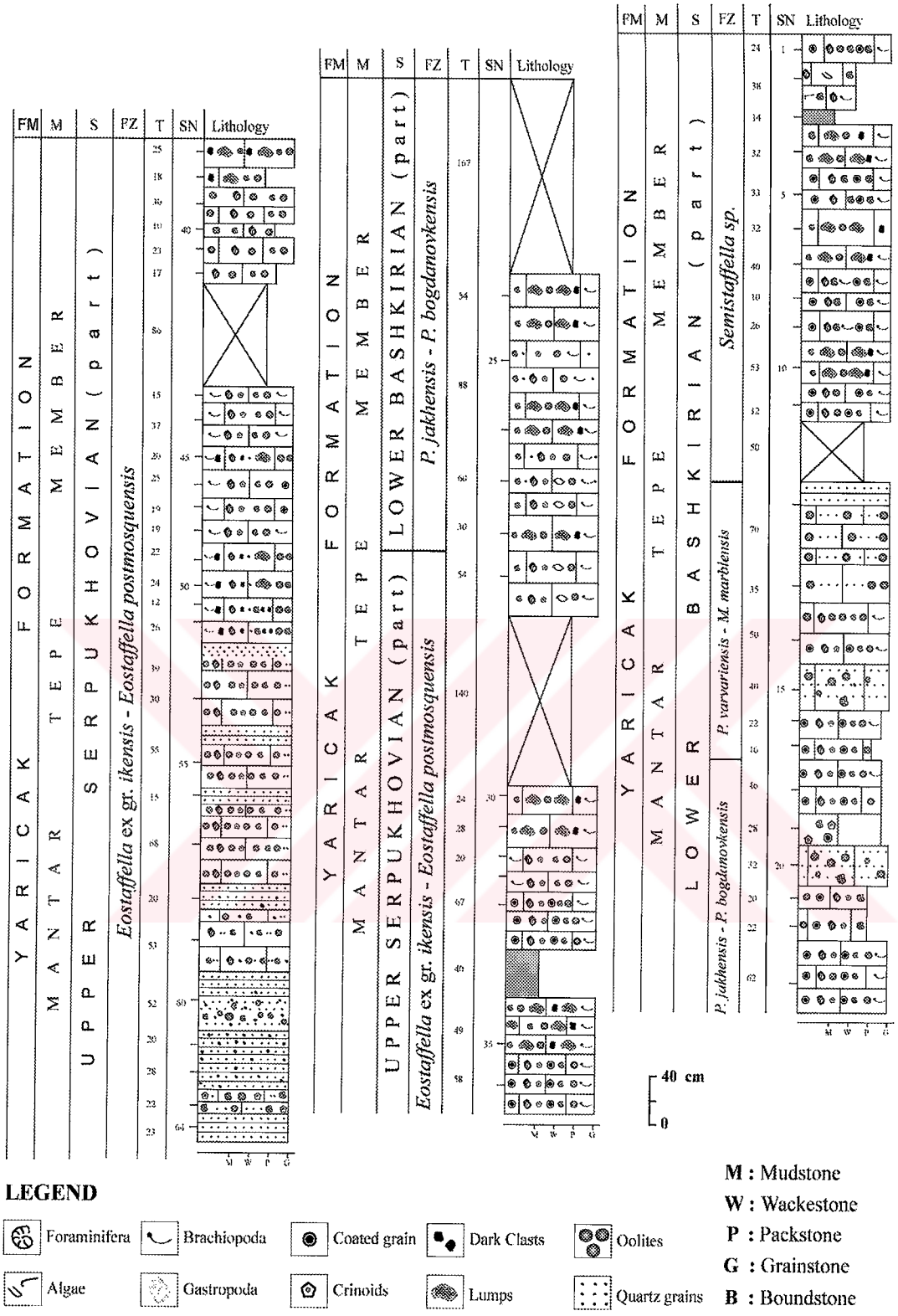


Figure 9. Lithostratigraphy of the measured section with biozones (FM: formation, M: member, FZ: foraminiferal zone, T: thickness, SN: sample no).

upper parts, sandy oolitic grainstones and quartz arenitic sandstones are dominant and finally they are overlain by oolitic and bioclastic grainstones (Figure 9).

2.2 Biostratigraphy

The Serpukhovian stage of the Yarıcak Formation, characterized by carbonates with quartz arenitic sandstone intercalations, is divided into 3 biostratigraphic zones by Altıner and Özgül (2001), namely, ST1, ST2 and ST3. ST3, *Eostaffella postmosquensis – Plectostaffella* ex gr. *bogdanovkensis* Zone, is considered to be equivalent of the Zapaltyubinsky and Voznesensky Horizons of the Russian Platform (Figure 8) (Table 1). In recent stage organizations of the Carboniferous, (Vachard and Maslo, 1996; Shcherbakov, 1997; Groves, 1999), this zone corresponds to the Upper Serpukhovian and Lower Bashkirian (Table 1). The Baskirian stage composed of an alternation of quartz arenitic sandstones and oolitic limestones is divided into 4 zones by Altıner and Özgül (2001) (Figure 8). The zone BT1 (*Semistaffella – Plectostaffella jakhensis* Zone), corresponds to the Syuransky in the Urals and Krasnopolyansky Horizon in the Eastern Russian Platform (Table 1).

The Serpukhovian stage is subdivided into four horizons; Tarussky, Steshevsky, Protvinsky and Zapaltyubinsky in the Russian Platform (Shcherbakov, 1997). Vdovenko et al. (1986) divided the Serpukhovian stage into three foraminiferal zones; Z1: *Pseudoendothyra globosa, Neoarchaediscus parvus*, Z2: *Eostaffellina protvae*, Z3: *Eosigmoilina explicata, Monotaxinoides subplana*. Shcherbakov (1997) recognized the Upper Serpukhovian by appearance of *Eostaffella ikensis*, *Bradyina* spp., *Biseriella parva*, *Pseudoglomospira subquadrata* and *Archaediscus krestovnikovi*.

Vdovenko et al. (1990) stated that the Upper Serpukhovian of Russian platform consists of Protvinsky, Zapaltyubinsky and Voznesensky Horizons. Protvinsky Horizon corresponds to the *Eostaffella protvae* Zone. The Zapaltyubinsky Horizon is calibrated by the zone of *Eostaffella explicata* and *Monotaxinoides subplana* Zones (Table 2). As for the Voznesensky Horizon, it corresponds to the *Plectostaffella bogdanovkensis* foraminiferal zone (Table 2).

Table 1. Upper Serpukhovian – Lower Bashkirian horizons in different regions.

	Russian Platform		Urals	In this study	North America	
Stages	Substages	Horizons	Horizons	Horizons	System	Series
Bashkirian	Lower	Prikamsky	Askynbashsky		Pennsylvanian (part)	Atokan
		Severokeltmensky	Akavassky			
		Krasnopolyansky	Syuransky	Syuransky		Morrowan
		Voznesensky	Bogdanovsky	Bogdanovsky		
Serpukhovian	Upper	Zapaltyubinsky	Ustsarbasky	Zapaltyubinsky	Mississippian (part)	Chesterian
		Protvinsky		Protvinsky		

However, later Voznesensky Horizon of Russian Platform is included in the Bashkirian stage (Vachard and Maslo, 1996).

The Bashkirian contains six horizons, Bogdanovsky, Syuransky, Akavassky, Askynbashsky, Tashastinsky and Asatausky Horizons. Sinitsyna and Sinitsyn (1987) divided the Bashkirian into six zones equivalent to the Bashkirian Horizons. The Lower Bashkirian zones are (1) *Plectostaffella bogdanovkensis* (Bogdanovsky Horizon), (2) *Eostaffella postmosquensis – E. pseudostruvei* zone (Syuransky Horizon), (3) *Pseudostaffella antiqua* zone (Akavassky Horizon), (4) *Ps. praegorskyi- Profusulinella staffelaeformis* zone (Askynbashsky Horizon) (Table 2).

The Lower Baskirian zonation was modified by Kulagina and Sinitsyna (1997) (Table 2). They assigned the Bogdanovsky through Akavassky Horizon

Table 2. Foraminiferal zones in different studies.

Stage	Turkey in this study, 2006	Turkey Altıner and Özgül, 2001	Askyn Section Kulagina and Sinitsyna, 1997	Donets Basin Vachard and Maslo, 1996	Russian Platform Vdovenko et al., 1990	Askyn Section Sinitsyna and Sinitsyn, 1987
	Foraminiferal Zones	**Foraminiferal Zones**	**Foraminiferal Zones**	**Foraminiferal Zones**	**Foraminiferal Zones**	**Foraminiferal Zones**
Lower Bashkirian		*Pseudostaffella antiqua grandis*	*Pseudostaffella praegorskyi Staffellaeformes staffellaeformis*	*Ozawainella umbonata Pseudostaffella praegorskyi Pseudonovella carbonica*		*Pseudostaffella praegorskyi - Profusulinella staffellaeformis*
		Pseudostaffella antiqua	*Pseudostaffella antiqua*	*Pseudostaffella antiqua*		*Pseudostaffella antiqua*
	***Semistaffella* sp.**	*Semistaffella – Plectostaffella jakhensis*	*Eostaffella pseudostruvei*	*Semistaffella variabilis Semistaffella* sp.		*Eostaffella postmosquensis- E. pseudostruvei*
	Millerella marblensis	*Eostaffella postmosquensis – Plectostaffella* ex gr. *bogdanovkensis*		*Millerella marblensis*	*Plectostaffella bogdanovkensis*	*Plectostaffella bogdanovkensis*
	Plectostaffella jakhensis - Plectostaffella bogdanovkensis			*Plectostaffella bogdanovkensis*		
Upper Serpukhovian	***Eostaffella* ex gr. *ikensis - E. postmosquensis***	*Eostafellina paraprotvae – Bradyina cribrostomata*			*Eostaffella explicata - Monotaxinoides subplana*	

to two zones and six subzones. According to the scheme, Bogdanovsky and Syuransky Horizons correspond to the *Eostaffella pseudostruvei* zone. Lower part of the Bogdanovsky is assigned to *Plectostaffella bogdanovkensis* subzone. The Upper Bogdanovsky and the Lower Syuransky are assigned to the *Semistaffella miniscularia* subzone and the Upper Syuransky is assigned to *Semistaffella variabilis* subzone. The Akavasky Horizon is calibrated by the *Pesudostaffella antiqua* Zone and its three subzones, *P. antiqua*, *P. antiqua posterior*, *P. antiqua grandis*.

According to Shcherbakov (1997), Lower Bashkirian in Urals includes three horizons; Syuransky, Akavasky, Askynbashky. Bogdanovsky Horizon is included in the lower part of the Syuransky Horizon.

In the studied section, the Upper Serpukhovian and Lower Bashkirian interval was divided into four foraminiferal zones (Table 2-3). The Lower zone (*Eostaffella* ex gr. *ikensis – E. postmosquensis* Zone) corresponds to the Upper Serpukhovian (Protvinsky – Zapaltyubinsky Horizons). However, the Upper three (*Plectostaffella bogdanovkensis – P. jakhensis* Zone, *Millerella marblensis* Zone and *Semistaffella* sp. Zone) correspond to the Lower Bashkirian comprising two Russian Horizons, namely Bogdanovsky and Syuransky.

2.2.1. *Eostaffella* ex. gr. *ikensis – E. postmosquensis* Zone

This zone covers the lower and middle parts of the measured section consisting of quartz arenitic sandstones and the sandy oolitic grainstones intercalated with quartz arenitic sandstones and the overlying oolitic, bioclastic grainstones and oolitic packstones (Figure 9). It also includes micritic limestone facies. It is from samples HB04-64 to HB04-28 (Table 3). It is characterized by the overlapping ranges of two taxa, *Eostaffella* ex gr. *ikensis* and *E. postmosquensis*. The upper boundary of this zone is characterized by the disappearance of *E.* ex. gr. *ikensis*. The lower boundary is characterized by the appearance of *E. postmosquensis* and *E. pseudostruvei*. This zone also includes some forms that do not pass into the Bashkirian stage, namely, *Bradyina cribrostomata*, *Biseriella parva*, and *E. tenebrosa*.

The zone contains a rich assemblage of foraminifera (Table 3): *Archaediscus postmoelleri* (Pl.III, figs. 1-3), *A. longus* (Pl. III, figs. 4, 5), *A. krestovnikovi* (Pl. III, figs. 6, 7), *A. moelleri* (Pl. III, fig. 9), *A. karreri* (Pl. III, fig. 8), *Paraarchaediscus koktjubensis* (Pl. IV, figs. 1, 11), *P. stilus* (Pl. IV, figs. 12-15), *P. ninae* (Pl. V, figs. 1-9), *P.* sp. A (Pl. V, figs. 10, 11), *Eosigmoilina* sp. (Pl. III, fig. 10), *Neoarchaediscus probatus* (Pl. VI, figs. 1-7), *N. subbaschkiricus* (Pl. VI, figs.8-18), *N. parvus* (Pl. VII, figs. 1, 2), *N. achimensis* (Pl. VII, figs. 3-6), *Astreoarchaediscus rugosus* (Pl. VII, figs. 15-17), *A. baschkiricus* (Pl. VII, figs. 18, 21), *Pseudoglomospira subquadrata* (Pl. I, figs. 13-17), *Paleonubecularia* sp. (Pl.II, figs. 9-11), *Paleotextularia* sp. (Pl. VIII, figs. 2-4), *Cribrostomum* sp. (Pl. VIII, fig. 5), *Climacammina* sp. (Pl. VIII, figs. 6, 7), *Diplosphearina inequalis* (Pl. I, figs. 1-4), *Tuberitina* sp. (Pl. I, figs. 5-7), *Pseudoendothyra luminosa* (Pl. XV, figs. 15, 16), *P.* spp. (Pl. XV, figs. 1-14), *Endothyra* spp. (Pl. X, figs. 5-12), *Planoendothyra* spp. (Pl. X, fig. 13), *Eostaffella pseudostruvei* (Pl. XII, figs. 1-6), *E. postmosquensis* (Pl. XII, figs. 7-13), *E. postproikensis* (Pl. XIII, figs. 3-6), *E. pinguis* (Pl. XII, figs. 20, 21), *E. hohsienica* (Pl. XII, figs. 22, 23), *E.* ex gr. *ikensis* (Pl. XIII, figs. 7-10), *E. tenebrosa* (Pl. XIII, fig. 11), *Biseriella parva* (Pl. VIII, figs. 8-17), *Globivalvulina bulloides* (Pl. VIII, fig. 18, Pl. IX, figs. 1-11), *G. granulosa* (Pl. VIII, figs. 1-15), *Bradyina cribrostomata* (Pl. X, figs. 14-17), *Mediocris mediocris* (Pl. XI, fig. 2), *Mediocris breviscula* (Pl. XI, fig. 3).

This zone is considered to be equivalent to the Protvinsky – Zapaltyubinsky Horizon in the Russian Platform and to the E2 Zone in the Western Europe (Vdovenko et al., 1990).

2.2.2. *Plectostaffella bogdanovkensis – P. jakhensis* Zone

The zone consists of oolitic grainstones, coated grain grainstone and oolitic packstones (Figure 9). It comprises the interval from samples HB04-27 to HB04-18 (Table 3). The zone is the interval lying between from the last appearance of *Eostaffella* ex gr. *ikensis* and the first occurrence of *Millerella marblensis*. This interval also corresponds to the first occurrences of *Plectostaffella bogdanovkensis* and *P. jakhensis*.

The following species are recorded in the zone (Table 3): *Archaediscus postmoelleri* (Pl.III, figs. 1-3), *A. longus* (Pl. III, figs. 4, 5), *A. krestovnikovi* (Pl. III, figs. 6, 7), *A.* sp. (Pl. III, figs.10-14), *Paraarchaediscus koktjubensis* (Pl. IV, figs. 1, 11), *Neoarchaediscus subbaschkiricus* (Pl. VI, figs.8-18), *N. timanicus* (Pl. V, figs.12-14), *N. parvus* (Pl. VII, figs. 1, 2), *Astreoarchaediscus rugosus* (Pl. VII, figs. 15-17), *A. baschkiricus* (Pl. VII, figs. 18, 21), *Globivalvulina bulloides* (Pl. VIII, fig. 18, Pl. IX, figs. 1-11), *G.* sp. (Pl. X, figs. 1-4), *Pseudoglomospira subquadrata* (Pl. I, figs. 13-17), *Paleonubecularia* sp. (Pl. II, figs. 9-11), *Paleotextularia* sp. (Pl. VIII, figs. 2-4), *Climacammina* sp. (Pl. VIII, figs. 6, 7), *Diplosphearina inequalis* (Pl. I, figs. 1-4), *Tuberitina* sp. (Pl. I, figs. 5-7), *Pseudoendothyra luminosa* (Pl. XV, figs. 15, 16), *Ps.* spp. (Pl. XV, figs. 1-14), *Endothyra* spp. (Pl. X, figs. 5-12), *Planoendothyra* spp. (Pl. X, fig. 13), *Plectostaffella bogdanovkensis* (Pl. XIV, fig. 1-5), *P. jakhensis* (Pl. XIV, fig. 6-9), *Eostaffella pseudostruvei* (Pl. XII, figs. 1-6), *E. postmosquensis* (Pl. XII, figs. 7-13), *E. postproikensis* (Pl. XIII, figs. 3-6), *E. pinguis* (Pl. XII, figs. 20, 21), *E. hohsienica* (Pl. XII, figs. 22, 23), *E. paraprotvae* (Pl. XIII, figs. 14-16).

This zone is equivalent of the Lower Bogdanovsky Horizon in the Urals and to Lower Voznesensky Horizon in the Donets Basin and the Russian Platform (Vachard and Maslo, 1996).

2.2.3. *Millerella marblensis* Zone

Detected between the sample HB04-17 and HB04-12 (Table 3), the zone comprises coated crinoidal packstones, bioclastic, oolitic grainstones with sand fragments and quartz arenitic sandstones (Figure 9). It is defined as the interval encompassing the first appearance of *Millerella marblensis* up to the first occurrence of *Semistaffella* sp. *P. varvariensis* is the characteristic taxon making its first appearance in this zone.

The following species are recorded in the zone (Table 3): *Archaediscus krestovnikovi* (Pl. III, figs. 6, 7), *Neoarchaediscus probatus* (Pl. VI, figs. 1-7), *N. timanicus* (Pl. V, figs.12-14), *N. achimensis* (Pl. VII, figs. 3-6), *N.* sp A (Pl. XVII, figs. 7-13), *A. baschkiricus* (Pl. VII, figs. 18, 21), *Globivalvulina bulloides* (Pl. VIII, fig. 18, Pl. IX, figs. 1-11), *G. scaphoidea* (Pl. IX, fig. 16), *G.* sp. (Pl.

X, figs. 1-4), *Pseudoglomospira subquadrata* (Pl. I, figs. 13-17), *Paleonubecularia* (Pl. II, figs. 9-11), *Paleotextularia* sp. (Pl. VIII, figs. 2-4), *Diplosphearina inequalis* (Pl. I, figs. 1-4), *Tuberitina* sp. (Pl. I, figs. 5-7), *Monotaxinoides* sp. (Pl. VIII, fig. 1), *Pseudoendothyra luminosa* (Pl. XV, figs. 15, 16), *P.* spp. (Pl. XV, figs. 1-14), *Endothyra* spp. (Pl. X, figs. 5-12)., *Planoendothyra* spp. (Pl. X, fig. 13), *Plectostaffella bogdanovkensis* (Pl. XIV, fig. 1-5), *P. jakhensis* (Pl. XIV, fig. 6-9), *P. varvariensis* (Pl. XIV, fig. 10, 11), *Eostaffella pseudostruvei* (Pl. XII, figs. 1-6), *E. postmosquensis* (Pl. XII, figs. 7-13), *E. postmosquensis acutiformis* (Pl. XII, figs. 14-17), *E. postproikensis* (Pl. XIII, figs. 3-6), *E. pinguis* (Pl. XII, figs. 20, 21), *E. cumberlandensis* (Pl. XIII, figs. 1, 2), *E. paraprotvae* (Pl. XIII, figs. 14-16) and *Millerella marblensis* (Pl. XI, figs. 7, 8).

The *Millerella marblensis* Zone corresponds to the Upper Bogdanovsky Horizon of Western Urals and Upper Voznesensky Horizon of the Russian Platform (Vachard and Maslo, 1996).

2.2.4. *Semistaffella* sp. Zone

Semistaffella sp. Zone is composed of oolitic, bioclastic grainstones and the algal packstone facies (Figure 9). Mudstone facies also occurs in the uppermost part of the zone (Figure 9). It comprises the sample interval HB04-11 – HB04-01 (Table 3). This zone is defined by the first occurrence of *Semistaffella* sp. The upper boundary of the zone is not defined in this study because the measured stratigraphic section ends within this zone.

Several foraminiferal species are present in this zone (Table 3) including: *Archaediscus longus* (Pl. III, figs. 4, 5), *Neoarchaediscus probatus* (Pl. VI, figs. 1-7), *N. timanicus* (Pl. V, figs.12-14), *N. subbaschkiricus* (Pl. VI, figs.8-18), *N. achimensis* (Pl. VII, figs. 3-6), *N.* sp. A (Pl. XVII, figs. 7-13), *Astreoarchaediscus rugosus* (Pl. VII, figs. 15-17), *A. baschkiricus* (Pl. VII, figs. 18, 21), *A. sp.* (Pl. VII, figs. 22), *Globivalvulina bulloides* (Pl. VIII, fig. 18, Pl. IX, figs. 1-11), *G. scaphoidea* (Pl. IX, fig. 16), *G.* sp. (Pl. X, figs. 1-4), *Pseudoglomospira subquadrata* (Pl. I, figs. 13-17), *Pseudoglomospira* sp. A (Pl. II, figs. 5, 8), *Pseudoglomospira* sp. B (Pl. II, figs. 7, 8), *Paleonubecularia* sp.

(Pl. II, figs. 9-11), *Paleotextularia* sp. (Pl. VIII, figs. 2-4), *Climacammina* sp. (Pl. VIII, figs. 6, 7), *Diplosphearina inequalis* (Pl. I, figs. 1-4), *Tuberitina* sp. (Pl. I, figs. 5-7), *Pseudoendothyra luminosa* (Pl. XV, figs. 15, 16), *P.* spp. (Pl. XV, figs. 1-14), *Endothyra* spp. (Pl. X, figs. 5-12), *Planoendothyra* spp. (Pl. X, fig. 13), *Plectostaffella bogdanovkensis* (Pl. XIV, fig. 1-5), *P. jakhensis* (Pl. XIV, fig. 6-9), *P. varvariensis* (Pl. XIV, fig. 10, 11), *Semistaffella* sp. (Pl. XIV, fig. 12-14), *Eostaffella pseudostruvei* (Pl. XII, figs. 1-6), *E. postmosquensis* (Pl. XII, figs. 7-13), *E. postmosquensis acutiformis* (Pl. XII, figs. 14-17), *E. pinguis* (Pl. XII, figs. 20, 21), *E. cumberlandensis* (Pl. XIII, figs. 1, 2), *E. paraprotvae* (Pl. XIII, figs. 14-16), *E.* sp. (Pl. XIII, figs. 12,13), *Millerella marblensis* (Pl. XI, figs. 7, 8) and *M. umbilicata* (Pl. XI, figs. 5, 6).

The *Semistaffella* sp. Zone corresponds to the Syuransky Horizon in the Urals, the Krasnopolyansky Horizon of the Russian Platform and the Feninsky Horizon in the Donets Basin.

2.3. Mid-Carboniferous Boundary

In this section, the criteria for determination of mid-Carboniferous boundary are discussed. The mid-Carboniferous boundary can be defined by conodonts, ammonoids and calcareous foraminifera (Brenckle, 1977).

The Upper Serpukhovian was subdivided into two horizons the Protvinsky and the Zapaltyubinsky and the Lower Bashkirian substage was subdivided into the Syuransky, Akavassky and Askynbashsky Horizons.

Reitlinger (1980) who introduced the *Plectostaffella bogdanovkensis* described the foraminifers from this horizon. Initially the Bogdanovsky Horizon included in the Upper Serpukhovian, however, it was reassigned to the lowest Bashkirian. Einor et al. (1979) and Semichatova et al. (1979), defined the mid-Carboniferous boundary between the Bogdanovsky and Syuransky Horizons. Ainsenverg et al. (1979) described the mid-Carboniferous boundary at the top of the Voznesensky Horizon. This was ratified in 1995 by the commission on the Carboniferous System and the mid-Carboniferous boundary was placed at the base Bogdanovsky Horizon, very closely approximates the base of the *Homoceras* genozone.

The international mid-Carboniferous boundary is defined by the appearance of the conodont species, *Declinognathodus noduliferous*. This level approximates the base of the *Homoceras* Zone in Western Europe. The contact between is defined between Zapaltyubinsky-Voznesensky Horizons in the Russian Platform and the Mississippian-Pennsylvanian subsystems in NA.

Gibshman and Akhmetshina (1990) also studied the mid–Carboniferous boundary and defined the boundary at the base of species *Declinognathodus noduliferous*. Kulagina and Sinitsyna (1997, 2003) defined that the base of the Bashkirian corresponded to the base of Bogdanovsky Horizon.

This study mainly focuses on the calcareous foraminifera in order to define the mid Carboniferous boundary.

2.3.1. Calcareous foraminifers across the mid- Carboniferous boundary

The mid-Carboniferous boundary coincides with the boundary between Protvinsky and Voznesensky in Russian Platform and at the base of the Bogdanovsky Horizon in the Urals. This boundary also corresponds to Mississippian-Pennsylvanian boundary in North America and is mainly defined by conodonts, ammonoids and calcareous foraminifers. Across this, boundary significant changes occurred in the calcareous foraminifers and particularly Fusulinaceans flourished. The first stage in the evolution of Fusulinaceans is marked by the appearance of *Plectostaffella* and *Semistaffella* (Einor et al., 1979). The appearance of *Globivalvulina bulloides* is also a marker for identifying the mid-Carboniferous boundary in North America (Groves, 1988). However, recent studies have shown that it occurs also below the mid-Carboniferous boundary in Eurasia, Artic Alaska and Turkey. Eosigmoilinid foraminifers (*Eosigmoilina robertsoni* and *Brenckleina rugosa*) are the zonal indices for Zapaltyubinsky and equivalent horizons. The boundary is defined by absence of these foraminifers. *Millerella marblensis* consistently appears within the Early Pennsylvanian.

The mid-Carboniferous boundary beds at the measured section in the Central Taurides are mainly composed of grainstones intercalated with quartz

arenites. Abundant fossil foraminifera are found in these beds. The mid-Carboniferous boundary is drawn at the base of the section 27 based on the first appearance and disappearance of foraminifers. The mid-Carboniferous boundary in the measured section is defined by the appearance of *Plectostaffella bogdanovkensis*, *P. jakhensis,* and the disappearance of *Eostaffella* ex gr. *ikensis* and *Bradyina cribrostomata.* Most Lower Carboniferous taxa from several faunal groups, including foraminifers, become extinct at this level and are replaced by typical Bashkirian forms. *P. bogdanovkensis* foraminiferal zone corresponds to the Voznesensky Horizon (Vdovenko et al., 1990). It is characterized by the presence of Bashkirian like eostaffellids (*E. postmosquensis, E. pseudostruvei*) and by the appearance of *Millerella marblensis*, *Globivalvulina bulloides* and *Plectostaffella.*

The mid-Carboniferous boundary is delineated between previously mentioned Upper Serpukhovian (Zapaltyubinsky) (*Eostaffella* ex gr. *ikensis – E. postmosquensis*) and Lower Bashkirian (Bogdanovsky) (*Plectostaffella bogdanovkensis – P. jakhensis*) biozones (Table 3).

Table 3. Foraminiferal distribution chart.

| Stage | Horizons | ZONES | Sample No | *Archaediscus longus* | *Archaediscus karreri* | *Archaediscus krestovnikovi* | *Archaediscus moelleri* | *Archaediscus postmoelleri* | *Archaediscus* sp. | *Asteroarchaediscus bashkirus* | *Asteroarchaediscus rugosus* | *Asteroarchaediscus* sp. | *Biserilla parva* | *Bradyina cribstomata* | *Bradyina* sp. | *Climacammina* sp. | *Cribrostomum* sp. | *Diplosphaerina inequalis* | *Eostigmoilina* sp. | *Eostafella cumberlandensis* | *Eostafella* ex gr. *ikensis* | *Eostafella hohsienica* | *Eostafella pinguis* | *Eostafella postmosquensis* | *Eostafella p. acutiformis* | *Eostafella postprotkensis* | *Eostafella pseudostruvei* | *Eostafella* sp. | *Eostafella teneborsa* | *Eostafellina paraprotvae* | *Endothyra* sp. | *Globivalvulina bulloides* | *Globivalvulina granulosa* | *Globivalvulina scaphoidea* | *Globivalvulina* sp. A | *Mediocris mediocris* | *Mediocris bresvicula* | *Millerella marblensis* | *Millerella* sp. A | *Millerella umbilicata* | *Monota.inoides* sp. | *Neoarchaediscus achimensis* | *Neoarchaediscus parvus* | *Neoarchaediscus probatus* | *Neoarchaediscus subbashkirus* | *Neoarchaediscus timanicus* | *Neoarchaediscus* spp. | *Paleonubecularia* sp. | *Paleotextularia* sp. | *Paraarchaediscus kobjuhensis* | *Paraarchaediscus ninae* | *Paraarchaediscus* sp. A | *Paraarchaediscus stilus* | *Parathuramminacea* | *Planoendothyra* sp. | *Pseudoendothyra luminosa* | *Pseudoendothyra* spp. | *Pseudoglomospira* sp. A | *Pseudoglomospira* sp. B | *Pseudoglomospira subquadrata* | *Plectostaffella bogdanovkensis* | *Plectostaffella jakhensis* | *Plectostaffella varvariensis* | *Semistaffella* sp. | *Tetrataxis* sp. | *Tuberitina* sp. |
|---|---|---

CHAPTER III

SEQUENCE STRATIGRAPHY

3.1 Historical Background

Sequence stratigraphy is the most recent paradigm in geological thought. Sequence stratigraphy has stemmed from the seismic stratigraphy of the 1970's. Seismic stratigraphy emerged in 1970's with the work of Vail et al. (1977). The seismic stratigraphic analysis stimulated a revolution in stratigraphy. This new method together with the global cycle chart was published by Vail et al. (1977). Seismic stratigraphy is a geologic approach to the stratigraphic interpretation of seismic data (Vail and Mitchum, 1977). Seismic sequence analysis is based on the depositional sequences. Depositional sequence is defined as a stratigraphic unit composed of a relatively conformable succession of genetically related strata and bounded at its top and base by unconformities or their correlative conformities (Mitchum et al., 1977). However, in 1963 Sloss had defined the sequence as an unconformity bounded rock-stratigraphic units of higher rank.

Seismic stratigraphy and global cycle chart were introduced as an inseparable package of new stratigraphic methodology. These ideas passed on to the sequence stratigraphy, as seismic stratigraphy evolved into sequence stratigraphy with the incorporation of outcrop and well data (Posamentier et al., 1988; Van Wagoner et al., 1988). Sequence stratigraphy is widely embraced as a new method of stratigraphic analysis by both industry and academic practitioners that has become a highly successful exploration technique in the natural resources searches (Catuneanu, 2002). Sequence stratigraphy is defined as the study of rock relationships within a chronostratigraphic framework of repetitive, genetically related strata bounded by surfaces of erosion or nondeposition, or their correlative conformities (Van Wagoner et al., 1988). Sequence is the fundamental unit of sequence stratigraphy. A sequence can be subdivided into system tracts which are composed of depositional systems, 3-D assemblages of

lithofacies (Van Wagoner et al., 1988). System tracts are defined by stacking patterns of parasequence sets or cycles. Cycle is defined as a relatively conformable succession of genetically related beds or bed sets bounded by marine flooding surfaces and their correlative surfaces (Van Wagoner et al., 1988).

Meter scale depositional cycles are fundamental stratigraphic units. Cyclicity is defined by the stratal repetition of physical and chemical characters of sedimentary rocks, such as, lithofacies and biofacies (Yang et al., 1998). This stratal regularity is the basis for establishing a high resolution cyclostratigraphy (Yang et al., 1998).

Although previous studies have focused on siliciclastic systems, sequence analysis can be readily applied to carbonate systems. Posamentier et al. (1988) described the eustatic controls on clastic deposition. Sarg (1988) discussed carbonate sequence stratigraphy. This study is the cornerstone for the recent cyclic studies on carbonates. Carbonates can be equally good recorder of high frequency sea level changes. Mainly, peritidal and shallow marine carbonates show shallowing upward meter-scale cyclicity. Shallowing upward cycles in shallow water carbonates have been interpreted as the sedimentological record of successive high frequency sea level changes (Goldhammer et al., 1987 and Strasser, 1988). Thus to recognize the cycles in carbonates, limestone microfacies analysis is the major tool.

This study documents a detailed study of cyclic sedimentation in the subtidal carbonate deposits of latest Serpukhovian – lowest Bashkirian deposits of Mantar Tepe Member consisting of mainly oolitic limestone with quartz arenite intercalations. In order to define cyclic sedimentation firstly detailed microfacies studies were carried out. Details of microfacies analysis will be discussed in the following section.

3.2 Microfacies Types and Depositional Environments

Previously the term microfacies is defined by only petrographic and paleontological criteria studied in thin sections however, today this term is referred to all sedimentological and paleontological data determined from rock

samples, polished slabs and thin sections (Flügel, 2004). Steenwinkel (1990) also defined facies types based on the total aspects of rock: lithology, outcrop features, petrography, bedding types, sedimentary structures and diagenesis. With the painstakingly examination of their sedimentological and paleontological features, microfacies studies reflect the history and depositional environments of carbonate rocks (Flügel, 2004). Microfacies determination is largely descriptive and microfacies types should be defined by microfacies criteria whose existence and abundance indicate the specific depositional settings (Flügel, 2004). Each lithofacies indicates a specific hydrodynamic environment. Microfacies types of carbonate rocks are not restricted to specific time intervals. Therefore, Wilson (1975) introduced the term standard microfacies types (SMF types) which can describe major depositional and biological controls and suggests major depositional settings. Wilson (1975) distinguished 24 standard microfacies types and used these standard microfacies types to differentiate the facies belts of a rimmed shelf. In addition, Flügel (2004) classified 26 standard microfacies types (SMF) for rimmed carbonate platforms (Figure 10) and also described 30 microfacies types for carbonate ramps as ramp microfacies types (RMF) (Figure 11). Some of these microfacies types correspond in their criteria to SMF types of rimmed carbonate platforms. SMF types are better defined than RMF because they are described based on more case studies.

In this study, the carbonates are named according to the Dunham Classification (1962) and 11 different microfacies in the measured section are determined by the analysis of bioclastic components, and sedimentological features observed in thin sections. Major microfacies types distinguished in the studied rocks are summarized in Table 4. The main lithofacies types are coated crinoidal grain packstone, bioclastic grainstone with foraminifera, coated bioclastic grainstone, oolitic grainstone, oolitic packstone-grainstone, oolitic packstone, aggregate-grain grainstone, mudstone-wackestone, sandy oolitic grainstone, sandy pelloidal packstone, and quartz arenite.

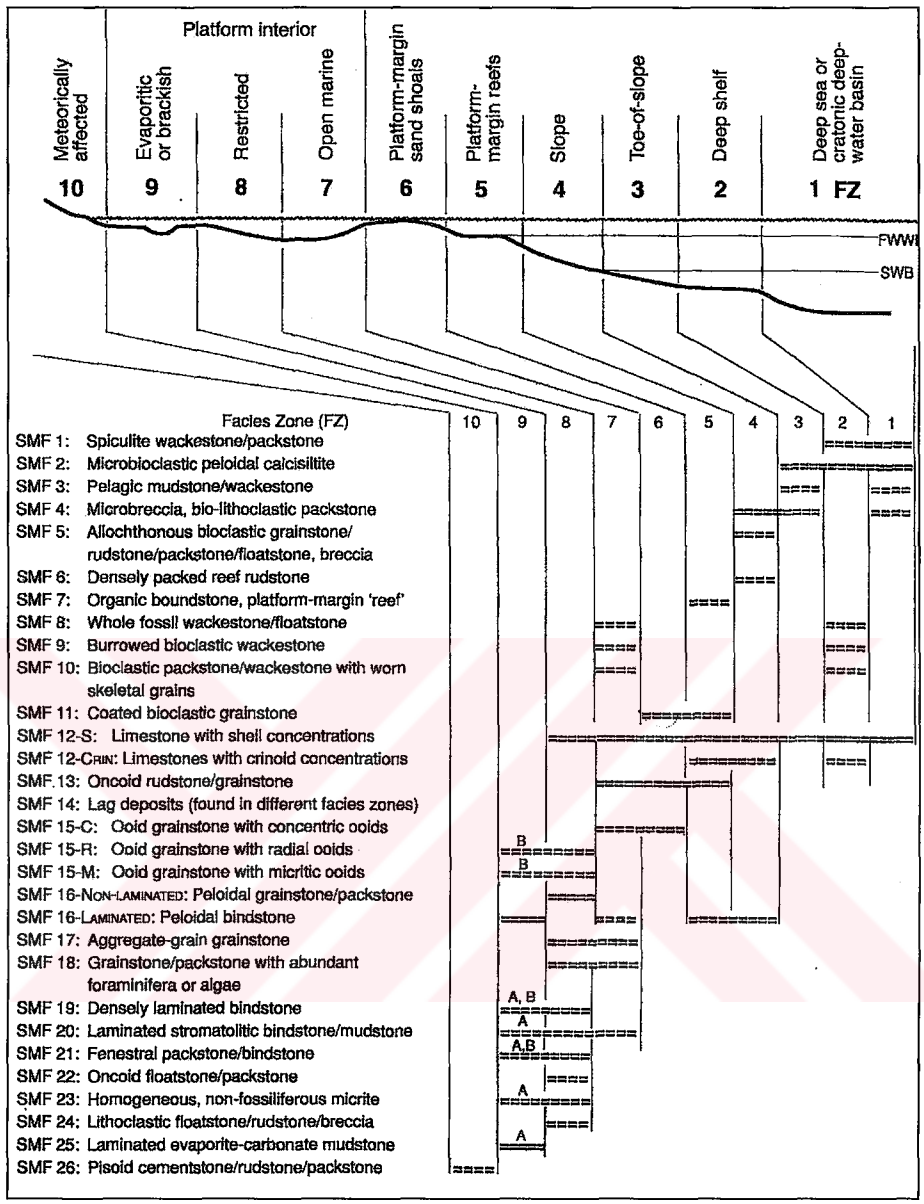


Figure 10. Distribution of Standard Microfacies (SMF) types in the Facies Zones (FZ) of the rimmed carbonate platform model (Flügel, 2004) (A: evaporitic, B: brackish).

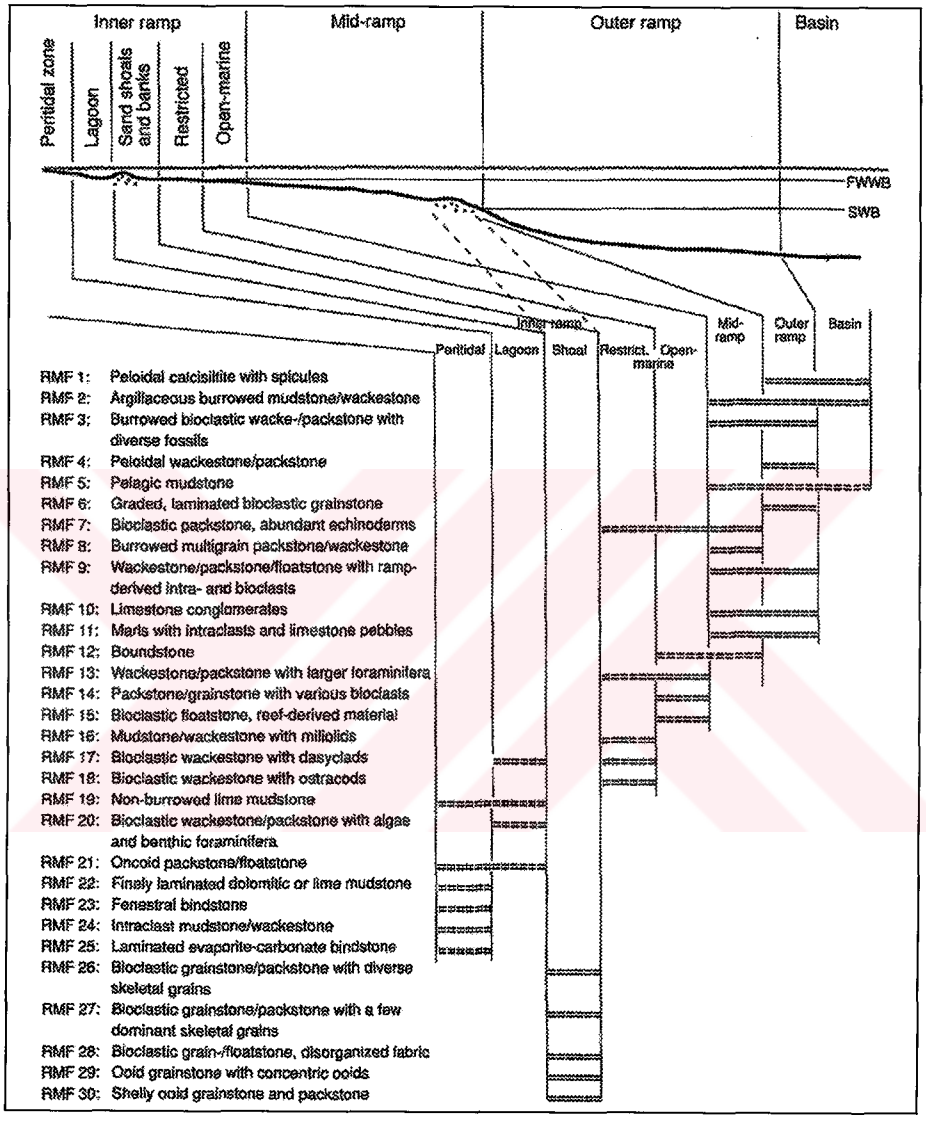


Figure 11. Generalized distribution of microfacies types in different parts of a homoclinal carbonate ramp (Flügel, 2004).

Table 4. Carbonate and siliciclastic facies and their depositional environments in the studied section.

No	Facies Type		Description	Grain types/fossils	Position within the cycle	Depositional Environment
1	Coated crinoidal packstone		Packstone which consists of bioclastic grains composed mainly of crinoids having micritic envelops	Crinoid fragments, gastropods, foraminifers, and bivalves	Base	Sand shoals and banks (Shoal)
2	Bioclastic grainstone with foraminifers		Grainstone with high abundance of benthic foraminifera and bioclasts	Foraminifers, brachiopoda fragments, echinid spines, gastropods and aggregate grains	Base	Sand Shoals (Shoal)
3	Coated bioclastic grainstone		Grainstone mainly composed of skeletal grains having micritic envelopes or biogenic encrustations	Foraminifers, crinoids and echinid fragments, gastropods, pelloids, lumps and bioclasts	Base - Middle	Sand Shoals (Shoal)
4	Oolitic grainstone	O1	Grainstone with oolites and dominantly bioclasts	Foraminifers, bioclasts, crinoids and echinid fragments, and gastropods	Middle	Sand Shoals (Shoal)
		O2	Oolitic grainstone with lumps	Lumps, radial oolites and aggregate grains	Top	Restricted Environment (Shoal)
		O3	Grainstone which consists of radial-fibrous oolites with quartz grains (~5%)	Oolites with radial structure and quartz grain	Top	Restricted Environment (Shoal)

Table 4. (Cont'd)

No	Facies Type	Description	Grain types/fossils	Position within the cycle	Depositional Environment
5	Oolitic packstone-grainstone	Packstone to grainstone composed of oolites and skeletal grains	Crinoids and echinid fragments, pellets, dark intraclasts, foraminifers and gastropods	Middle	Sand Shoals (Shoal)
6	Oolitic packstone	Packstone with micritic matrix composed of oolites. Grains are incontact with each other.	Oolites (radial and concentric), crinoids, foraminifers, and lumps	Top	Landward direction of the Sand Shoal (Shoal)
7	Aggregate-grain grainstone	Grainstones which consists of aggregate grains with mainly intraclasts, lumps, and dark clasts.	Foraminifers, intraclasts, lumps and micritized grains	Base-Middle-Top	Restricted Platform Interior (Shoal)
8	Mudstone - wackestone	No fossils or few fossils, homogenous lime mud	Unfossiliferous	Top	Lagoon Platform interior (Lagoonal – Restricted)
9	Sandy oolitic grainstone	Packstone composed of quartz grains (~25%) and oolites with micritic matrix	Pellets, foraminifers, oolites with radial structure, crinoids and echinid fragments	Base	Restricted Environment (Landward side)
10	Sandy pelloidal packstone	Pelloidal packstone which contains ~25% quartz grains	Pellets and quartz grains	Middle	Restricted Environment (Landward side)
11	Quartz arenitic sandstone	Sandstone composed very fine sand to silt sized quartz grains	Quartz grains, unfossiliferous	Top	Shore (Landward side)

3.2.1. Coated crinoidal packstone (CP)

Coated crinoidal packstone microfacies exhibits micritic envelops around crinoid fragments and bioclasts (Figure 12). Other components are superficial oolites, pelloids, dark intraclasts, foraminifers, bioclasts, brachiopods and gastropods.

Crinoids require open marine, moderately agitated conditions just below the wave base (Wilson, 1975). Therefore, this facies indicates an open marine environment with moderate energy. It is deposited seaward of the bioclastic grainstone. This facies is equivalent of FZ 5 of Flügel (2004).

3.2.2. Bioclastic grainstone with abundant foraminifers (BG)

The main components of this facies are fossils. Its particles are mainly foraminifers (Figure 13.A, B, C, D, E, and F). Other very common components are crinoid fragments, brachiopods and dark intraclasts (Figure 13.A, B, C, E, and F). This microfacies type corresponds to bioclastic grainstone with diverse skeletal grains (Flügel, 2004). It also includes fewer amounts of ooids (Figure 13.A, B). Cement is formed by sparitic calcite.

This type of facies forms extensive sheets generally seaward of oolitic grainstone shoals and grades down dip into skeletal grainstone or coated crinoidal packstone (Al-Tawil and Read, 2003). They constitute high energy skeletal banks and sheets deposited seaward of ooid shoal, in wave agitated settings. This type of microfacies corresponds to the FZ 5 and FZ 6 of Flügel (2004).

3.2.3. Coated bioclastic grainstone (CG)

In this type of facies, most of the grains are coated and exhibit micrite envelopes. This lithofacies also includes foraminifers (such as eostaffellids, archaediscids, paleotextularids, unilocular and irregularly coiled bilocular forms etc.), crinoids, gastropods, brachiopods and echinid fragments (Figure 14). In addition to these small coated grains, lumps and dark intraclasts occur in this type of lithofacies. It has sparry calcite cement. This lithofacies occurs in areas of constant wave action at or above wave base (Flügel, 2004).

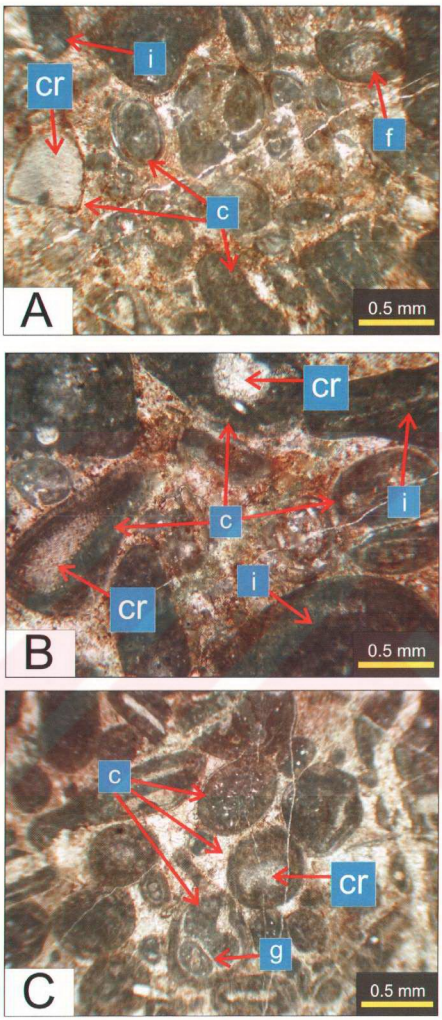


Figure 12. Photomicrographs of coated crinoidal packstone lithofacies, (c: coated grain, cr: crinoid fragment, f: foraminifer, g: gastropod and i: intraclast), (A-B-C: HB04-33).

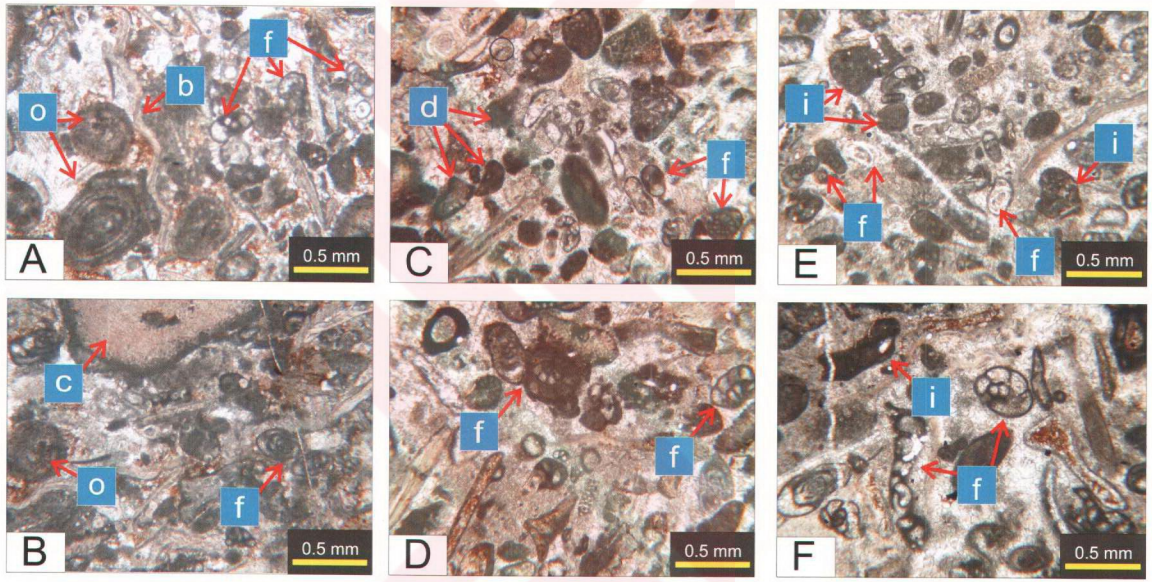


Figure 13. Photomicrographs of bioclastic grainstone with abundant foraminifers lithofacies, (b: brachiopod fragment, c: crinoid fragment, f: foraminifer, i: intraclast and o: oolite) (A-B: HB04-05 and C-D-E-F: HB04-11).

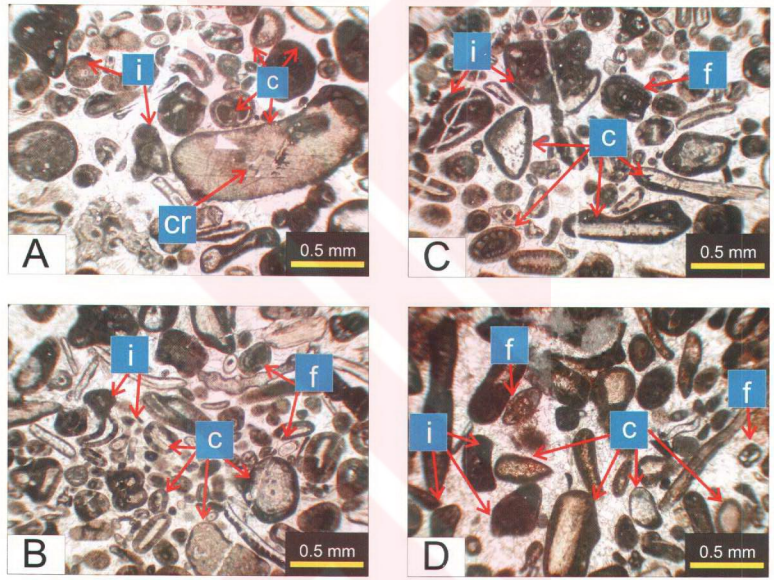


Figure 14. Photomicrographs of coated bioclastic grainstone lithofacies, (c: coated grain, cr: crinoid fragment, f: foraminifer, i: intraclast), (A-B-C: HB04-33 and D: HB04-47).

It forms seaward direction of oolitic grainstone shoals. According to Flügel (2004) and Wilson (1975) facies zonation, this lithofacies corresponds to FZ 6 (Figure 10, 11).

3.2.4. Oolitic grainstone (O1, O2, O3)

This microfacies consists of mainly medium ooids cemented by a sparry calcite (Figure 15). Cement is formed by sparitic calcite. This facies is grouped into three subfacies, namely O1; O2; O3. O1 (Oolitic grainstone with bioclasts) is moderately sorted and includes mainly foraminifers and bioclasts (Figure 15. A-B). It also includes intraclasts, fragmented crinoids and echinids, pellets. A variety of grains serve as nuclei including intraclasts, bioclasts and skeletal fragments, especially foraminifers tests. O2 (oolitic grainstone with lump) is different from the O1 type and is composed of mainly lumps and intraclasts (Figure 15. C-D). O3 (oolitic grainstone with quartz sands) is characterized by abundant, well sorted ooids and quartz grains (Figure 15. E-F). The laminae of the ooid cortices are radially structured or exhibit radial fibrous structures. This type of microfacies corresponds to the SMF 15-R of Flügel (2004). SMF 15 is described as the ooid grainstone and "R" represents the radial microfabric of ooid cortices.

This oolitic grainstone facies is deposited under high energy environments in platform margin sand shoals and platform interior open marine environments. O1 is deposited in sand shoals. The presence of lumps in O2 indicates the shallowing character. It is deposited in the landward of sand shoal, restricted environments. O3 facies mainly occurs in restricted environments of platform interiors. This oolitic grainstone facies is equivalent of FZ 6 and FZ 7 of Wilson (1975) and Flügel (2004) depositional environment models.

3.2.5. Oolitic packstone-grainstone (OPG)

Radial fibrous and concentric ooids are major components of this microfacies. It consists of mainly ooids and lesser amounts of fossils and their fragments. The nuclei are composed of bioclast fragments, foraminifers, echinid

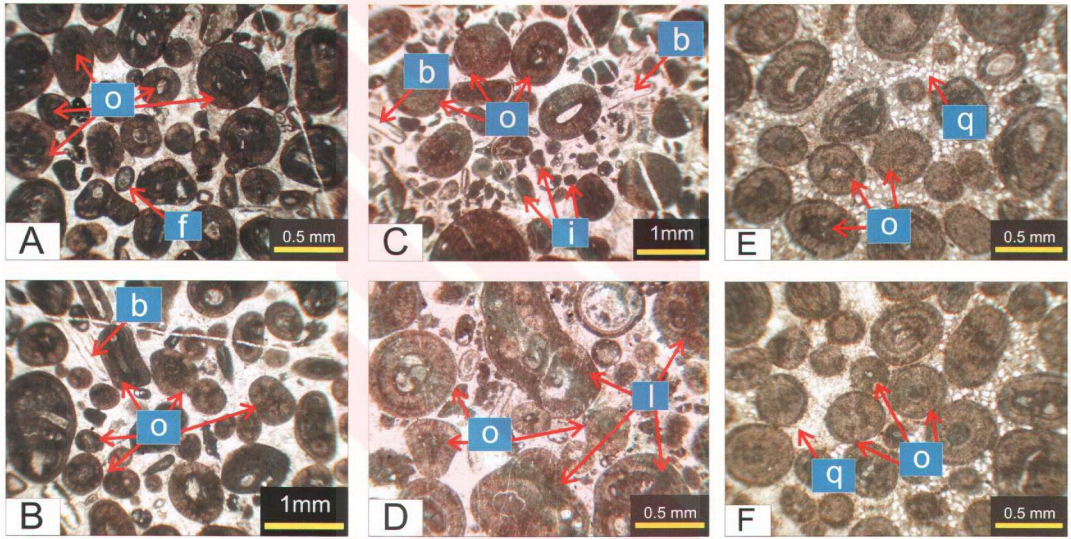


Figure 15. Photomicrographs of oolitic grainstone lithofacies. A-B: oolitic grainstone with bioclasts (O1 type), C-D: oolitic grainstone with lumps and aggregate grains (O2 type), E-F: oolitic grainstone with quartz sands (O3 type), (b: bioclast, f: foraminifer, i: intraclast, l: lump, o: ooid, q: quartz grain) (A-B: HB04-41, C-D: HB04-28, E-F: HB04-20).

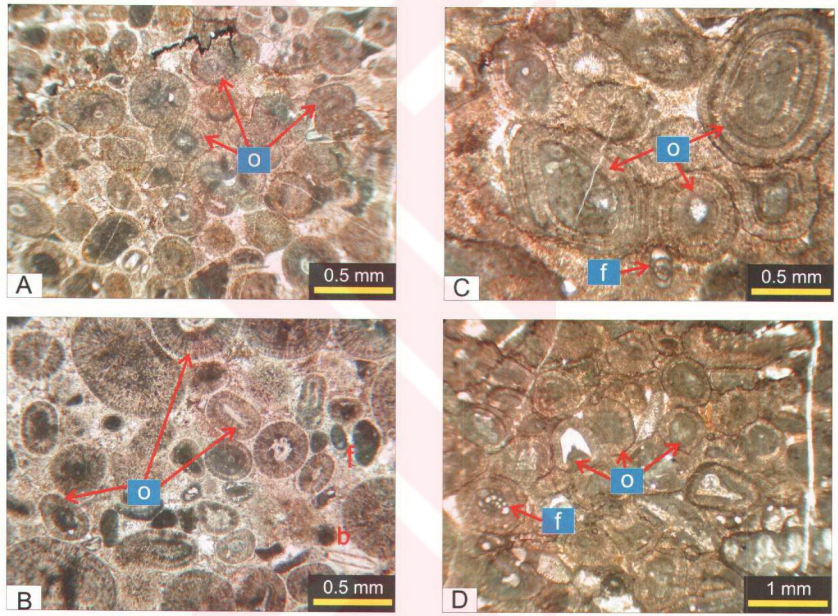


Figure 16. Photomicrographs of oolitic packstone-grainstone (A-B) and oolitic packstone lithofacies (C-D), (b: bioclast, f: foraminifer, o: oolite), (A-B: HB04-21, C-D: HB04-40).

fragments and dark clasts (Figure 16.A-B). This facies is poorly washed. They are linked with sparitic to microsparitic calcite cement and sometimes micrite.

The radial fibrous and poorly washed micritic matrix indicates that this facies may form under low to moderate energy. This facies occurs landward of the shoal. It corresponds to the FZ 7 of Flügel (2004).

3.2.6. Oolitic packstone (OP)

Radial fibrous and concentric ooids are major components of this microfacies. The nuclei are composed of bioclast fragments, foraminifers, echinid fragments and dark clasts (Figure 16. C-D).

The ooids are bounded together with micritic matrix. This indicates that this facies may form under low to moderate energy. This is deposited landward side of the oolitic sand shoal. The presence of lumps also indicates the low to moderate energy depositional environment. It corresponds to the FZ 7 of Flügel (2004).

3.2.7. Aggregate-grain grainstone (AG)

This type of lithofacies is associated with pelloids, intraclasts, coated and micritized grains (skeletal grains). Aggregate grains are composite grains consisting of ooids, skeletal materials bounded together by organic film and dark intraclasts (Figure 17). The skeletal grains are foraminifers, such as paleotextularids, forms with pseudoendothyrids, unilocular forms, biseriamminids and eostaffellids, and echinid fragments (Figure 17). This facies has sparry calcitic cement.

The presence of aggregate grains indicates low to moderate, changing water energy levels. Grainstones predominantly consisting of aggregate grains are characteristic parts of platforms formed during sea level highstand phases (Flügel, 2004). This grainstone lithofacies is equivalent of FZ 7 and FZ 8 of Flügel (2004) defined for open and restricted shallow platforms.

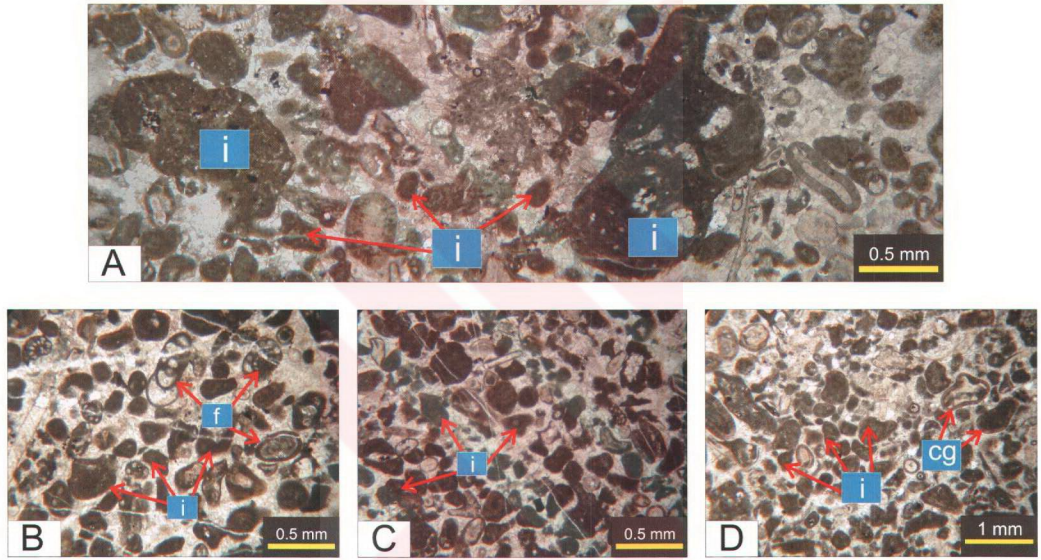


Figure 17. Photomicrographs of aggregate grain grainstone lithofacies (cg: coated grains, i: intraclasts, f: foraminifera), (A: HB04-50; B: HB04-52; C: HB04-51; D: HB04-49).

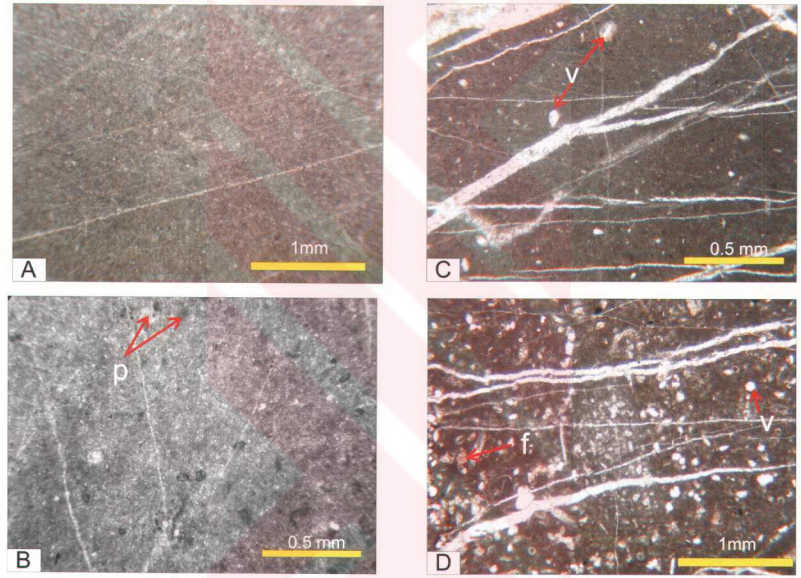


Figure 18. Photomicrographs showing mudstone-wackestone lithofacies (f: fossil fragments, p: pellet, v: vug), (A-B: HB04-03 and C-D: HB04-34).

2.8. Mudstone-wackestone (M)

Massive mudstone and lagoonal wackestone lithofacies are grouped into this facies. The mudstone is characterized by the high abundance of lime mud. It is poorly fossilliferous to unfossilliferous and contains pellets (Figure 18. A, B).

Lagoonal wackestone is composed of mainly micrite (Figure 18. C, D). It contains vugs and few fossils which indicates that this facies is deposited in a lagoonal environment.

This massive lithofacies occurs in low energy, lagoonal setting behind the high energy sand shoals. This microfacies corresponds to SMF 23 (Non-laminated homogenous micrite and microsparite) of Flügel (2004). This micritic facies caps some of the cycles within the measured section. Mudstone-wackestone facies corresponds to FZ 9 of Flügel (2004).

3.2.9. Sandy oolitic grainstone (SO)

This type of microfacies consists mainly of oolites and quartz grains. It also includes lesser amounts of skeletal grains such as foraminifers, bioclasts and crinoids and echinid fragments (Figure 19). Pellets are also found in this facies. The grains are cemented by sparry calcite. The beds characterized by this microfacies type usually overlie the levels characterized by sandy pelloidal packstone facies. The contact between these two facies is gradational.

This facies mainly occur at the base of the bottom cycles which are recognized at the bottom of the measured section. It is equivalent of FZ 10 of Flügel (2004).

3.2.10. Sandy pelloidal packstone (SP)

This type of microfacies is unfossiliferous, very fine grained, and composed of well rounded peloids, fine grained subangular quartz grains and rare ooids and skeletal fragments (Figure 20). It has micritic matrix.

Sandy pelloidal packstone microfacies is probably the equivalent of coastal eolinate quartz-pelloidal lithofacies of Al-Tawil et al. (2003) and Al-Tawil and Read (2003) and is generally devoid of fossils. Al-Tawil et al. (2003) stated that these types of microfacies are interpreted as coastal colinates on the

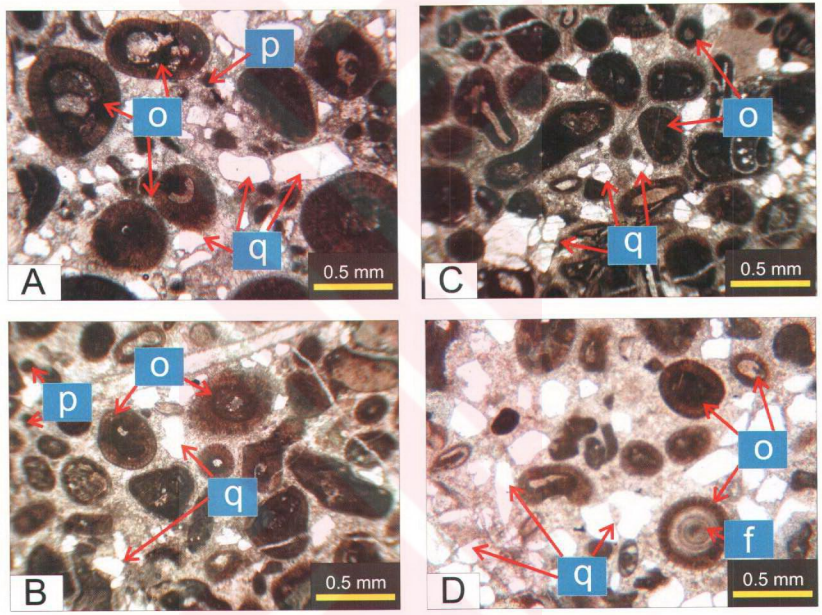


Figure 19. Photomicrographs of sandy oolitic grainstone lithofacies, (f: foraminifer, o: ooid, q: quartz grain, p: pellet), (A: HB04-59; B-C: HB04-63; D: HB04-60).

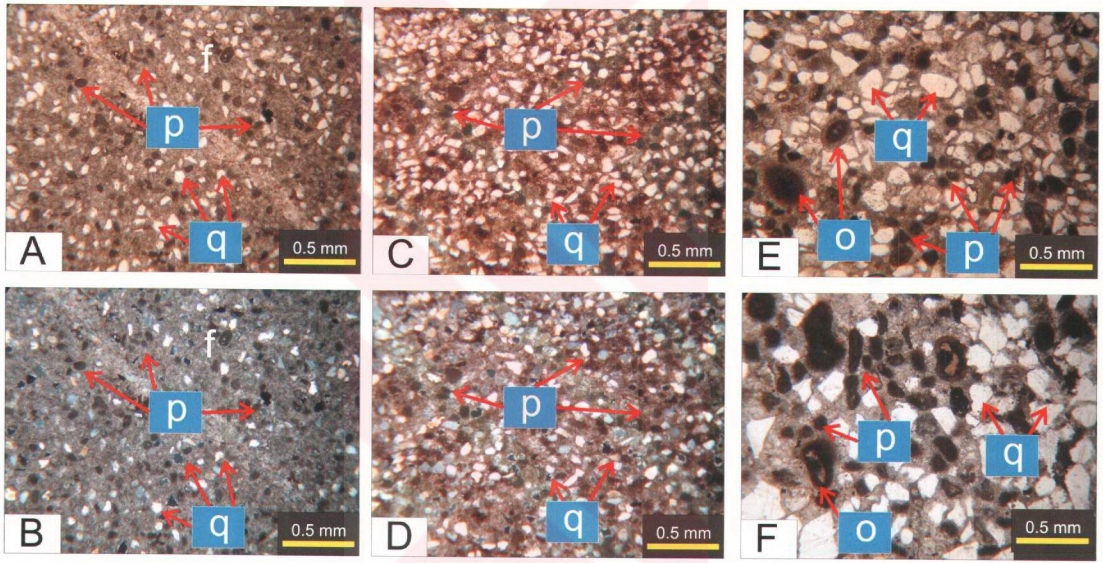


Figure 20. Photomicrographs of sandy pelloidal packstone lithofacies (f: foraminifer, o: ooid, p: pellet, q: quartz grain), (A-B: HB04-62; C-D: HB04-61; E: HB04-60 and F: HB04-53).

basis of abundant quartz and pelloid grains lithology, very fine to fine sand couplets and lack of in-situ fossils. However, these may also occur in shallow marine tidal environments with high sediment influx. It corresponds to FZ 10 of Flügel (2004).

3.2.11. Quartz arenitic sandstone (S)

This microfacies totally consists of very fine sand to silt sized quartz grains. Fossils and other constituents are absent in this type facies. It comprises more than 95 % quartz grains (Figure 21). yellowish coloris characteristic for this facies and display herringbone cross-bedding (Figure 22). The micritic cement is particularly observed between grains.

The herringbone cross-bedding indicates that the quartz arenite was deposited in intertidal or possibly a foreshore environment (Khalifa, 2005). This microfacies deposited during the regressive phase. Cycles mainly at the bottom of the studied section is capped by this facies.

Based on the detailed microfacies analysis, previously published standard microfacies belts of Wilson (1975) and Flügel (2004) and the successive occurrence of microfacies types along the section a depositional model (Figure 23) has been constructed for the Serpukhovian – Bashkirian boundary beds. According to this model, mainly four major depositional belts have been envisaged. These are (1) Continental to clastic shoreline, (2) Restricted lagoonal, (3) Shoal and (4) open marine. In continental to clastic shoreline belt, there is high amount of sediment influx. The quartz arenitic sandstone facies, the sandy pelloidal packstones and sandy oolitic grainstone facies are deposited towards the seaward direction in this belt. The restricted lagoonal belt includes mudstone-wackestone facies. The shoal facies belt includes the aggregate grain grainstone, the oolitic packstone, the oolitic packstone/grainstone, the oolitic grainstones, bioclastic, the coated grain grainstone and the coated crinoidal packstone facies. Although, the open marine facies belt has never been observed in the studied section, the presence of the mud-rich coated crinoidal packstone facies indicates that open marine mudstones should be found in close proximity

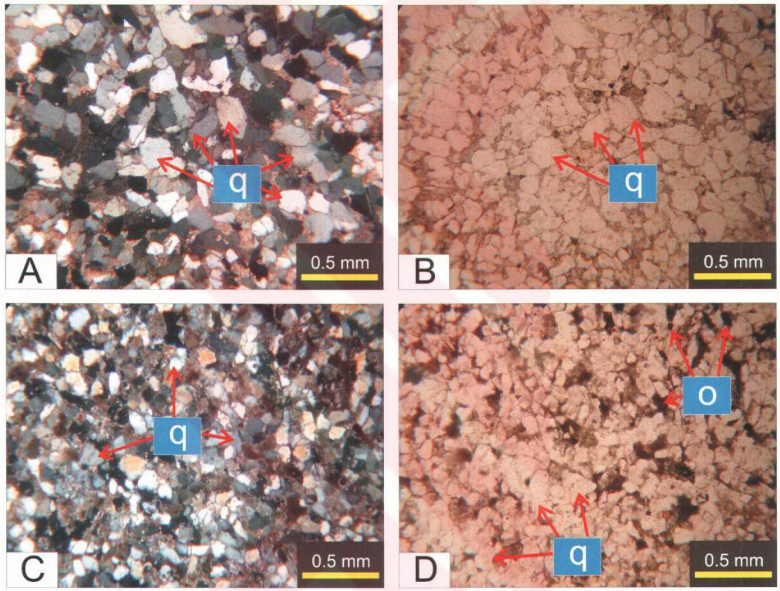


Figure 21. Photomicrographs of the quartz arenitic sandstone lithofacies, o: opaque mineral, q: quartz grain (A, B: HB04-12; C,D: HB04-64).

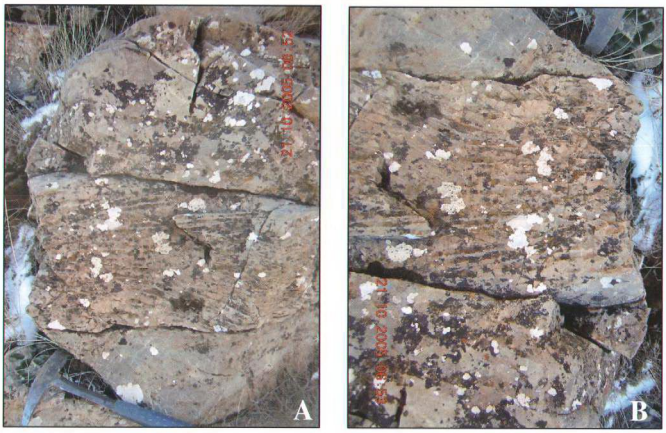


Figure 22. Close-up view of quartz arenite displaying herringbone cross-bedding.

of the shoal belt whose seaward depositional limit is controlled by the wave base (Figure 23).

3.3 Meter-scale shallowing upward cycles (Parasequences)

Parasequences are the building blocks of the sequence stratigraphy. Shallowing upward cycles are named as parasequences. The Parasequence is a relatively conformable succession of bed or bedsets bounded by marine flooding surfaces and their correlative surfaces (Van Wagoner et al., 1988). Shallow marine carbonates are the best indicators of sea level fluctuations since their deposition is dependent on the parameters such as, water depth, energy, and faunal content (Goldhammer et al., 1990). Shallowing-upward meter-scale carbonate cycles (parasequences) tend to be systematically arranged within larger scale successions (parasequence sets). Stacking patterns of the meter-scale cycles can be used to define large scale sequences, systems tracts and long-term relative sea-level fluctuations (Osleger and Read, 1991; Goldhammer et al., 1990).

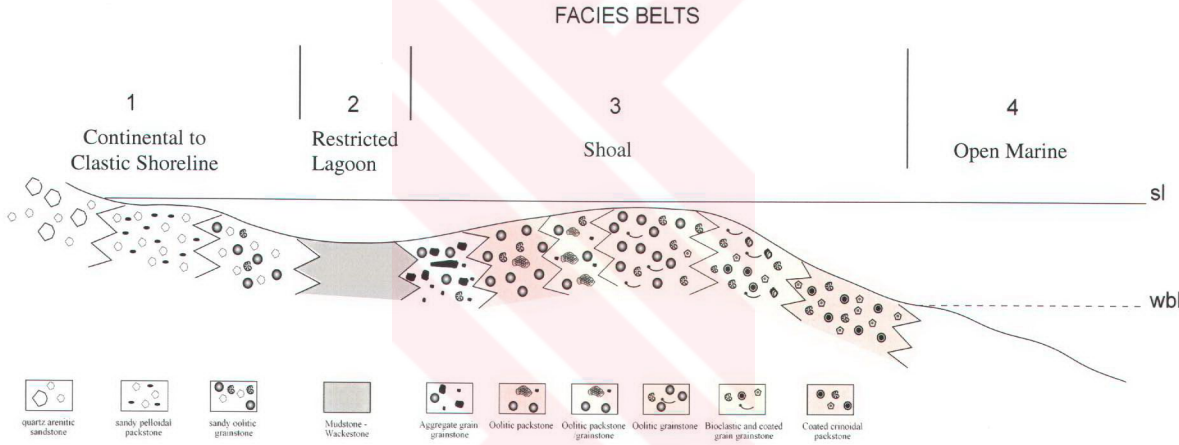


Figure 23. Composite model illustrating the microfacies distribution of Serpukhovian – Bashkirian boundary beds in the studied section.

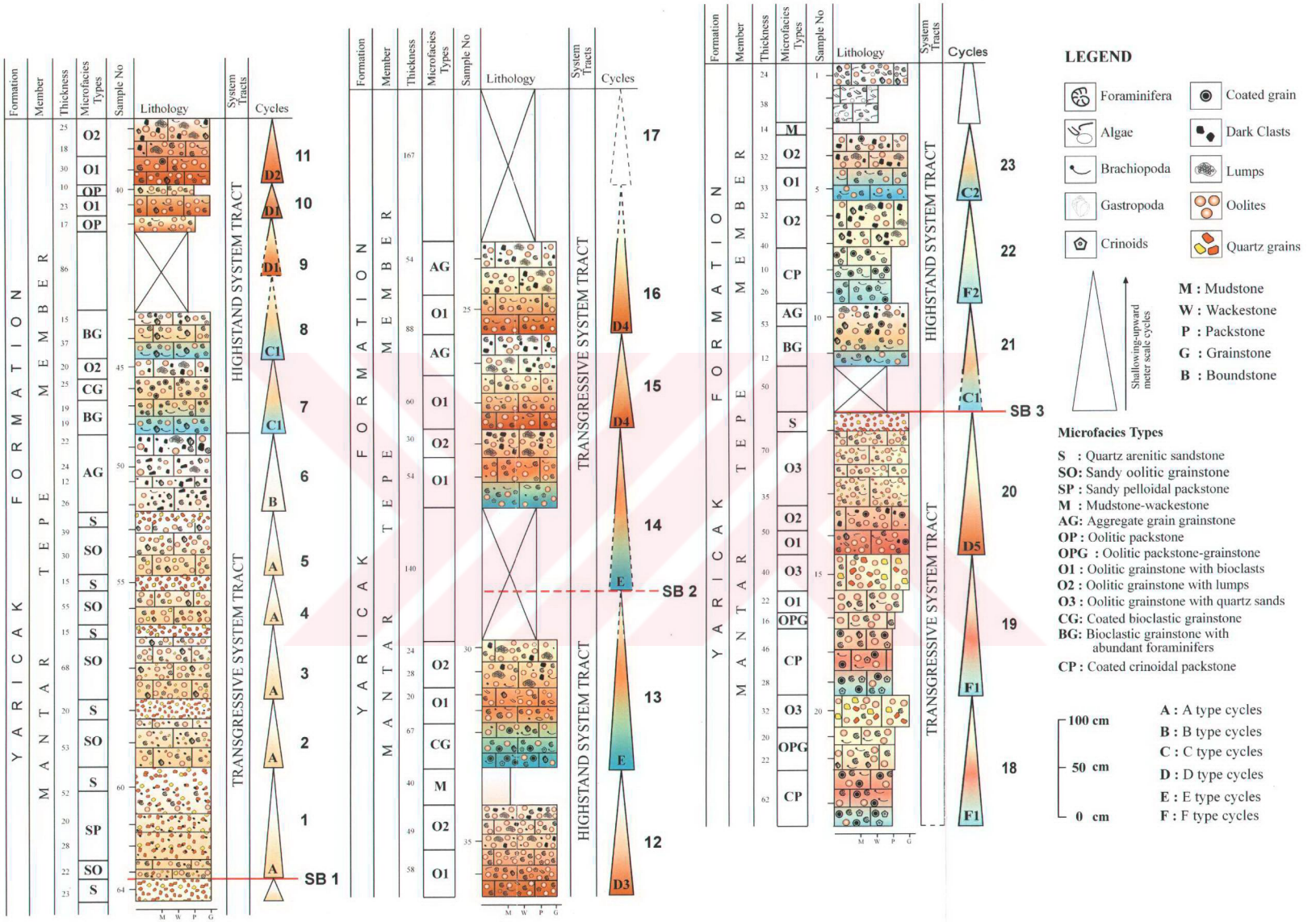


Figure 24. Columnar section of the studied section showing meter scale cycles.

In this study, a section was measured to define the shallowing upward meter-scale cycles across the mid-Carboniferous boundary in the Hadim region. The measured section is 25.64 m thick and contains 23 shallowing upward cycles (Figure 24). Individual cycles range from 33 to 180 cm in thickness. Average thickness of the cycles is about 1,08 m. These cycles are defined by the stacking pattern of microfacies types defined in previous chapter. Different types of cycles are observed in the measured section based on the detailed analysis of microfacies and grouped into six main and ten sub-types cycles. The cycles within the studied section are mainly characterized by high energy deposits.

3.3.1 Types of shallowing upward cycles (Parasequences)

According to the vertical association and faunal content of different microfacies, six main types and ten sub-types are recognized in this study. These are mainly shallow subtidal in character. As previously stated, these cycles are shallowing-upward meter-scale cycles, but the subaerial exposure structures are not seen at the top of the cycles. However, the presence of mud, lumps and quartz grains indicates the shallowing trend. The discrimination of cycles is based on the superimposed subenvironments.

3.3.1.1 A type cycles

A type cycles are characterized by sandy and silty facies with quartz fragments (Figure 25). They are dominant at the lower part of the measured section (Figure 24) and begin with the sandy oolitic grainstone facies containing mainly quartz grains, oolites and some fossils. This facies is followed upward with unfossiliferous sandy pelloidal packstone and finally the cycle is capped by quartz arenitic sandstones.

3.3.1.2 B type cycles

This type of cycle is mainly represented by aggregate grain grainstone facies (Figure 25). The characteristic feature of the cycle is the gradual grain size increase from bottom to top as the indicator of the decrease in the rate of sea-

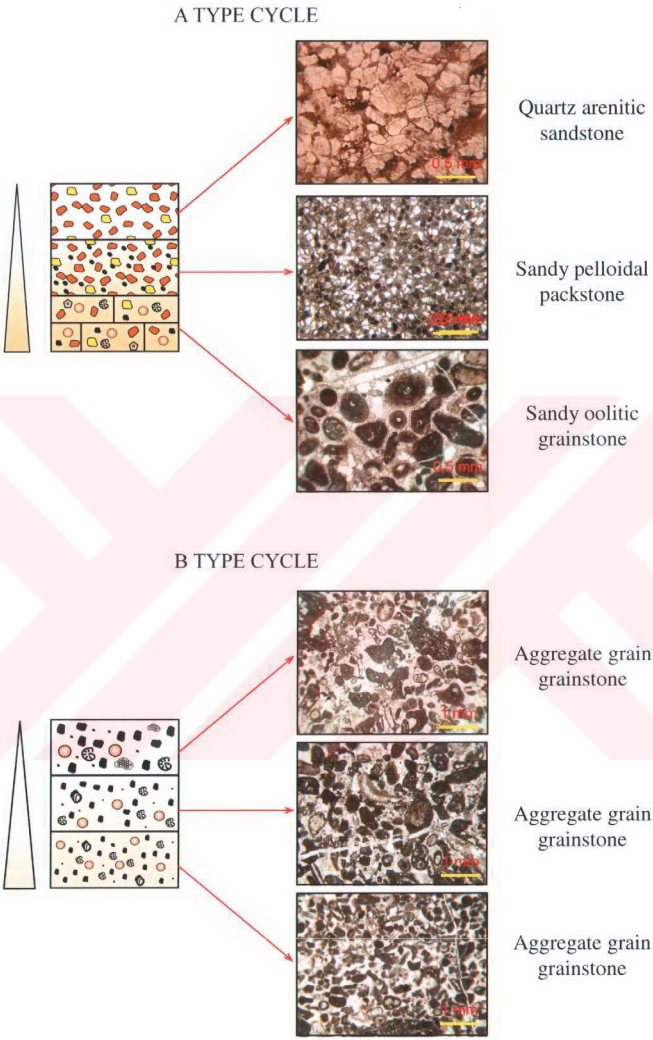


Figure 25. A type cycle (Cycle 2), B type cycle (Cycle 6) and photomicrographs of microfacies deposited within these cycles.

level rise. In the aggregate grain grainstone facies, the grain size of clasts, lumps and biological elements show a marked coarsening at the cycle tops (Figure 25).

3.3.1.3 C type cycles

That C type cycle with bioclastic grainstones starts at its base. Two sub-types have been defined, namely, C1 and C2 (Figure 26). C1 starts with bioclastic grainstones. This facies is followed upwards by the coated grain grainstone facies. The cycle ends with the oolitic grainstone facies with lumps which indicates a shallowing trend (Figure 26-C1). In the C2 cycle, aggregate grain grainstones overlie the bioclastic grainstones and the cycle is capped by lagoonal mudstone facies (Figure 26-C2).

3.3.1.4 D type cycles

This type of cycle is characterized by the dominance of oolitic grainstones. It starts with the oolitic grainstone facies with bioclasts (O1 facies). According to the internal variations, within the cycle D, five sub-types are identified. D1 sub-type starts with oolitic grainstones and is capped by oolitic packstones (Figure 27-D1). However, D2 sub-type is capped with oolitic grainstones with lumps (O2 facies) (Figure 27-D2). This capping facies indicates a shallowing trend since lumps occur in low-moderate energy environments. D3 sub-type is similar to D2 and starts with oolitic grainstones and then is followed by the oolitic packstone/grainstone facies. This cycle ends with lagoonal mudstone-wackestone facies (Figure 28-D3). The marked appearance of lagoonal mudstone-wackestone facies at the top of the cycle indicates the relative sea level fall. Among other types of cycles, D4 type cycle is capped by the aggregate grain grainstone facies (Figure 28-D4). However, in the D5 sub-type cycle, the oolitic grainstone with quartz grains was deposited on top of the oolitic grainstone facies with bioclasts. Finally, quartz arenitic sandstone facies caps this cycle (Figure 29-D5) indicating a very clear shallowing trend leading to subaerial exposure.

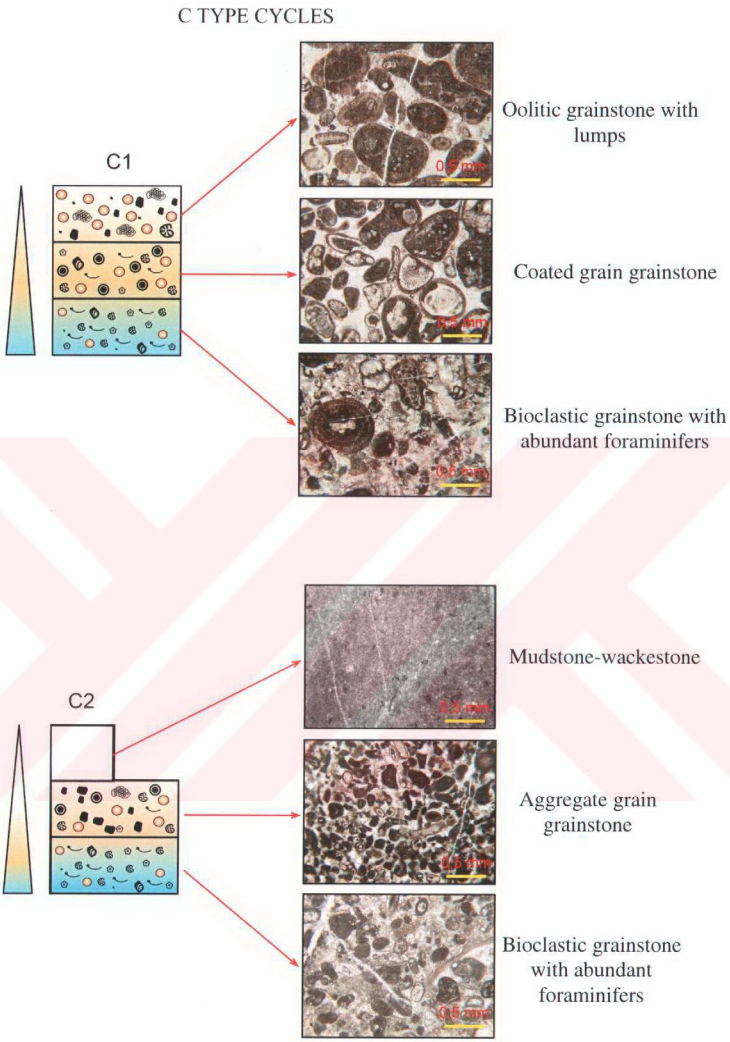


Figure 26. C1 type cycle (Cycle 21); C2 type cycle (Cycle 23) and photomicrographs of microfacies deposited within these cycles.

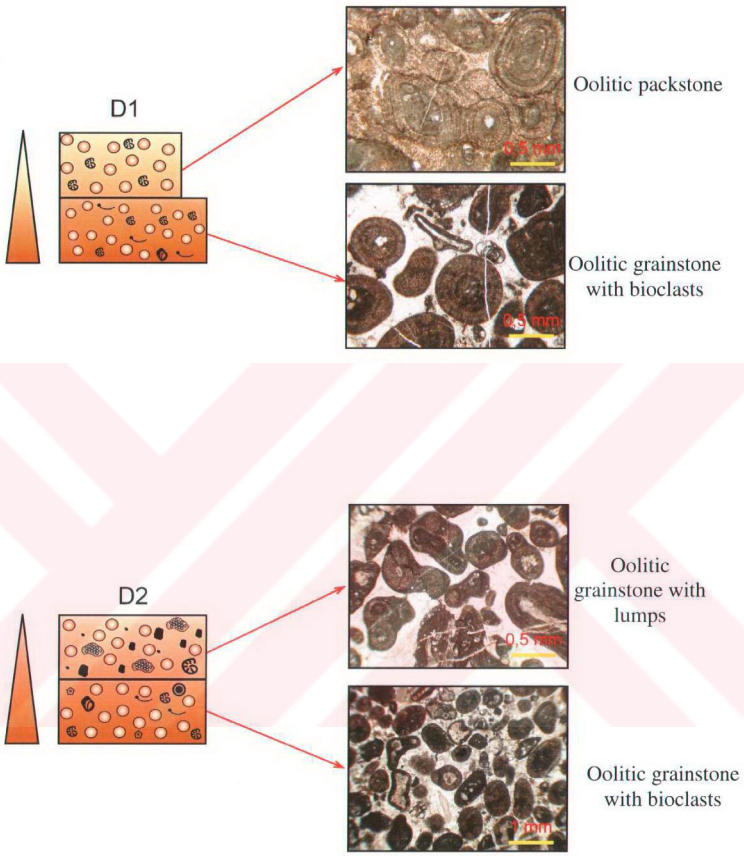


Figure 27. D1 type cycle (Cycle 10); D2 type cycle (Cycle 11) and photomicrographs of microfacies deposited within these cycles.

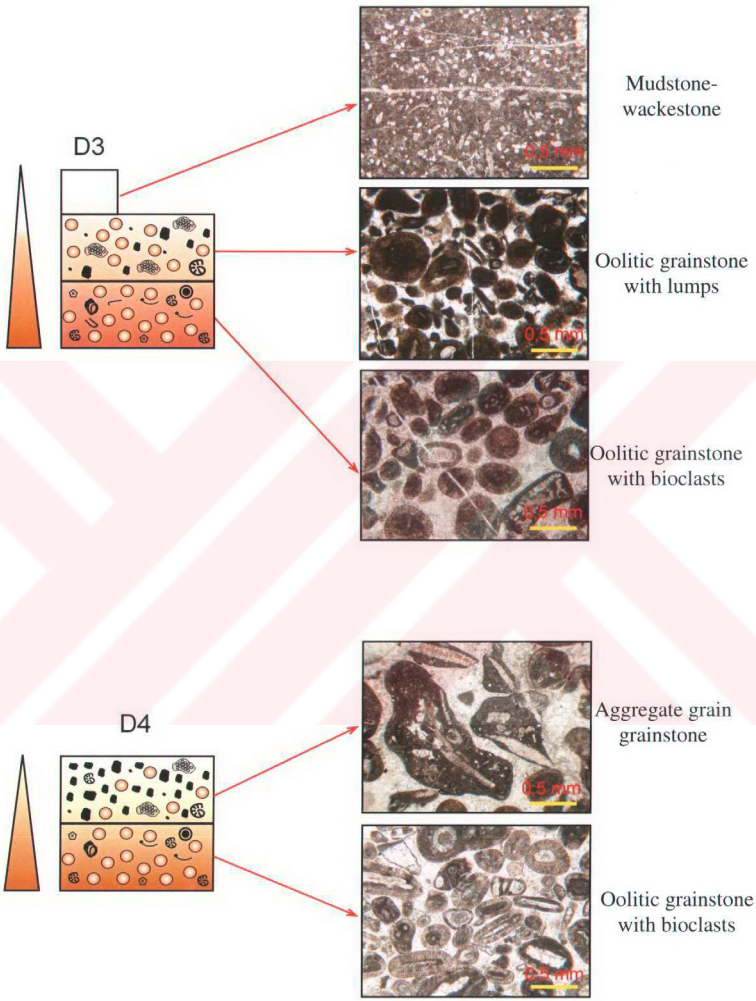


Figure 28. D3 type cycle (Cycle 12) D4 type cycle (Cycle 15) and photomicrographs of microfacies deposited within these cycles.

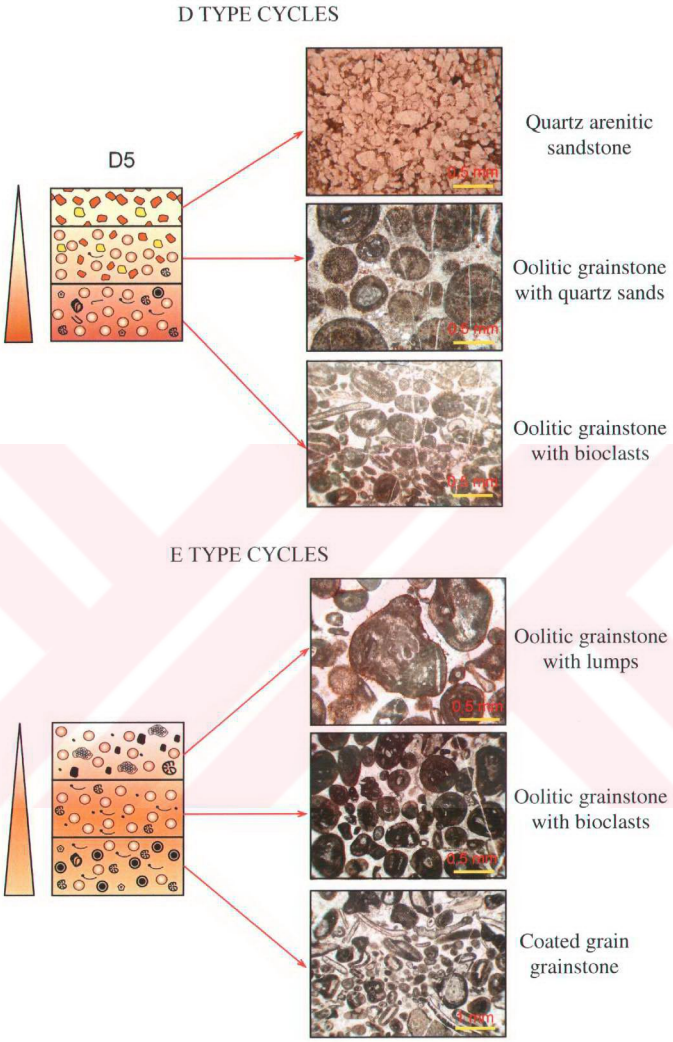


Figure 29. D5 type cycle (Cycle 20); E type cycle (Cycle 13) and photomicrographs of microfacies deposited within these cycles.

3.3.1.5 E type cycles

This cycle type consists of the coated grain grainstone facies at the bottom. Oolitic grainstones with bioclasts follow this facies and the cycle is capped by oolitic grainstones with lumps which show a clear shallowing period (Figure 29-E).

3.3.1.6 F type cycles

F type cycle is mostly characterized by crinoidal coated packstone facies. This type of cycle is composed of two different subcycles (F1 and F2) which start with this facies, however, the capping microfacies of these subcycles are different (Figure 30). Oolitic packstone/grainstone facies follow over the coated crinoidal packstone facies and the cycle is capped by oolitic grainstones with quartz fragments in the F1 cycle (Figure 30-F1). F2 cycle ends with oolitic grainstones with lumps (Figure 30-F2).

3.3.2. Origin and Duration of Cycles

The vertical succession of the microfacies delineates shallowing upward cycles which show the first deepening and then shallowing trends. Vertical stacking patterns analysis is made by the fact that facies, stratal thickness and unconformities in carbonate rocks are systematically grouped within a hierarchy of chronostratigraphic units (Lehrmann and Goldhammer, 1999).

The sedimentary record has stratigraphic cycles of different orders, defined by duration, first order (>100 my), second order (10-100 my), third order (1-10 my), fourth order (0.1-1 my) and fifth order (0.01-0.1 my) (Lehrmann and Goldhammer, 1999; Goldhammer et al., 1993; Goldhammer et al. 1990).

The driving mechanisms of these cycles are primarily eustatic and tectonic events. The first-order cycles relate to plate reorganization (Vail et al., 1977), second-order cycles are driven by tectonics and change in ocean basin volumes (Read, 1995). The mechanism responsible for the third order cycles is not so clear. Third order cycles are probably eustatic in origin and relate to ice volume.

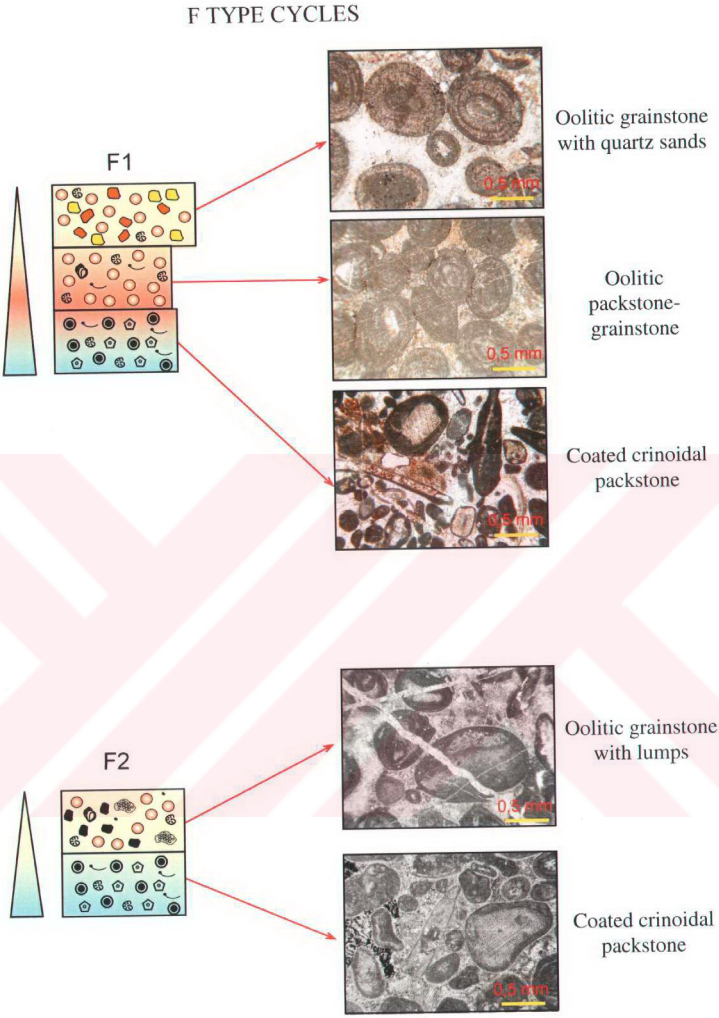


Figure 30. F1 type cycle (Cycle 18); F2 type cycle (Cycle 22) and photomicrographs of microfacies deposited within these cycles.

High frequency, 4th, 5th or higher order, shallowing upward depositional cycles are the building blocks of large scale lower frequency (3rd order) depositional sequences in carbonates. High frequency cycles are climatically driven sea level changes and their amplitude depends on the global ice volume, the records of ocean volume changes, climate, subsidence and compaction (Goldhammer et al., 1990 and Read, 1995).These short periods lie within the range of the Milankovitch frequency band and glacio-eustasy caused by drastic climatic change (Einsele et al., 1991). These higher order cyclic patterns can be identified as Milankovitch cycles. These climatic variations are resulted from cyclic changes in the orbital parameters of the Earth. These orbital parameters are the eccentricity, the obliquity and the precession.

The eccentricity which varies particularly at periods of about 100 ky (more accurately 95 and 105 ky) and approximately 400 ky is caused by eccentricity fluctuations of the Earth's orbit around the Sun (Weedon, 2003). The obliquity is the deviation of the Earth's axis of rotation from a vertical axis on the orbital plane. The precession is the precessional movement of the Earth as a result of gravitational pull of the Sun and expresses a certain relationship between the obliquity and the eccentricity. The obliquity and precession cycles have dominant periodicities of approximately 23 ky and 19 ky for precession and 41ka for obliquity in the Quaternary period. The Carboniferous precession has dominant periodicities about 19.5 ky and 16.6 ky and the amplitude of the obliquity is found to have had a period of 31.1 ky (Collier et al., 1990).

Cyclic sedimentation has been documented for Carboniferous strata worldwide, has been attributed to sea level fluctuations driven by climatic changes (Read, 1995; Ross and Ross, 1987). Glacioeustatic cycles are controlled by the fluctuations in the volume of ice accumulation at the poles in response to climate warming and cooling (Lever, 2004). The higher frequency cycles are caused by the waxing and waning of polar ice-caps (Read, 1995). Icehouse periods are driven by the 100.000 year cyclicity of eccentricity (House, 1995 and Read, 1995). Sea level fluctuations are high during the icehouse times (Read, 1995). Periods with glacial icehouse climatic conditions are characterized by

high amplitudes of relative change in sea level (Rankey, 1999; Veevers and Powel, 1987 and Read, 1995).

Table 5 displays the correlation of glacial periods during Serpukhovian – Bashkirian interval based on different studies. Most of the studies indicates that this interval was under the effect of glacial activity. The shallowing upward meter scale cycles in the studied section might be deposited during the glacial (icehouse) period (Late Serpukhovian – Early Bashkirian) (Table 5). However, these deposits may also be deposited under the interglacial water conditions.

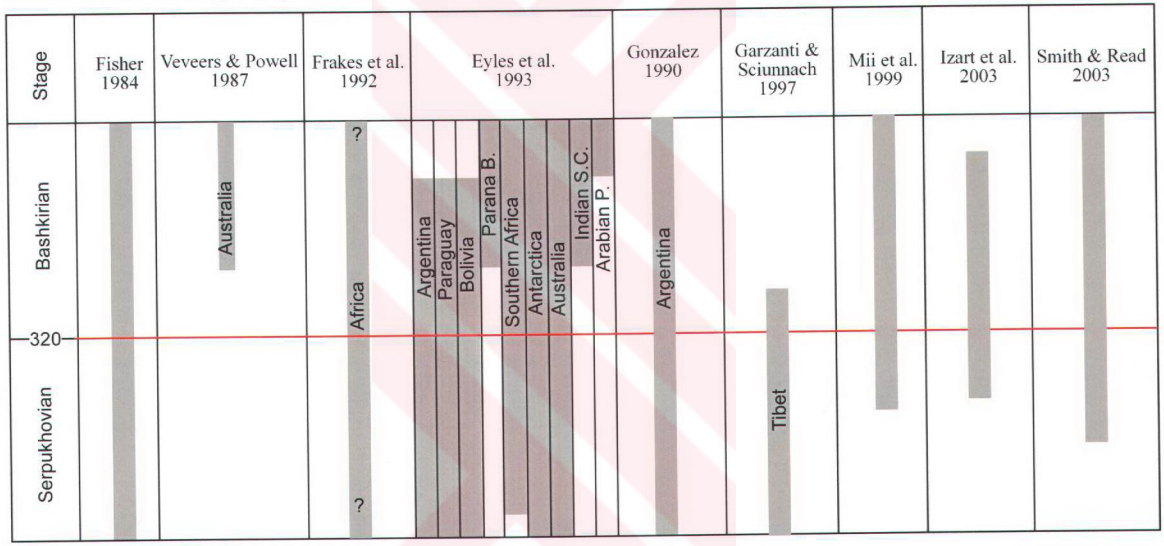
The measured cyclic deposits, in the Hadim region, are correlative with the sequence boundaries of Donets defined by Izart et al. (2003). In the studied section, three sequence boundaries are defined. The first one is at the bottom of the section, the second one is in the middle part and the last one is at the upper part of the measured section. The duration of the studied section is calculated as approximately 2 My based on the cycles in Donets determined by Izart et al. (2003). In this study, 20 shallowing upward cycles (parasequences) are determined within the depositional succession between SB1 and SB3. The average duration of a cycle is approximately 100 ky which corresponds to the Milankovitch eccentricity cycle. During the icehouse, the eccentricity cycles are dominant so the cycles in this study are the eccentricity cycles.

3.4. Sequence stratigraphic interpretation

A sequence stratigraphic interpretation is put forward based on the microfacies associations of shallowing upward cycles (parasequences). Because of the absence of exposure surfaces and erosional boundaries, the vertical evolution of microfacies and the interaction of cycle types within the section is examined to define the system tracts within the measured section. Two main sequences and three sequence boundaries have been identified by the presence of quartz arenitic sandstone facies. A and B type cycles dominated by quartz sand fragments are interpreted as transgressive system tract of the sequence 1 (Figure 24). C and D type cycles which mainly consists of oolitic and bioclastic grainstones are the highstand system tract deposits (Figure 24). D and E type cycles are interpreted as transgressive system tract of the sequence 2. F and D5

type cycles are the following highstand system tract deposits (Figure 24). Above the sequence boundary 3, the highstand deposits of the sequence 3 is defined by the C and F type cycles (Figure 24).

Table 5. Correlation of glacial periods around mid-Carboniferous boundary based on different studies.



CHAPTER IV

RESPONSE OF FORAMINIFERS TO CARBONATE CYCLICITY

4.1. Response of foraminifers to carbonate cyclicity

Microfossil data provide useful tools for studying the response of cycles. The abundance of foraminifera is important criteria in determining shallowing upward cycles. In this thesis, a quantitative study is carried out to determine the biological response, especially of calcareous foraminifera, to carbonate cyclicity in shallow subtidal carbonate deposits. The measured section consisting mainly of limestone contains various types of fossils, such as fusulinids, smaller foraminifers, echinids, crinoids, gastropods, brachiopods. The predominant forms are calcareous foraminifera in the facies and therefore, mainly calcareous foraminifera were used for this study. In order to test the response of foraminifers to cyclicity within the studied succession, a number of counting experiment has been carried out with point counter. In general, the abundance of foraminifera increases in bioclastic and coated-grain grainstone facies which occur at the bottom of cycles and decreases in sandy oolitic grainstone and sandstone facies which mainly caps the cycles.

The main calcareous foraminifera groups used in the point counting are archaediscids, eostaffellids, irregularly coiled bilocular forms, unilocular forms, endothyrids, pseudoendothyrids, paleotextularids and biseriamminids (Appendix B). Their detail descriptions will be given in the systematic paleontology chapter.

4.1.1. General descriptions of the counted forms

1. Archaediscids: They have a proloculus and a single undivided chamber that coils from completely skew to completely planispiral. The interior of the second chamber, the lumen, varies from closed to open. The two-layered wall is composed of typically thicker, light colored, hyaline layer and an inner thin, dark microgranular zone which is nearly absent in some genera. The counted genera

of this group are *Archaediscus*, *Paraarchaediscus*, *Neoarchaediscus* and *Asteroarchaediscus*.

2. Eostaffellids: They are characterized by a dark microgranular wall. The test is small, discoidal and has a rounded and subangular periphery. They are generally planispiral, but some forms show shifts in coiling direction. It includes both evolute and involute forms. The genera are *Eostaffella*, *Millerella*, *Mediocris, Plectostaffella* and *Semistaffella*.

3. Irregularly coiled bilocular forms: They consist of a spherical proloculus followed by a glom spirally coiled undivided second chamber. The second chamber is streptospirally coiled. Irregularly coiled bilocular forms include two main forms. One, which is represented by *Pseudoglomospira,* is composed of a thin, dark, microgranular wall. The other one, *Paleonubecularia,* has a coarsely agglutinated wall.

4. Unilocular forms: These forms are characterized by small, unilocular to bilocular tests. The shape of the test is globular, spherical, subspherical or slightly irregular. These unilocular to bilocular specimens consist of parathuramminacean foraminifers.

Two major genera belonging to this group of forms are *Tuberitina* and *Diplosphaerina.* The former has a dark, coarsely perforate microgranular calcite wall and the second genus is composed of dark microgranular calcite, thin imperforate or very finally perforate wall. In addition to these, there are also other unidentified parathuramminacean foraminifers.

5. Paleotextularids: These forms are characterized by uncoiled, biserially arranged chambers. The wall is composed of outer, dark microgranular layer and inner, yellowish, pseudofibrous layer. Some forms have single aperture, *Paleotextularia* and some have cribrate aperture, *Cribrostomum.*

6. Endothyrids: These forms have thin, undifferentiated, homogenous, dark microgranular calcite wall. Some of the forms in this category have secondary deposits which include thickenings on the anterior side at the join, basal deposits such as, spines and various shape projections, and continous ridges parallel to septa. These forms include genera *Endothyra* and *Planoendothyra*. *Planoendothyra* is distinguished from *Endothyra* by coiling pattern, the latter of

which is typically more or less involute and skew coiled throughout. However, *Planoendothyra* has involute, highly skewed initial and planispiral, evolute outer volutions.

7. Biseriamminids: These forms are characterized by a biserially-coiled chamber arrangement. Coiling is planispiral or trochospiral and involute. These forms include *Globivalvulina* and *Biseriella*. *Biseriella* differs from *Globivalvulina* in its undifferentiated, microgranular wall. The latter one has a wall consisting of a central light layer bracketed by darker, microgranular layers.

8. Pseudoendothyrids: Forms in this group is characterized by a recrystallized wall. The coiling is similar to *Eostaffella*. However, it differs from *Eostaffella* in its recrystallized diaphanotheca. The included genus is *Pseudoendothyra*.

4.1.2. Interpretation of response of calcareous foraminifers

Within the studied section, foraminiferal assemblages are diverse. The abundance of foraminifera displays a good response to sedimentary cyclicity. The total abundance of counted foraminifera points out the deepening and shallowing responses in the studied section (Figure 31-39).

In most of the cycles, the total abundance of counted forms displays good response to cyclicity (Figure 31). In A type parasequences, which are mainly characterized by quartz sand fragments, the total abundance decreases towards the upper part of the cycle (see cycle 1-5, Figure 31). In B type parasequences (see cycle 6, Figure 31), there are some variations within the parasequence but the total abundance is less at the top of the parasequence. The total abundance in C1 cycles exhibits variations and there is no clear response because this facies mainly consists of oolitic grainstones characterized by similar foraminiferal abundance within the cycle. In these cycles, the presence of lumps and intraclasts indicate the shallowing trend. On the other hand, C2 cycles (see cycle 23, Figure 31) capped by the mudstone-wackestone facies, point out a significant decrease in foraminiferal abundance. All subtypes of D type cycle give good response to sedimentary cyclicity. In these subtypes, D4 cycle type displays reverse relationship that means the bottom of the cycle mostly consists of less calcareous foraminifera however the top contains abundant calcareous foraminifera (see

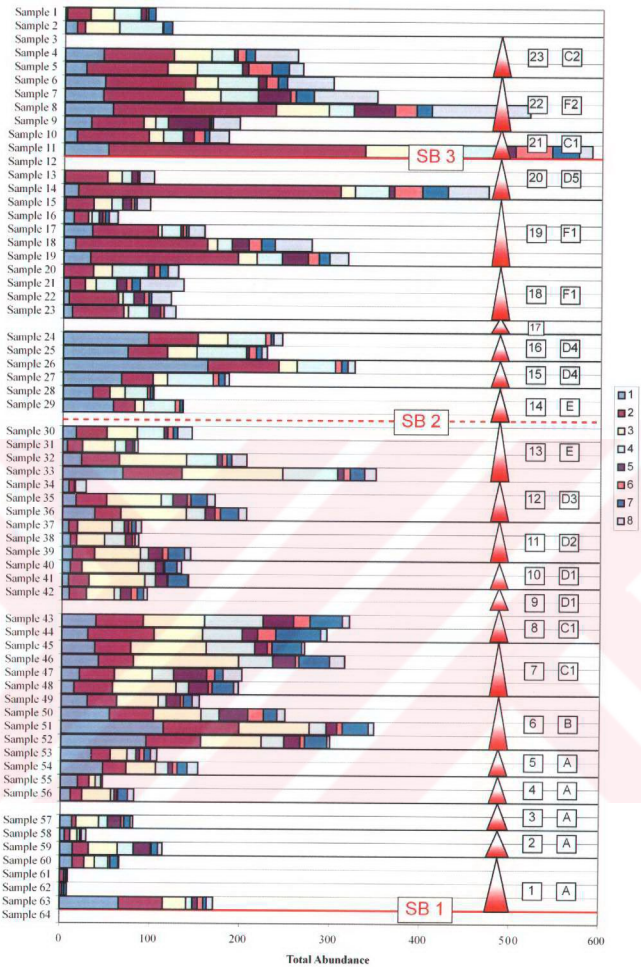


Figure 31. Point counting results of total abundance for determining the response of foraminifers to cyclicity (1: archaediscids, 2: eostaffellids, 3: irregularly coiled bilocular forms, 4: unilocular forms, 5: paleotextularids, 6: endothyrids, 7: biseriamminids, 8: pseudoendothyrids).

cycle 15, 16, Figure 31). The foramiferal responses are not significant in E and F type cycles (see cycle 13, 14, 18, 22, Figure 31).

The responses of archaediscids (Figure 32) and eostaffellids (Figure 33) are similar to those of the total abundance of foraminifera (Figure 31). These forms display good reponses to sedimentary cyclicity in A, B and E type cycles and D2, D3, D5 and F2 subtypes (see cycle 1-5, 7, 11, 12, 13, 22, Figure 32 and Figure 33). However, the faunal variations within the C1 and F1 type cycles (see cycle 7, 18, 19, Figure 32 and Figure 33) are not significant. As observed in the variations of the total abundance of foraminifera, the abundance of these forms point out reverse responses in D4 cycles (see cycle 15, 16 Figure 32 and Figure 33).

The responses of unilocular forms, paleotextularids, irregularly coiled forms, and biseriamminids are similar to each other. In A type cycles, the bottom mostly consists of abundant foraminifera and the top contains less abundant foraminifera (see cycle 1-5, Figure 34-37). There are some varitions in B, C, D and E type cycles (see cycle 6, 7, 18, Figure 34-37). Unlike the other faunal groups, the abundance of unilocular forms decrases toward the upper part of D4 cycles (see cycle 15, 16, Figure 34). In F2 cycles, the case is different, the abundance of the paleotextularids and irregularly coiled bilocular forms decreases (see cycle 22, Figure 35, 36), as the abundance of the unilocular forms and biseriamminids increases towards the upper part (see cycle 22, Figure 34, 37).

However, pseudoendothyrids (Figure 38) and endothyrids (Figure 39) do not give any remarkable response since they do not display any significant changes in abundance.

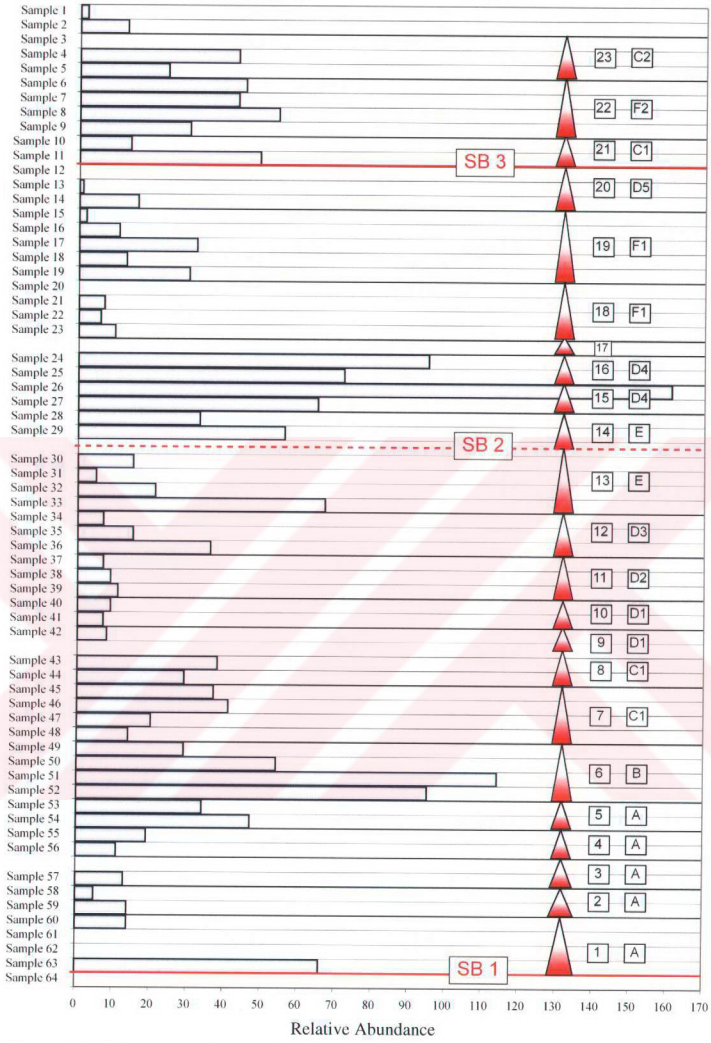


Figure 32. Point counting results of archaediscids for determining the response of foraminifers to cyclicity.

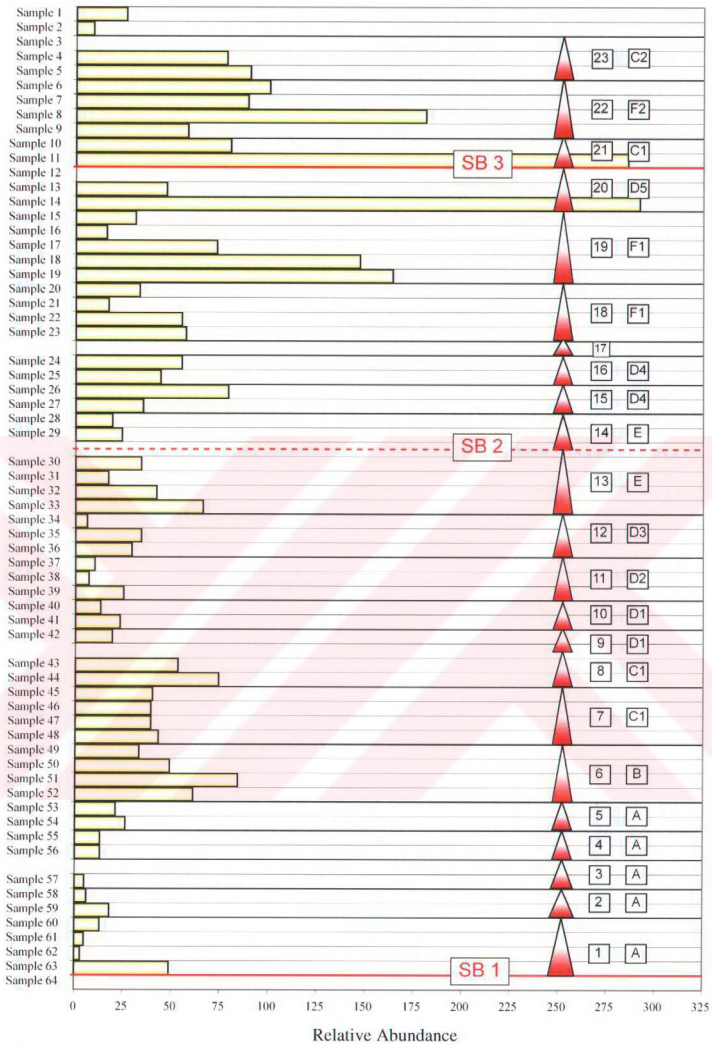


Figure 33. Point counting results of eostaffellids for determining the response of foraminifers to cyclicity.

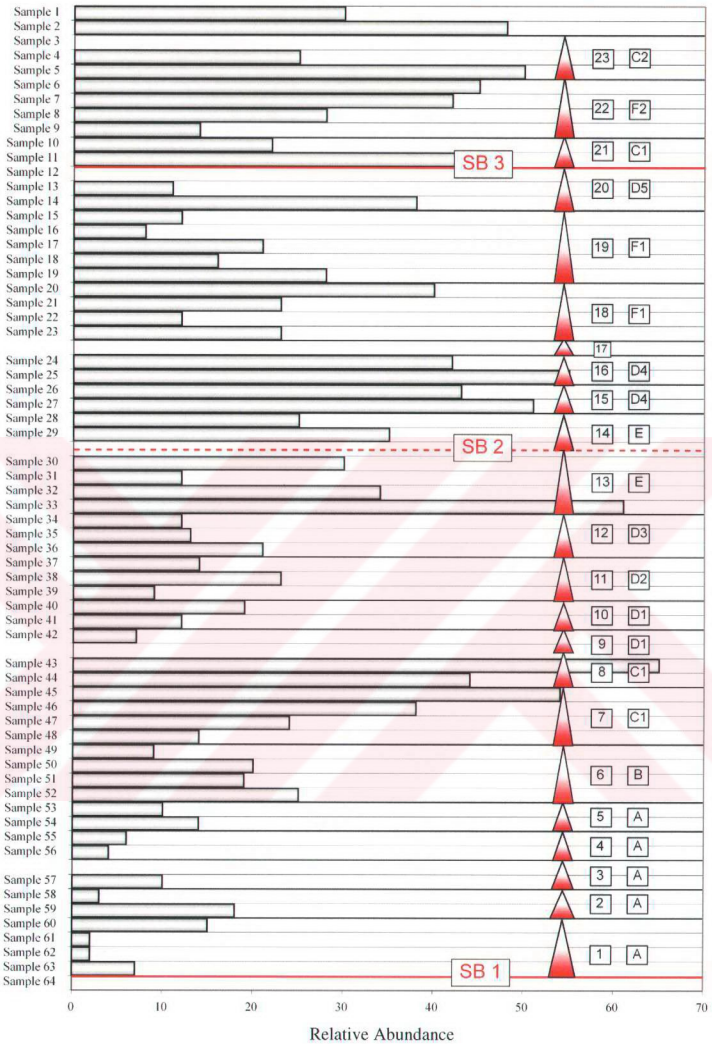


Figure 34. Point counting results of unilocular forms for determining the response of foraminifers to cyclicity.

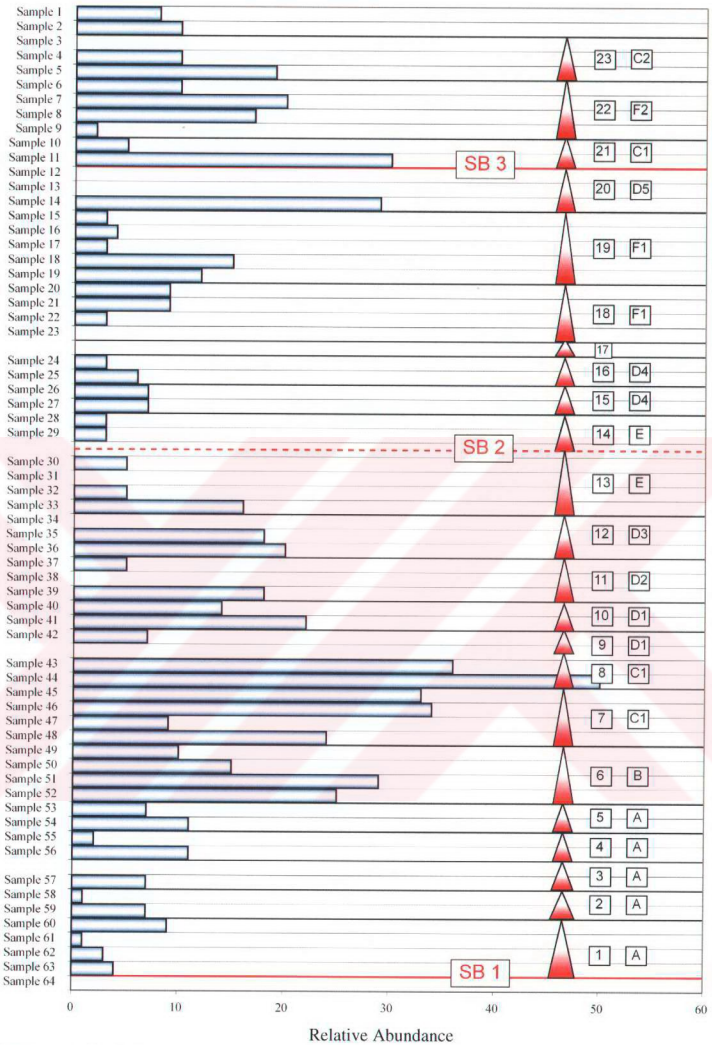


Figure 35. Point counting results of paleotextularids for determining the response of foraminifers to cyclicity.

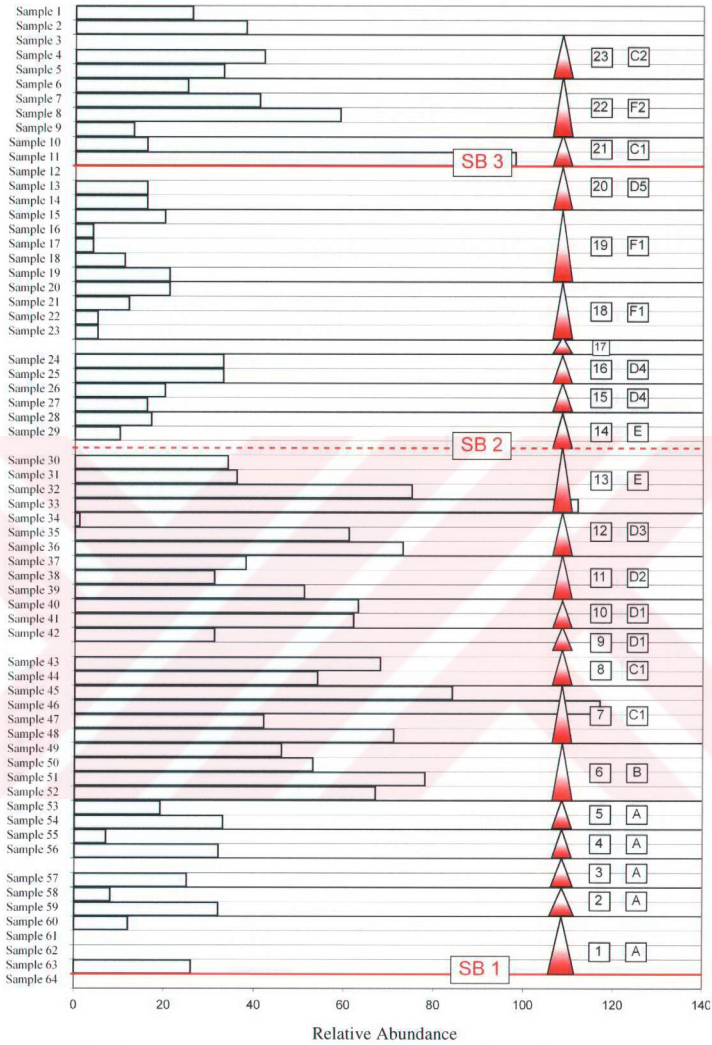


Figure 36. Point counting results of irregularly coiled bilocular forms for determining the response of foraminifers to cyclicity.

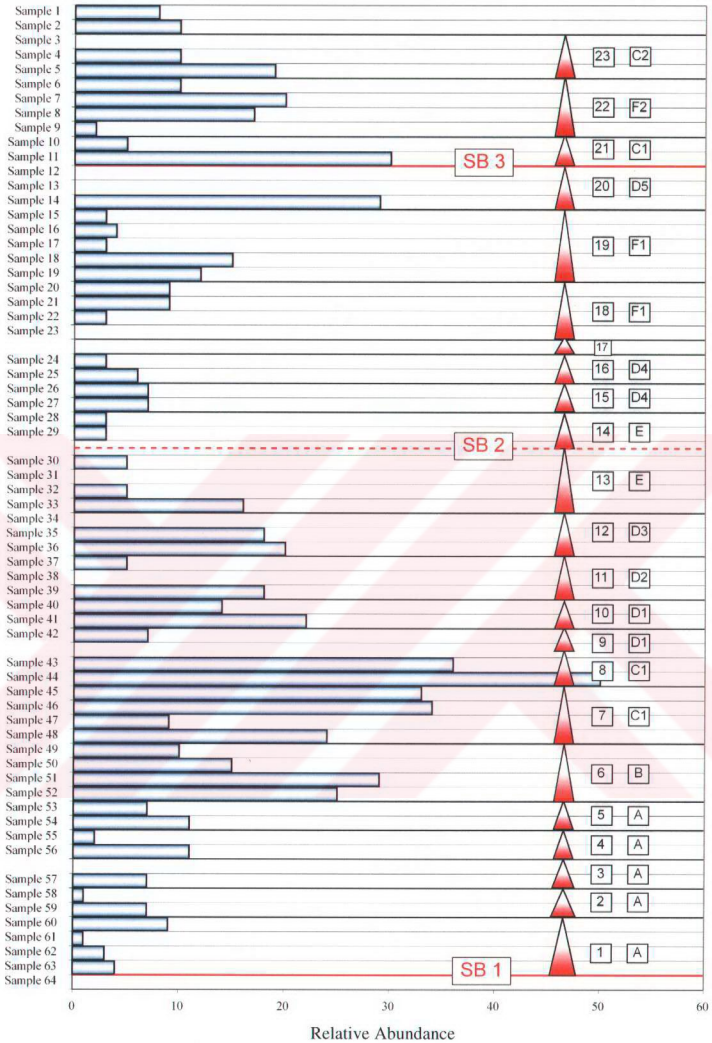


Figure 37. Point counting results of biseriamminids for determining the response of foraminifers to cyclicity.

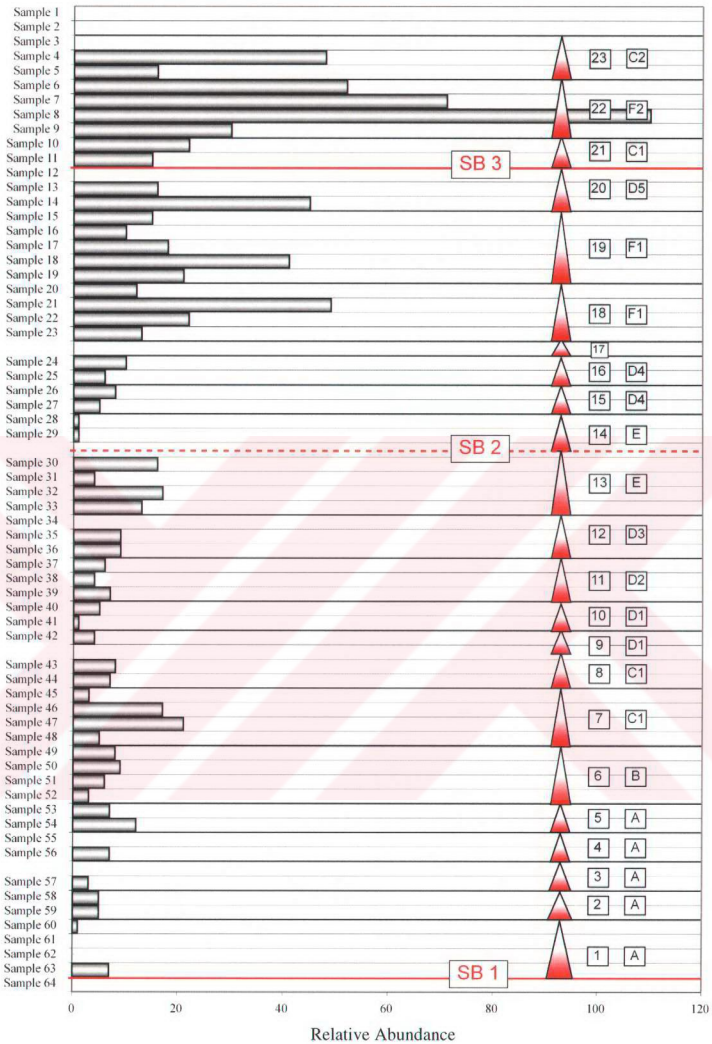


Figure 38. Point counting results of pseudoendothyrids for determining the response of foraminifers to cyclicity.

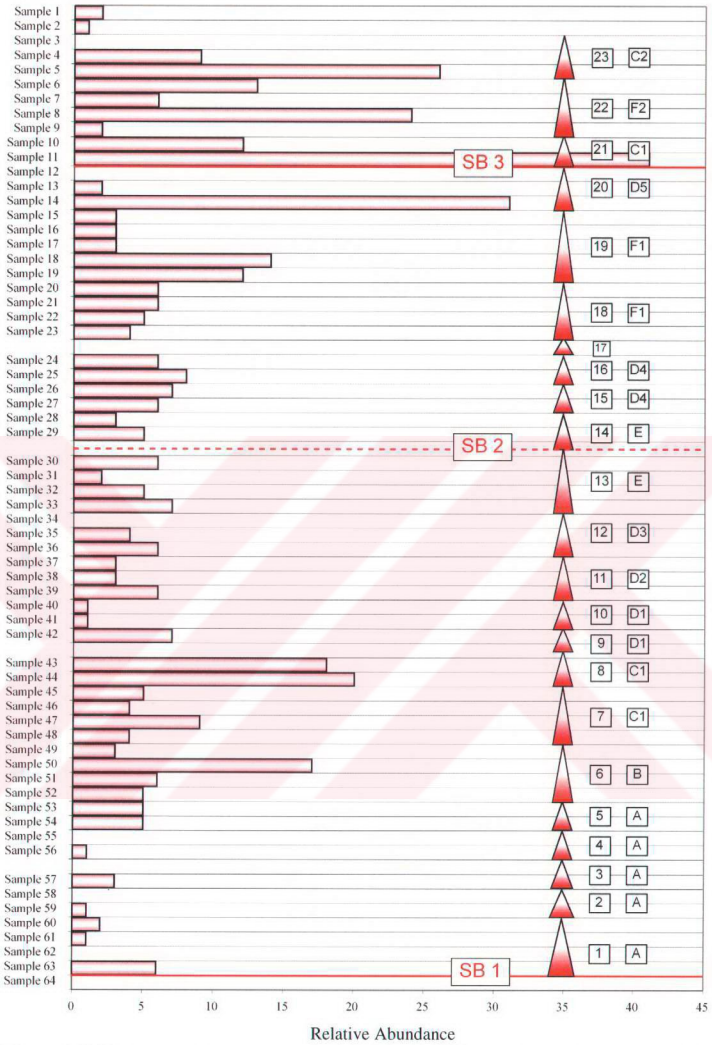


Figure 39. Point counting results of endothyrids for determining the response of foraminifers to cyclicity.

CHAPTER V

SYSTEMATIC PALEONTOLOGY

A systematic micropaleontological study was carried out on calcareous foraminifera from systematically collected samples along the measured section. Identifications were based entirely on thin sections. Important taxonomic parameters in the identification of foraminifers include wall structure, manner of coiling, the diameter or length, width, number of volutions, number of chambers per volution, peripheral shape and secondary deposits.

Loeblich and Tappan (1988) is used mainly for the suprageneric and generic classifications. In addition, for Archaediscids Brenckle's classification (Brenckle and Marchant, 1987) are followed. It should be noted that the taxonomical study given in this chapter are brief descriptions of available taxa rather than detailed definitions with complete synonym lists. The main aim in this chapter is to show that this study was carried out with an objective taxonomic criteria within a well constructed taxonomic frame.

SUPERFAMILY PARATHURAMMINACEA BYKOVA, 1955

Family Archaesphaeridae Malakhova, 1956

Genus *Diplosphearina* Derville, 1952

Type species: *Diplosphaerina inequalis* Derville, 1931

Diplosphaerina inequalis Derville, 1931

Pl. I, figs. 1-4

1931. *Diplosphaerina inequalis* Derville; pl. 18, figs. 77-80.

1969. *Neotuberitina maljavkini (*Mikhailov) var *grandis* Reitlinger; Manukalova-Grebeniuk et al., pt.1: pl. 1, fig. 14; pt3: pl.1 fig. 17; pl.17, fig. 29

1973. *Eotuberitina reitlingerae* Miklukho-Maklai; Brenckle, pl. 2, figs. 4, 5

1980. *Diplosphaerina inequalis* Derville; Rich, pl. 1, figs. 7, 9-15, 18; pl. 4, figs. 4, ,7-9

1983. *Diplosphaerina inequalis* Derville; Groves, pl. 1, figs. 2-4

1995. *Diplosphaerina inequalis* Derville; Altıner and Savini, pl. 4, figs. 4-5

Description:

Test is minute, free or attached and consisting of one or two chambers. Chambers range from spherical to crescent and hemispherical. Wall is dark, microgranular calcite, imperforate or finely perforate.

Dimensions (mm):

Height : 0,150 – 0,237

Basal Diameter: 0,310 – 0,440

Thickness of wall: 7 – 8 μm

Stratigraphic Distribution:

Specimens were recovered from Upper Serpukhovian and Lower Bashkirian.

Family Tuberitinidae Miklukho-Makloy, 1958

Genus *Tuberitina* Galloway and Harlton, 1928

Type species: *Tuberitina bulbacea* Galloway and Harlton, 1928

Tuberitina sp.

Pl. I, figs. 5-7

Description:

Chambers are hemispherical. Wall is dark, microgranular calcite which is coarsely perforate. *Tuberitina* differs from *Diplosphaearina* in its thicker, coarsely perforate wall.

Dimensions (mm):

Height: 0,111 – 0,177

Basal Diameter: 0,133 – 0,200

Thickness of wall: 11 – 12 μm

Stratigraphic Distribution:

Specimens were recovered from Upper Serpukhovian and Lower Bashkirian.

Family Pseudoammodiscidae

Genus *Pseudoglomospira* Bykova, 1955

Type species: *Pseudoglomospira devonica,* Bykova, 1955

Pseudoglomospira subquadrata Potievskaya and Vakerchuk in Brazhnikova et al., 1967

Pl. I, figs. 13-17; Pl. II, figs. 1-4

1967. *Glomospira subquadrata* Potievskaya and Vakerchuk in Brazhnikova et al., p. 139-140, pl. 19, fig. 5; pl. 20, fig. 1; pl. 51, figs. 4-6

1968. *Glomospira* sp.; Aisenverg et al., pl. 7, figs. 21-23

1981. *Pseudoglomospira subquadrata* Potievskaya; Altıner, pl. 2, figs. 32-33.

1983. *Pseudoglomospira subquadrata* Potievskaya; Aisenverg et al., pl. 1, figs. 23-27

1991. *Hemigordiellina subquadrata* Potievskaya; Vachard and Beckary, pl. 4, figs.26, 27

1992. *Pseudoglomospira* spp., Groves, pl. 1, figs. 1-7

1995. *Pseudoglomospira subquadrata* Potievskaya; Altıner and Savini, pl. 4, figs. 32-33

Description:

Coiling is streptospiral defining a square shaped form. The height of the second chamber increases very slowly. The number of the turns is four to five.

Dimension (mm):

Diameter : 0,15 – 0,17

Thickness of wall: 6 – 11 μm

Remarks:

This species is different from other *Pseudoglomospira* species in having a square-like appearance.

Stratigraphic Distribution:

The stratigraphic range is from Visean, Serpukhovian to Bashkirian (Vachard and Beckary, 1996). Specimens were recovered from Upper Serpukhovian to Lower Bashkirian.

Pseudoglomospira sp. A

Pl. II, figs. 5,6

Description:

It consists of a spherical proloculus followed by a glomosprially coiled non-septate second tubular chamber. Wall is dark microgranular.

Dimensions (mm):

Diameter : 0,27 – 0,30

Thickness of wall: 9 μm

Remarks:

This species has large dimensions. This form differs from *P. subquadrata* in having larger dimensions and a much irregular shape.

Stratigraphic Distribution:

Specimens were recovered from Upper Serpukhovian to Lower Bashkirian.

Pseudoglomospira sp. B

Pl. II, figs. 7,8

Description:

It has small circular proloculus. Proloculus is followed by non septate tubular second chamber which coils streptospirally initially and later coils planispirally. Wall is thin microgranular.

Dimensions (mm):

Diameter : 0,15 – 0,20

Thickness of wall: 6 μm

Remarks:

It differs from *Pseudoglomospira* sp. A in having smaller dimensions of the test.

Stratigraphic Distribution:

Specimens were recovered from Upper Serpukhovian to Lower Bashkirian.

Genus *Paleonubecularia* Reitlinger, 1950

Type Species: *Paleonubecularia fluxa,* Reitlinger 1950

Paleonubecularia sp.

Pl. II, figs. 9-11

Description:

Test is typically encrusting. It consists of glomospirally to meandering coiled undivided second tubular chamber. Wall is calcareous, agglutinated with large adventitious grains.

Dimension (mm):

Thickness of wall: 16 – 32 μm

Stratigraphic Distribution:

Specimens were recovered from Upper Serpukhovian through Lower Bashkirian.

SUPERFAMILY ARCHAEDISCACEA Cushman, 1928

Family Archaediscidae Cushman, 1928

Subfamily Archaediscinae, Cushman, 1928

Genus *Archaediscus* Brady, 1873

Type species: *Archaediscus karreri* Brady, 1873

Archaediscus postmoelleri Potievskaya, 1958

Pl. III, figs. 1-3

1958. *Archaediscus postmoelleri* Potievskaya, pl. 3, fig. 2, 3

1969. *Archaediscus postmoelleri* Potievskaya; Manukalova-Grebeniuk et al., pl. 27, fig.2

1968. *Archaediscus postmoelleri* Potievskaya; Aisenverg et al., pl. 24, fig. 1,2

Description:

Test is discoidal. Coiling is initially streptospiral and later becomes oscillatory planispiral. The periphery of the test is subrounded. The wall is composed of a single hyaline layer.

Dimensions (mm):

Diameter : 0,254 – 0,265
Width : 0,176 – 0,194
W/D Ratio : 0,692 – 0,732

Remarks:

This species differs from other archaediscid species in having a thicker wall. The coiling pattern, initially streptospiral and later planispiral, is also characteristic for this species.

Stratigraphic Distribution:

Specimens were recovered from Upper Serpukhovian through Lower Bashkirian.

Archaediscus longus Potievskaya, 1958

Pl. III, figs. 4, 5

1958. *Archaediscus longus* Potievskaya, p. 20-21, pl. 2, fig. 8, 9

1968. *Archaediscus longus* Potievskaya; Aisenverg et al., pl. 24, fig. 1-2

1993. *Archaediscus longus* Potievskaya; Brenckle and Grelecki, pl. 6, fig.11-12

1979. *Neoarchaediscus longus* Potievskaya; Semichatova et al., pl. 8, fig. 1

Description:

Test shape is discoidal. Coiling is sigmoidal in initial volutions, changing to oscillatory planispiral. Final two to three volutions are evolute. The number of whorls is about six. Wall has hyaline radial layer.

Dimensions (mm):

Diameter : 0,273 – 0,318
Width : 0,103 – 0,130

W/D Ratio : 0,377– 0,408

Remarks:

Archaediscus longus is different from *Archaediscus krestovnikovi* Rauser-Chernousova by having more irregular outer volutions and the latter one has extensively sigmoidally coiled initial volutions.

Stratigraphic Distribution:

Specimens were recovered from Upper Serpukhovian through Lower Bashkirian.

Archaediscus krestovnikovi Rauser-Chernousova, 1948

Pl. III, figs.6, 7

1948. *Archaediscus krestovnikovi* Rauser-Chernousova, p. 10, pl. 2, figs. 18-20

1954. *Archaediscus krestovnikovi* Rauser-Chernousova var. *krestovnikovi* Rauser-Chernousova; Grozdilova and Lebedeva, pl. 7, figs. 2, 3

1968. *Archaediscus* ex gr. *krestovnikovi* Rauser-Chernousova; Aisenverg et al., pl. 17, fig. 8, 10

1979. *Archaediscus krestovnikovi* Rauser-Chernousova; Brazhnikova in Aisenverg et al., pl. 5, fig.4

1981. *Archaediscus (Archaediscus)* ex gr. *krestovnikovi* Rauser-Chernousova; Altıner, pl.4, figs. 27-32; pl. 8, figs. 1-6, 7-9

1990. *Archaediscus krestovnikovi* Rauser-Chernousova; Vdovenko et al., pl. 1, fig. 28

1993. *Archaediscus krestovnikovi* Rauser-Chernousova; Brenckle and Grelecki, p.1, fig.15, 17, 18

1996. *Archaediscus krestovnikovi* Rauser-Chernousova; Mamet, pl. 1, fig.4

1997. *Archaediscus krestovnikovi* Rauser-Chernousova; Brenckle et al., pl.2, fig. 28

1999. *Archaediscus krestovnikovi* Rauser-Chernousova; Özkan, p. 51, 52, pl. 2, fig. 15

Description:

Test is discoidal. Coiling is initially sigmoidal, outer volutions are planispiral. There are five whorls. Tubular chamber is open with flat floor. Wall is hyaline-radial.

Dimensions (mm):

Diameter : 0,215 – 0,333

Width : 0,091 – 0,111

W/D Ratio : 0,333 – 0,423

Remarks:

Archaediscus krestovnikovi is similar to *Paraarchaediscus koktjubensis* in the coiling type. However, this specimen is different from the latter one by its one layered hyaline wall. The latter has a double layer, inner microgranular and outer of hyaline.

Stratigraphic Distribution:

The stratigraphic distribution of this form is from Visean through Serpukhovian (Vdovenko et al., 1990).

Archaediscus karreri Brady, 1873

Pl. III fig. 8

1873. *Archaediscus karreri* Brady, p. 286-290, pl. 11, figs. 1-6

1960. *Archaediscus karreri* Brady; Grozdilova and Lebedeva, pl. 11, fig. 2

1967. *Archaediscus karreri* Brady; Brazhnikova et al., pl. 14, fig. 7

1968. *Archaediscus karreri* Brady; Aisenverg et al., pl. 17, fig.1,2

1990. *Archaediscus* ex gr. *Archaediscus karreri* Brady; Nemirovskaya et al., pl. 5, fig. 14

1993. *Archaediscus karreri* Brady; Brenckle and Grelecki, p. 12, 14, p. 1, fig.2-3

Description:

The shape is lenticular. Second tubular chamber is open. Coiling is initially sigmodial changing the direction in the last one to two volutions. Whorls are involute. The number of whorls is around five. The height of lumina increases rapidly with the growth of the test. Wall is thick, hyaline with distinct radial structure.

Dimensions (mm):

Diameter : 0,628

Width : 0,383

W/D Ratio : 0,610

Remarks:

Due to the single layered hyaline wall, this group is placed within the genus *Archaediscus*. This species differs from *A. karreriformis* Brady, by the presence of distinct radial structure. The *A. karreri* differs from *A. nanus* in its larger dimensions. The coiling pattern of *A. karreri* similar to *P. koktjubensis* although its shape is more ovoid and the latter one has double layered wall.

Stratigraphic Distribution:

The stratigraphic range of A. *karreri* is Lower Carboniferous (Brady, 1873). Some specimens were documented from the Upper Serpukhovian in this study.

Archaediscus moelleri Rauser-Chernousova, 1948

Pl.III, fig.9

1948. *Archaediscus moelleri* Rauser-Chernousova; p. 231, pl. 15, figs. 14, 15

1954. *Archaediscus moelleri* var *moelleri* Rauser-Chernousova; Grozdilova and Lebedeva, pl. 5, fig. 6

1960. *Archaediscus moelleri* Rauser-Chernousova; Grozdilova and Lebedeva, pl. 10, fig. 7

1967. *Archaediscus moelleri* Rauser-Chernousova; Brazhnikova et al., pl. 17, fig. 6; pl.14, fig. 6

1968. *Archaediscus moelleri* Rauser-Chernousova; Aisenverg et al., pl. 17, fig.4, 6

1980. *Archaediscus moelleri* Rauser-Chernousova; Rich, pl. 15, figs. 1-3

1982. *Archaediscus moelleri* Rauser-Chernousova; Rich, pl. 6, figs. 5, 6

1983. *Archaediscus moelleri* Rauser-Chernousova; Aisenverg et al., pl.21, fig.5, 6, 10

1989. *Archaediscus moelleri* Rauser-Chernousova; Fewtrell et al., pl. 3.12, fig. 15

1993. *Archaediscus moelleri* Rauser-Chernousova; Brenckle and Grelecki, pl.3, fig.3, 4, 9

1999. *Archaediscus moelleri* Rauser-Chernousova; Özkan, p. 47, 48, pl. 2, figs. 5-10

Description:

Test is lenticular with a rounded to angular periphery. Surface is smooth. Coiling is skewed throughout, but the last one to two whorls show decreasing asymmetry of coil. There are four to six volutions. Interior coiling is involute and outer two volutions are evolute. Wall is hyaline-radial.

Dimensions (mm):

Diameter : 0,410

Width : 0,289

W/D Ratio : 0,704

Remarks:

Archaediscus moelleri differs from *A. gigas*, in its much smaller dimensions. The small number of whorls and the inflated lenticular form differentiate this form from *A. karreri*.

Stratigraphic Distribution:

The stratigraphic range of this form is from Upper Visean and Serpukhovian (Dain and Grozdilova, 1953). Our specimens were recorded in the Upper Serpukhovian.

Archaediscus spp.

Pl.III, figs. 11-14

Description:

Under *Archaediscus* spp., we group several forms with small discoidal tests. Number of whorls varies from three to five. The coiling is initially streptospiral but the last whorls are sigmoidal to planispiral. Initial whorls are involute and the final two to three whorls are evolute. Wall is composed of single hyaline layer which is characteristic of *Archaediscus*.

Dimensions (mm):

Diameter : 0,232 – 0,311

Width : 0,114 – 0,116

W/D Ratio : 0,372– 0,491

Remarks:

This taxonomical unit differs from *A. longus* in its initially streptospiral coiling and less oscillatory coiling in the last whorls.

Stratigraphic Distribution:

Specimens were recovered from Upper Serpukhovian and Lower Bashkirian.

Genus *Eosigmoilina* Ganelina, 1956

Eosigmoilina sp.

Pl. III, fig. 10

Description:

Test is small. The coiling axis shifts and forms a different coiling pattern. Proloculus is followed by undivided tubular chamber which is coiled in varying planes that produce a sigmoidal spire. The wall is composed of hyaline radial layer.

Dimensions (mm):

Diameter : 0,186

Width : 0,089

W/D Ratio : 0,478

Remarks:

This genus is different from other genera except *Brenckleina* due to the coiling type. The coiling plane of last whorl is 90° to the inner volutions which are coiled in approximately same plane. It differs from *Brenckleina* in the absence of initial occlusions of the chambers.

Stratigraphic Distribution:

The stratigraphic range of this form is from Serpukhovian (Brenckle and Grelecki, 1993). This form is a good marker for the determination of mid-Carboniferous boundary. The specimen is recovered in Upper Serpukhovian (Zapaltyubinsky Horizon).

Subfamily Kasachstanodiscinae Marfenkova, 1983

Genus *Paraarchaediscus* Orlova, 1955

Type Species: *Paraarchaediscus dubitabilis* Orlova, 1955

Paraarchaediscus koktjubensis Rauser-Chernousova, 1948

Pl. IV figs. 1-11

1948. *Paraarchaediscus koktjubensis* Rauser-Chernousova, p. 10-11, pl. 3, figs. 1-3

1960. *Paraarchaediscus koktjubensis* Rauser-Chernousova; Grozdilova and Lebedeva, pl. 11, fig. 3, 4

1968. *Paraarchaediscus koktjubensis* Rauser-Chernousova; Aisenverg et al., pl.17, fig. 7

1982. *Archaediscus moelleri* Rauser-Chernousova; Rich, pl. 6, figs. 3, 4, 7, 11

1983. *Archaediscus krestovnikovi* var *koktjubensis* Rauser-Chernousova; Aisenverg et al., pl. 21, fig.3, 4

1990. *Archaediscus* ex gr. *Archaediscus krestovnikovi* (aff. *Archaediscus krestovnikovi koktjubensis*) Rauser-Chernousova; Gibshman and Akhmetshina, pl. 3, fig. 1

1993. *Paraarchaediscus koktjubensis* Rauser-Chernousova; Brenckle and Grelecki, pl. 1, fig.10-11, pl. 2, figs. 18, 19

1993. *Paraarchaediscus koktjubensis* Rauser-Chernousova; Ueno and Nakazawa, fig. 4.1-5

1997. *Paraarchaediscus* aff. *Paraarchaediscus koktjubensis* Rauser-Chernousova; Brenckle et al., pl. 2, fig. 12

Description:

Test is lenticular with a narrow rounded periphery. Interior coiling is involute, sigmoidal, outer two volutions are evolute and oscillatory to planispiral. The number of volutions is five to six. Wall is composed of inner thin dark microgranular and outer thick hyaline layers. Lateral thickenings are developed.

Dimensions (mm):

Diameter : 0,225 – 0,387

Width : 0,098 – 0,204

W/D Ratio : 0,435 – 0,527

Remarks:

This form was initially proposed as a variety of *Archaediscus krestovnikovi*. The coiling pattern resembles *Archaediscus krestovnikovi*, but the wall composition of this form is assigned to the genus *Paraarchaediscus*.

Stratigraphic Distribution:

The stratigraphic range of *Paraarchaediscus koktjubensis* is originally assigned to the Visean but later considered to be Serpukhovian (Brenckle and Grelecki, 1993). Specimens were recognized in the Upper Serpukhovian and lowermost part of the Lower Bashkirian.

Paraarchaediscus stilus Grozdilova and Lebedeva in Grozdilova, 1953

Pl. IV, figs. 12-15

1953. *Paraarchaediscus stilus* Grozdilova and Lebedeva in Grozdilova, p. 110-111, pl. 4, figs. 19, 20

1993. *Paraarchaediscus stilus* Grozdilova and Lebedeva in Grozdilova, Brenckle and Grelecki, pl. 6, figs. 3, 4

1982. *Archaediscus stilus* Grozdilova and Lebedeva in Grozdilova, Rich, pl. 6, figs. 8-10.

Description:

Test is discoidal in shape. Initial volutions are sigmoidal, later volutions are planispiral. It is involute in the initial stage and evolute in the last two whorls. There are four to five volutions. The floor of chamber is convex. It consists of a clear outer hyaline radial layer and less clear inner dark microgranular layer.

Dimensions (mm):

Diameter : 0,209 – 0,250

Width : 0,080 – 0,092

W/D Ratio : 0,368 – 0,382

Remarks:

P. stilus resembles *P. koktjubensis*. It differs from *P. koktjubensis* having a more complete sigmoidal coiling around the proloculus. The test shape and arrangement of coiling of *P. stilus* resembles *N. probatus* but the former one has only hyaline radial layer.

Stratigraphic Distribution:

The stratigraphic range of *P. stilus* is Middle Carboniferous, Bashkirian but specimens also occur in the upper part of Lower Carboniferous, Visean (Brenckle and Grelecki, 1993). Specimens were reported mainly from Upper Serpukhovian in this study.

Paraarchaediscus ninae Grozdilova and Lebedeva, 1954

Pl. V, figs. 1-9

1954. *Paraarchaediscus ninae* Grozdilova and Lebedeva; pl.6, figs. 9, 10

1993. *Paraarchaediscus ninae* Grozdilova and Lebedeva; Brenckle and Grelecki, pl.6, fig. 11, pl.7, fig.1

Description:

Test is discoidal, slightly tapering toward the periphery. It has a rounded periphery. Coiling is more or less oscillatory, changing direction abruptly between third and fourth volutions. Except the last volution, wall composition is double layered, microgranular and hyaline.

Dimensions (mm):

Diameter : 0,188 – 0,393

Width : 0,084 – 0,177

W/D Ratio : 0,446 – 0,450

Remarks:

This form is placed within *Paraarchaediscus* since it has a double layered wall. The bimodal coiling pattern is characteristic of this species. This form resembles *Paraarchaediscus koktjubensis,* however, it has a well-defined initial streptospiral coiling.

Stratigraphic Distribution:

The stratigraphic range of this form is from Upper Serpukhovian and Lower Bashkirian (Brenckle and Grelecki, 1993). In this study, specimens were recovered from Upper Serpukhovian (Zapaltyubinsky Horizon).

Paraarchaediscus sp.

Pl. V, figs. 10, 11

Description:

This species is characterized by a lenticular shape and more or less planispiral coiling. Volutions are four to five. The height of lumen increases rapidly in the final whorls. Initial volutions are involute and last whorl is evolute. The wall is composed of an inner dark microgranular wall and outer hyaline radial layers.

Dimensions (mm):

Diameter : 0,393 – 0,460

Width : 0,116 – 0,138

W/D Ratio : 0,295 – 0,300

Remarks:

The wall composition of this form is similar to *Paraarchaediscus*. This form resembles *P. stilus*. The latter differs from this form in its initial sigmoidal coiling pattern.

Stratigraphic Distribution:

The stratigraphic distribution of this form in the studied section is in Upper Serpukhovian (Zapaltyubinsky Horizon).

Family Asteroarchaediscidae Miklukho-Maklai, 1957

Subfamily Asteroarchaediscinae, Miklukho- Maklai, 1957

Genus *Neoarchaediscus* Miklukho-Maklai, 1956

Type species: *Archaediscus incertus* Grozdilova and Lebedeva, 1954

Neoarchaediscus timanicus Reitlinger, 1950

Pl. V, figs. 12-14

1950. *Archaediscus timanicus* Reitlinger, pl. 18, fig. 4

1953. *Neoarchaediscus timanicus* Reitlinger; Dain and Grozdilova, pl. 3, figs.18-20

1969. *A. timanicus* Reitlinger; Manukhalova-Grebeniuk et al., pl. 28, figs. 16-19

1969. *Neoarchaediscus* ex gr. *timanicus* Reitlinger; Manukhalova-Grebeniuk et al., pl. 8, fig. 38

1979. *Neoarchaediscus timanicus* Reitlinger; Potievskaya in Einor et al., pl. 21, fig.30

1979. *Neoarchaediscus timanicus* Reitlinger; Brazhnikova in Aisenverg et al., pl. 12, figs. 34, 35

1983. *Neoarchaediscus* aff. *probatus* Reitlinger; Aisenverg et al., pl. 21, fig. 33

1993. *Neoarchaediscus timanicus* Reitlinger; Brenckle and Grelecki, pl. 4, figs.20, 21

1999. *Neoarchaediscus timanicus* Reitlinger; Özkan, p. 62, 63, pl. 3, figs. 20-22

Description:

Test is small, laterally compressed. It has rounded to rectangular outline. Tubular second chamber forms four to five whorls. Inner whorls are involute and outer one is evolute. It is glomospiral in the initial stage and planispiral in the later stage with a small change in the position of the axis. Wall is hyaline radial.

Dimensions (mm):

Diameter : 0,164 – 0,189

Width : 0,072 – 0,088

W/D Ratio : 0,439 – 0,465

Remarks:

This form is distinguished by its very small size. It is similar to *Archaediscus krestovnikovi* but differs from it in having occluded inner volutions.

Stratigraphic Distribution:

The stratigraphic range of *N. timanicus* is from Upper Serpukhovian through Lower Bashkirian (Dain and Grozdilova, 1953). In this study, specimens

have been recorded from Bogdanovsky and Lower Syuransky Horizon (Lower Bashkirian).

Neoarchaediscus probatus Reitlinger, 1950

Pl. VI, figs. 1-7

1950. *Archaediscus probatus* Reitlinger, pl. 18, fig.9

1954. *Archaediscus incertus*; Grozdilova and Lebedeva, pl. 7, figs.14, 15

1983. *Neoarchaediscus* aff. *probatus* Reitlinger; Aisenverg et al., pl. 21, figs. 35

1988. *Neoarchaediscus* ex gr. *probatus* Reitlinger; Groves, figs. 11.22-25

1993. *Neoarchaediscus probatus* Reitlinger; Brenckle and Grelecki, pl. 4, figs. 1, 2, 14, 15; pl.6, figs. 5, 6

1999. *Neoarchaediscus probatus* Reitlinger; Özkan, p. 60, 61, pl. 3, figs. 18, 19

Description:

Test is lenticular. The undivided tubular chamber forms five to six volutions. Inner whorls are involute and last whorl is evolute. The initial two to three volutions have a closed lumen which exhibit stellate outline. Initial coiling is sigmoidal becoming oscillatory planispiral in outer volutions. The remaining two to four volutions have a smooth, open lumen. Wall is composed of a thick light colored hyaline layer.

Dimensions (mm):

Diameter : 0,179 – 0,393

Width : 0,082 – 0,129

W/D Ratio : 0,458 – 0,328

Remarks:

The coiling pattern of this species is similar to *Archaediscus krestovnikovi,* but differs from that in the inner occluded and sigmoidal portion of the coiling. It differs from *Neoarchaediscus timanicus* in having greater width to diameter ratio and greater number of volutions. The latter one has smaller dimensions.

Stratigraphic Distribution:

The stratigraphic distribution of this form is from Upper Serpukhovian through Lower Bashkirian (Aisenverg et al., 1983). The specimens were recovered from uppermost part of Upper Serpukhovian to Lower Bashkirian.

Neoarchaediscus subbaschkiricus Reitlinger, 1949

Pl. VI, figs. 8-18

1949. *Asteroarchaediscus subbaschkiricus* Reitlinger, pl. 1, figs. 8a-b

1950. *Asteroarchaediscus subbaschkiricus* Reitlinger, pl. 18, fig.8

1968. *Asteroarchaediscus subbaschkiricus* Reitlinger; Aisenverg et al., pl. 24, fig. 8

1969. *Neoarchaediscus subbaschkiricus* Reitlinger; Malakhova-Grebeniuk et al., pl. 27, figs. 39-42; pl. 28, figs. 1,2; pl. 7, fig. 38; pl. 10, fig. 2; pl.5, figs. 21,33; pl. 6, figs. 1,2; pl. 11, fig.20; pl.13, fig.5

1979. *Asteroarchaediscus subbaschkiricus* Reitlinger; Brazhnikova in Aisenverg et al., pl. 2, figs. 18, 19

1983. *Neoarchaediscus subbaschkiricus* Reitlinger; Aisenverg et al., pl. 22, figs. 8, 9

1993. *Neoarchaediscus* cf. *subbaschkiricus* Reitlinger; Ueno and Nakazawa, figs. 4.6-8

1994. *Neoarchaediscus* cf. *subbaschkiricus* Reitlinger; Ueno et al., fig.3.24

1999. *Neoarchaediscus subbaschkiricus* Reitlinger; Özkan, p. 56, 57, pl. 3, figs. 5-7

Description:

Test is small and lenticular. Periphery is rounded. Proloculus is followed by a skew coiled non-septate second chamber. The chamber enlarges gradually through growth. Outer volutions tend to be oscillatory planispiral. The number of volutions is five to six. Initial volutions are occluded and outer volutions are open. Last whorl is evolute. Wall is calcareous and consists of a clear hyaline layer.

Dimensions (mm):

Diameter : 0,155 – 0,214

Width : 0,090 – 0,129

W/D Ratio : 0,580 – 0,602

Remarks:

The early stage of the test of *Neoarchaediscus subbaschkiricus* resembles that of *Asteroarchaediscus baschkiricus*. The evolute coiling and high lumen of

the last whorls are the characteristic features of this form. This form resembles *N. postrugosus* but can be distinguished from the latter species in having a thick lenticular test with a larger width to diameter ratio.

Stratigraphic Distribution:

The stratigraphic range of this form is uppermost Serpukhovian through Lower Bashkirian (Dain and Grozdilova, 1953). In this study, specimens were recovered from the Upper Serpukhovian and Lower Bashkirian.

Neoarchaediscus parvus Rauser-Chernoussova, 1948

Pl. VII, figs. 1, 2

1948. *Neoarchaediscus parvus* Rauser-Chernoussova, p. 233, pl. 16, figs. 9-12

1973. *Neoarchaediscus* cf. *N. parvus* Rauser-Chernoussova; Brenckle, pl. 9, figs. 11-15.

1979. *Asteroarchaediscus parvus* Rauser-Chernoussova; Potievskaya in Einor et al., pl. 12, fig. 19

1980. *Neoarchaediscus parvus* Rauser-Chernoussova; Rich, pl. 16, figs. 5-11

1982. *Neoarchaediscus parvus* Rauser-Chernoussova; Rich, pl. 6, figs. 14-16

1990. *Neoarchaediscus* ex gr. N. *parvus* Rauser-Chernoussova; Nemirovskaya et al., pl. 5, fig. 17

1990. *Neoarchaediscus parvus* Rauser-Chernoussova; Vdovenko et al., pl. 1, fig. 22

1993. *Neoarchaediscus parvus* Rauser-Chernoussova; Ueno and Nakazawa, fig.4.13-17

1996. *Neoarchaediscus parvus* Rauser-Chernoussova; Mamet, pl. 1, fig. 5

Description:

Test is discoidal with a rounded periphery. Whorls are involute, the final whorl is evolute. It has rough surface. Second tubular chamber forms three to four volutions. Coiling is skewed in initial volutions. The final whorls are planispiral or slightly skewed. The lumina are closed and have a stellate appearance in inner volutions. Lumina in the outer two volutions are open. The wall is composed of light colored, finely fibrous calcite.

Dimensions (mm):

Diameter : 0,183 – 0,205

Width : 0,110 – 0,118

W/D Ratio : 0,575 – 0,601

Remarks:

This form is referable to the genus *Neoarchaediscus* because it has open lumina in outer one to two volutions. It has a large proloculus.

Stratigraphic Distribution:

The stratigraphic range of this for is from Lower Carboniferous, Upper Visean, Serpukhovian stage (Ueno and Nakazawa, 1993). The specimens were recovered from Upper Serpukhovian through lowermost Bashkirian.

Neoarchaediscus achimensis Grozdilova and Lebedeva, 1954

Pl. VII, figs. 3-6

1954. *Neoarchaediscus achimensis* Grozdilova and Lebedeva, p. 53-54, pl. 5, fig. 13; pl. 6, fig. 1

1969. *Neoarchaediscus achimensis* Grozdilova and Lebedeva; Manukalova-Grebeniuk, pl.28, figs. 13-15; pl.4, fig. 19; pl. 13, fig. 37

1993. *Neoarchaediscus achimensis* Grozdilova and Lebedeva; Brenckle and Grelecki, p. 31-32, pl.7, figs.1, 2

1994. *Neoarchaediscus achimensis* Grozdilova and Lebedeva; Groves, figs.3-31-33

2003. *Neoarchaediscus achimensis* Grozdilova and Lebedeva; Brenckle and Milkina, pl.5, fig. 28

Description:

Test is ovoid with convex lateral sides and a rounded to acute periphery. It has outer smooth surface. The two or three initial whorls are glomospiral. The median portion of the test seems to be set off from the outer part, due to the irregular coiling of the spiral. Tubular chamber is initially occluded becoming open with flat to slightly convex floor. The number of volutions is five to six. Wall is hyaline-radial.

Dimensions (mm):

Diameter : 0,267 – 0,542

Width : 0,213 – 0,411

W/D Ratio : 0,758 – 0,797

Remarks:

Its exterior shape and the arrangement of the whorls are reminiscent of *A. moelleri.* However, it differs from *A. moelleri* in the structure of the inner whorls.

Stratigraphic Distribution:

The stratigraphic range of this for is from Serpukhovian through Lower Bashkirian (Brenckle and Grelecki, 1993). The specimens were recovered from the uppermost part of Upper Serpukhovian (Zapaltyubinsky Horizon) through lowermost Bashkirian (Bogdanovsky and Lower Syuransky Horizons).

Neoarchaediscus spp.

Pl. VII, figs. 7-13

Description:

This group is characterized by single layered hyaline radial wall. Initial volutions are occluded and involute. The final two volutions are open and evolute. There are five volutions. Due to the occlusion structures in the inner whorls, this group is placed into *Neoarchaediscus.*

Dimensions (mm):

Diameter : 0,262 – 0,350

Width : 0,109 – 0,162

W/D Ratio : 0,416 – 0,462

Stratigraphic Distribution:

Specimens were recovered from Upper Serpukhovian through Lower Bashkirian.

Genus *Asteroarchaediscus*, Miklukho-Maklai, 1956

Type Species: *Archaediscus baschkiricus* Krestovnikov-Theodorovitch, 1936

Asteroarchaediscus rugous Rauser-Chernousova, 1948

Pl. VII, figs. 14-17

1948. *Archaediscus rugosus* Rauser – Chernousova, p. 11, pl. 3, figs. 4-6

1953. *Archaediscus ex* gr. *rugosus* Rauser - Chernousova; Dain and Grozdilova, pl. 4, figs. 1-3

1967. *Asteroarchaediscus* ex gr. *rugosus* Rauser - Chernousova; Brazhnikova et al., pl. 21, fig. 2

1969. *Asteroarchaediscus rugosus* Rauser - Chernousova; Manukalova-Grebeniuk et al., pl. 12, figs. 31,32; pl. 28, figs. 3-5

1973. *Asteroarchaediscus gnomellus*, Brenckle, pl. 9, figs. 2-6

1979. *Asteroarchaediscus rugosus* Rauser - Chernousova; Potievskaya in Einor et al., pl. 12, fig. 23

1983. *Asteroarchaediscus rugosus* Rauser - Chernousova; Groves, pl. 3, figs. 3-7

1983. *Neoarchaediscus* ex gr. *rugosus* Rauser - Chernousova; Aisenverg et al., pl. 22, figs. 10, 11

1988. *Asteroarchaediscus* ex gr. *rugosus* Rauser - Chernousova; Groves, fig. 11. 1-7

1990. *Asteroarchaediscus* ex gr. *rugosus* Rauser - Chernousova; Gibshman and Akhmetshina, pl. 3, figs. 8-10

1990. *Asteroarchaediscus* ex gr. *rugosus* Rauser - Chernousova; Nemirovskaya et al., pl. 5, fig. 16

1993. *Asteroarchaediscus* ex gr. *rugosus* Rauser - Chernousova; Makhlina et al., pl. 20, fig. 26

1994. *Asteroarchaediscus rugosus* Rauser - Chernousova; Ueno et al., figs.3.29-30

1993. *Asteroarchaediscus rugosus* Rauser - Chernousova; Brenckle and Grelecki, pl. 2, fig. 6

2003. *Asteroarchaediscus rugosus* Rauser - Chernousova; Brenckle and Milkina, pl. 6, fig. 34

Description:

Test is discoidal. The early whorls are glomosprially coiled. Later whorls slightly change their axis of coiling. Tubular chamber is occluded except in last volution. The number of volution is five to six. Wall is hyaline radial.

Dimensions (mm):

Diameter : 0,229 – 0,304

Width : 0,131 – 0,139

W/D Ratio : 0,457 – 0,572

Remarks:

Asteroarchaediscus rugosus is distinguished from *Asteroarchaediscus baschkiricus* by its smaller W/D ratio. It is similar to *N. parvus* but the latter one has smaller dimensions. *N. parvus* is identical to *A. rugosus* except for smaller dimensions and occlusion which occurs in all volutions.

Stratigraphic Distribution:

The stratigraphic range of this species is from Upper Visean through Lower Bashkirian (Dain and Grozdilova, 1953). Our specimens were recorded from Upper Serpukhovian and Lower Bashkirian.

Asteroarchaediscus baschkiricus Krestovnikov- Theodorovitch, 1936

Pl. VII, figs. 18-21

1936. *Archaediscus baschkiricus* Krestovnikov and Theodorovitch, p. 87, tf. 1-3

1953. *Archaediscus baschkiricus* var. *baschkiricus* Krestovnikov and Theodorovitch; Dain and Grozdilova, pl. 3, fig. 12

1960. *Asteroarchaediscus baschkiricus* Krestovnikov and Theodorovitch; Grozdilova and Lebedeva, pl. 11, fig. 9

1969. *Asteroarchaediscus baschkiricus* Krestovnikov and Theodorovitch; Manukhalova et al., pl. 27, figs. 37, 38

1979. *Asteroarchaediscus baschkiricus* Krestovnikov and Theodorovitch; Brazhnikova in Aisenverg et al., pl. 5, fig. 42

1988. *Asteroarchaediscus* ex gr. *baschkiricus* Krestovnikov and Theodorovitch; Groves, figs.11. 8-14

1990. *Asteroarchaediscus baschkiricus* Krestovnikov and Theodorovitch;

Gibshman and Akhmetshina, pl. 3, figs. 16, 17

1990. *Asteroarchaediscus* ex gr. *baschkiricus* Krestovnikov and Theodorovitch; Nemirovskaya and others, pl. 5, fig. 18

1991. *Asteroarchaediscus baschkiricus* Krestovnikov and Theodorovitch; Vachard and Beckary, pl. 4, figs. 21, 22

1996. *Asteroarchaediscus baschkiricus* Krestovnikov and Theodorovitch; Mamet, pl. 1, fig. 6

1997. *Asteroarchaediscus baschkiricus* Krestovnikov and Theodorovitch; Brenckle et al., pl. 2, fig.21

1999. *Asteroarchaediscus baschkiricus* Krestovnikov and Theodorovitch; Özkan, p. 53-54, pl. 3, figs. 1-4

2003. *Asteroarchaediscus baschkiricus* Krestovnikov and Theodorovitch; Brenckle and Milkina, pl. 5, fig.17

Description:

Test is small and lenticular. Outline is oval in axial section. There are four or five volutions. Initial whorls are involute but final one is evolute. Except final whorl, all volutions are occluded. Coiling is oscillatory planispiral. Wall is thick, hyaline radial.

Dimensions (mm):

Diameter : 0,204 – 0,214

Width : 0,117 – 0,140

W/D Ratio : 0,573 – 0,654

Remarks:

This form is similar to *A. rugosus* but it differs from the latter by its convex sides.

Stratigraphic Distribution:

The stratigraphic range of *Asteroarchaediscus baschkiricus* is from Upper Visean through Bashkirian (Vdovenko et al., 1990). Specimens were recovered from Protvinsky-Zapaltyubinsky Horizon (Upper Serpukhovian) to Bogdanovsky and Lower Syuransky (Lower Bashkirian).

Asteroarchaediscus sp.

Pl. VII, figs. 22-23

Description:

The absence of microgranular wall and occlusion of all volutions are the characteristic features for this group. Proloculus is large and the shape of the test is biconvex. The coiling pattern is oscillatory planispiral. The second tubular chamber forms three to four volutions. Wall is hyaline.

Dimensions (mm):

Diameter : 0,243– 0,286

Width : 0,156 – 0,231

W/D Ratio : 0,641 – 0,800

Remarks:

This species similar to *N. parvus* but the occlusions of all volutions differentiate this form from the latter one.

Stratigraphic Distribution:

This form was recovered from the uppermost Serpukhovian (Zapaltyubinsky Horizon) and Lower Bashkirian (Bogdanovsky and Syuransky Horizons).

Family Lasiodiscidae Reitlinger, 1956

Genus *Monotaxinoides* Brazhnikova and Yartseva, 1956

Type species: *Monotaxinoides transitorius* Brazhnikova and Yartseva, 1956

Monotaxinoides sp.

Pl. VIII, fig. 1

Description:

The second tubular chamber is a very low trochospirally coiled and the test is nearly flat. The wall is microgranular.

Remarks:

Only few specimens were recovered so the specification could not be done.

Stratigraphic Distribution:

The specimens were recorded from Lower Bashkirian.

SUPERFAMILY PALAEOTEXTULARIACEA Galloway, 1933

Family Paleotextulariidae Galloway, 1931

Genus *Paleotextularia* Schubert, 1921

Type species: *Paleotextularia schellwieni* Galloway and Ryniker, 1930

Paleotextularia sp.

Pl. VIII, figs. 2-4

Description:

Test is rectilinear. It consists of biserially arranged, inflated chambers. Septa are long and curved. Aperture is simple and a slit like at the base of final chamber. Wall is composed of an inner hyaline layer and an outer dark, microgranular layer that contains adventitious grains.

Dimensions (mm):

Length : 1.160 – 1,315

Width : 0,536 – 0,768

W/L Ratio: 0,462 – 0,584

Thickness of wall : 0,087

Stratigraphic Distribution:

Our specimens were recovered from Upper Serpukhovian to Lower Bashkirian within the measured section.

Genus *Cribrostomum* Möller, 1879

Type Species: *Cribrostomum textulariforme* Möller, 1879

Cribrostomum sp.

Pl. VIII, fig. 5

Description:

It has biserially arranged four pairs of chambers. Septa are moderately long and broadly curved. Wall is composed of double layer. One is dark granular

outer layer and second one is thin discontinuous fibrous calcite layer. Aperture is cribrate in the last chambers.

Dimensions (mm):

Length : 1.31

Width : 0,802

W/L Ratio: 0,612

Thickness of wall : 0,05

Remarks:

Cribrostomum sp. differs from *Paleotextularia* species in having a cribrate aperture. It also differs from *Climacammina* which is initially biserial then uniserial.

Stratigraphic Distribution:

Specimens were recovered from Upper Serpukhovian.

Genus *Climacammina* Brady in Etheridge, 1873

Type species: *Textularia antiqua* Brady in Young and Armstrong, 1871

Climacammina sp.

Pl. VIII, figs. 6, 7

Description:

Test is composed of initially biserially later uniserially arranged seven pairs of chambers. Test is mm long and mm wide. This form has a thick wall consisting of an outer dark granular layer and a clear fibrous inner layer which may be discontinuous.

Dimensions (mm):

Length : 1.318

Width : 0,726

W/L Ratio: 0,06

Thickness of wall : 0,087

Stratigraphic Distribution:

Our specimens were recorded from Upper Serpukhovian and lower Bashkirian.

Family Biseriamminidae Chernysheva, 1941

Subfamily Biseriammininae Chernysheva, 1941

Genus *Biseriella* Mamet, 1974

Type species: *Globivalvulina parva*, Chernysheva, 1948

Biseriella parva Chernysheva, 1948

Pl. VIII, figs. 8-17

1948. *Globivalvulina parva* Chernysheva, p. 249, pl. 13, figs. 1-4

1968. *Globivalvulina parva* Chernysheva; Aisenverg et al., pl. 12, figs. 11-13

1979. *Globivalvulina* ex gr. *parva* Chernysheva; Brazhnikova in Aisenverg et al., pl. 5, figs.22-23

1980. *Biseriella parva* Chernysheva; Rich, pl. 5, figs. 2, 3, 6, 7, 10

1981. *Globivalvulina parva* Chernysheva; Altıner, pl. 23, figs. 18-23

1983. *Globivalvulina* ex gr. *parva* Chernysheva; Aisenverg et al., pl. 1, figs. 26, 27; pl. 6, fig. 15

1988. *Biseriella parva* Chernysheva; Groves, figs.4. 1-9

1989. *Biseriella parva* Chernysheva; Fewtrell et al., pl. 3.9, fig. 4; pl. 3.12, fig. 2

1990. *Biseriella parva* Chernysheva; Gibshman and Akhmetshina, pl. 2, figs. 10-15

1992. *Biseriella parva* Chernysheva; Groves, pl. 4, figs. 8-13

1995. *Biseriella parva* Chernysheva; Altıner and Savini, pl. 5, figs. 26-29

1996. *Biseriella parva* Chernysheva; Mamet, pl.1, fig. 28

1999. *Biseriella parva* Chernysheva; Özkan, p. 66-67, pl. 5, figs.1-11

2003. *Biseriella parva* Chernysheva; Brenckle and Milkina, pl. 6, figs. 1-3

Description:

Test is small and subglobular coiling is trochospiral in early portion tends toward a more planispiral coil in the latest stages. Proloculus is followed by rapidly expanding biserially arranged chambers. Wall is dark and composed of fine grained "tectum". Aperture is simple.

Dimensions (mm):

Diameter : 0,247 – 0,319

Width : 0,148 – 0,200

Thickness of wall: 8 – 11 μm

Remarks:

Biseriella parva differs from morphological similar *G. bulloides* in its undifferentiated, microgranular wall, smaller size, and lesser number of chambers. Groves (1988) stated that most specimens assignable to *Biseriella* can be accommodated within *B. parva.*

Stratigraphic Distribution

The stratigraphic range of *B. parva* is from Serpukhovian through Lower Bashkirian (Groves, 1988). Specimens were recovered from Upper Serpukhovian (Protvinsky-Zapaltyubinsky Horizon).

Genus *Globivalvulina* Schubert, 1921

Type species: *Valvulina bulloides* Brady, 1876

Globivalvulina bulloides Brady, 1876

Pl. VIII, fig. 18; Pl. IX, figs. 1-11

1876. *Valvulina bulloides* Brady, pl. 4, figs. 12-15

1967. *Globivalvulina scaphoidea* Reitlinger; Brazhnikova and others, pl. 22, fig.3

1983. *Globivalvulina* ex gr. *pulchra* Reitlinger; Aisenverg and others, pl. 12, figs. 16, 21, 22

1988. *Globivalvulina bulloides* Brady; Groves, p. 383-384, figs.14 (10-16)

1990. *Globivalvulina bulloides* Brady; Gibshman and Akhmetshina, pl. 2, figs. 1-8

1991. *Globivalvulina* ex gr. *bulloides* Brady; Vachard and Beckary, pl. 3, fig.16

1992. *Globivalvulina bulloides* Brady; Groves, pl. 4, figs.14-19

1995. *Globivalvulina bulloides* Brady; Altıner and Savini, pl. 5, figs. 1-3

1996. *Globivalvulina bulloides* Brady; Mamet, pl. 1, fig. 29

1999. *Globivalvulina bulloides* Brady; Özkan, p. 68-69, pl. 5, figs.12-19

2003. *Globivalvulina bulloides* Brady; Brenckle and Milkina, pl. 6, fig.4

Description:

Test is comparatively large, slightly compressed bilaterally. Central clear layer more or less continuously developed in final few chambers in earlier portions of test it may be inconsistently developed or absent. The number of pair of chambers varies from four to five. The whorl height rapidly increases.

Dimensions (mm):

Diameter : 0,304 – 0,410

Width : 0,359 – 0,431

W/D Ratio: 0,846 – 0,951

Thickness of wall: 11 – 15 μm

Remarks:

Globivalvulina bulloides is similar to *B. parva* but the main discrimination is its large size and well developed central clear layer and great number of chambers. *G. bulloides* is considered a seniour synonym of *G. moderata* (Groves, 1988). The supposed difference was thought to be wall thickness. Examinations by P. L. Brenckle (in Groves, 1988) revealed that these two species do not differ in any character as well as wall thickness. Most thick-walled forms formerly identified as *G. bulloides* should be assigned to *G. granulosa.*

Stratigraphic Distribution:

The stratigraphic range of *G. bulloides* is from Upper Serpukhovian (Zapaltyubinsky Horizon) through latest Carboniferous (Groves, 1988). Our specimens were recovered from Upper Serpukhovian to Lower Bashkirian. The appearance of *G. bulloides* characterizes the base of the Pennsylvanian in North America (Groves, 1988).

Globivalvulina granulosa Reitlinger, 1950

Pl. IX, figs. 12-15

1950. *Globivalvulina granulosa* Reitlinger; pl. 17, figs.4-9

1981. *Globivalvulina granulosa* Reitlinger; Altıner, pl. 24, figs. 5-7, 9?

1992. *Globivalvulina granulosa* Reitlinger; Groves, pl. 4, figs. 20-24

1995. *Globivalvulina granulosa* Reitlinger; Altıner and Savini, pl. 6, figs. 4, 5

1999. *Globivalvulina granulosa* Reitlinger; Özkan, p. 70-71, pl. 5, figs. 20-22

Description :

Test is large and almost planispiral increasing rapidly in width. The test is composed of four pair of chambers. Chamber size increases uniformly. Wall is granular with inclusions of small light colored crystals. The thickness of the wall increases rapidly in the final chambers.

Dimensions (mm):

Diameter : 0,313 – 0,352

Width : 0,180 – 0,218

W/D Ratio : 0,575 – 0,619

Thickness of wall: 15 – 29 μm

Remarks:

This form is different from others in its thick walled, coarsely granular test. Its large size differentiates it from others. It differs from *G. bulloides* in having thicker wall.

Stratigraphic Distribution:

The stratigraphic range is Middle Carboniferous (Reitlinger, 1950). In this study, specimens were recovered from Upper Serpukhovian.

Globivalvulina scaphoidea Reitlinger, 1949

Pl. IX, fig. 16

1949. *Globivalvulina scaphoidea* Reitlinger, pl. 1, fig. 5

1969. *Globivalvulina* ex gr. *scaphoidea* Reitlinger; Manukalova-Grebeniuk, pl. 8, fig.8; pl.11, fig. 4

1979. *Globivalvulina scaphoidea* Reitlinger; Brazhnikova in Aisenverg et al., pl. 5, fig.24.

1982. *Globivalvulina scaphoidea* Reitlinger; Villa, pl. 2, fig. 4

1983. *Globivalvulina scaphoidea* Reitlinger; Aisenverg et al., pl. 12, figs. 17, 18

Description:

Test is small, compressed bilaterally and composed of five pairs of chambers. Coiling straightens out as it expands, giving the transverse section of the test an elongate oval shape. Wall is dark and finely granular.

Dimensions (mm):

Diameter : 0,273

Width : 0,108

W/D Ratio: 0,395

Thickness of wall: 6 μm

Remarks:

Characteristic features of this form are its small dimensions and the sharp size increase of the last chamber. It differs from *Biseriella parva* by the sharp and uneven growth of its last chamber.

Stratigraphic Distribution:

The stratigraphic range is Lower and Middle Carboniferous (Reitlinger, 1949). Specimens were recovered from Lower Bashkirian.

Globivalvulina sp.

Pl. X, figs. 1-4

Description:

Test is of medium size and coiling is planispiral. It is composed of five pair of chambers. Chambers expand regularly in size but, the last chamber enlarges more. The number of biserial chambers pairs in the last volution is five. Wall is dark granular calcite.

Dimensions (mm):

Diameter : 0,316 – 0358

Width : 0,128 – 0,178

W/D Ratio: 0,405 – 0,497

Thickness of wall: 10 – 11 μm

Remarks:

This form differs from *G. bulloides* in having a more rapid expansion of its last chamber. It differs from *B. parva* in its larger size.

Stratigraphic Distribution:

Specimens were recovered from Upper Serpukhovian to Lower Bashkirian.

SUPERFAMILY ENDOTHYRACEA BRADY, 1884

Family Endothyridae Brady, 1884

Subfamily Endothyrinae Brady, 1884

Genus *Endothyra* Phillips, 1846

Type species: *Endothyra bowmani* Phillips, 1846

Endothyra spp.

Pl. X, figs. 5-12

Description:

A broad range of morphologies is represented in this group. They have a discoidal test. Coiling is initially skewed and the final volution is nearly planispiral. There are secondary floor coverings and projections. Wall is calcareous microgranular.

Dimensions (mm):

Diameter : 0,322 – 0,641

Thickness of wall: 0,014 – 0,020

Stratigraphic Distribution:

Specimens were recorded from Upper Serpukhovian and Lower Bashkirian.

Genus *Planoendothyra* Reitlinger in Rauser-Chernousova and Fursenko, 1959

Type species: *Endothyra aljutovica*, Reitlinger, 1950

Planoendothyra sp.

Pl. X, fig. 13

Description:

Test is discoidal, laterally compressed with a broadly rounded periphery. Initial volutions are involute and highly skewed. The outer volution is evolute and planispirally coiled. Rate of expansion of coil is very rapid. Wall is dark, microgranular. Secondary floor coverings are developed.

Dimensions (mm):

Diameter : 0,301 – 0,344

Thickness of wall: 0,014 – 0,017

Stratigraphic Distribution:

Specimens were recorded from Upper Serpukhovian and Lower Bashkirian.

Family Bradyinidae Reitlinger, 1950

Genus *Bradyina* Möller, 1878

Type species: *Bradyina nautiliformis* Möller,1878

Bradyina cribrostomata Rauser-Chernousova and Reitlinger in Rauser-Chernousova and Fursenko, 1937

Pl. X, figs. 14-17

1937. *Bradyina cribrostomata* Rauser-Chernousova and Reitlinger in Rauser-Chernousova and Fursenko, figs. 231 – 234

1960. *Bradyina cribrostomata* Rauser-Chernousova and Reitlinger in Rauser-Chernousova and Fursenko; Grozdilova and Lebedeva, pl. 8, fig. 3

1968. *Bradyina cribrostomata* Rauser-Chernousova and Reitlinger in Rauser-Chernousova and Fursenko; Aisenverg et al., pl. 13, fig. 2

1969. *Bradyina cribrostomata* Rauser-Chernousova and Reitlinger in Rauser-Chernousova and Fursenko; Manukalova-Grebeniuk, pl. 4, figs.12-14; pl. 5, fig. 1

1988, *Bradyina cribrostomata* Rauser-Chernousova and Reitlinger in Rauser-Chernousova and Fursenko; Groves, figs. 14.23-14.28

1996. *Bradyina cribrostomata* Rauser-Chernousova and Reitlinger in Rauser-Chernousova and Fursenko; Mamet, pl. 1, fig.20

2003. *Bradyina cribrostomata* Rauser-Chernousova and Reitlinger in Rauser-Chernousova and Fursenko; Brenckle and Milkina, pl. 6, fig. 41

Description:

The number of volutions is two to three. Test is nautiloid, planispiral and involute. The number of chambers in final volution is six. Chambers are

hemispherical and slightly convex. Wall is composed of thick granular keriotheca.

Dimensions (mm):

Diameter : 0,920 – 1,228

Width : 1,054 – 1,414

Thickness of wall: 70 – 100 μm

Remarks:

Bradyina cribrostomata differs from *B. nautiliformis* in its considerably smaller size and more chambers per volution and from *B. rotula* in its thicker wall and fewer chambers per volution.

Stratigraphic Distribution:

The stratigraphic range is from Upper Serpukhovian and Lower Bashkirian (Syuransky) (Groves, 1988). Our specimens were recovered from Upper Serpukhovian.

Bradyina sp.

Pl. X, fig. 18

Description:

It has a thin keriothecal wall. There are two to three volutions. The size of the chamber increases rapidly. The number of chambers in final volution is seven to eight. It is planispirally coiled.

Dimensions (mm):

Diameter : 1,225

Thickness of wall: 40 (μm)

Remarks:

The thinner wall of this specimen distinguishes it from *B. cribrostomata.*

Stratigraphic Distribution:

Specimens were recovered from Upper Serpukhovian (Protvinsky-Zapaltyubinsky Horizons).

SUPERFAMILY TETRATAXACEA GALLOWAY, 1933

Family Tetrataxidae Galloway, 1933

Genus *Tetrataxis* Ehnenberg, 1854

Type species: *Tetrataxis conica* Ehrenberg, 1854

Tetrataxis sp.

Pl. XI, fig. 1

Description:

Test is conical, trochospirally coiled with an umbilical cavity and has four to five volutions. Chambers are elongate. Wall is composed of a double layer. It consists of a dark inner microgranular layer and a yellowish pseudofibrous outer layer.

Dimensions (mm):

Height : 0.350

Basal Diameter : 0,716

Thickness of wall: 0,032

Remarks:

The trochospiral coiling and double layered wall, are characteristic features of *Tetrataxis*. Only one specimen was recovered. The paucity of material precludes specification.

Stratigraphic Distribution:

Specimen is recovered from Upper Serpukhovian.

SUPERFAMILY FUSULINACEA MOLLER, 1878

Family Eostaffellidae Mamet in Mamet, Mikhailoff and Mortelmans, 1970

Genus *Mediocris* Rozovskaya, 1961

Type species: *Eostaffella mediocris* Vissanorova, 1948

Mediocris mediocris Vissarionova, 1948

Pl. XI, fig. 2

1948. *Eostaffella mediocris* Vissarionova, pl. 14, figs. 7-9

1954. *Eostaffella mediocris* Vises. var. *mediocris* Vissarionova; Grozdilova and Lebedeva, pl. 13, figs. 9,10

1960. *Mediocris mediocris* Vissarionova; Grozdilova and Lebedeva, pl. 13, fig.13

1967. *Mediocris mediocris* Vissarionova; Brazhnikova and others, pl. 8, fig.14; pl. 10, fig. 6

1968. *Mediocris mediocris* Vissarionova; Aisenverg et al., pl. 10, fig. 6; pl. 19, fig. 20

1981. *Mediocris mediocris* Vissarionova; Altıner, pl. 28, figs. 15-18

1993. *Mediocris mediocris* Vissarionova; Ueno and Nakazawa, figs.5.1-5

1999. *Mediocris mediocris* Vissarionova; Özkan, p. 95-97, pl. 10, figs. 21-26

Description:

Shell is small and discoidal with rounded periphery. There are three to four volutions. Initial volutions are skewed and outer ones are essentially planispiral and gradually expand. Wall is undifferentiated, dark microgranular. Secondary deposits are a micrite plug in umbilical region.

Dimensions (mm):

Diameter : 0,363

Width : 0,194

W/D Ratio : 0,534

Remarks:

This form differs from *M. breviscula* by its greater width to diameter ratio.

Stratigraphic Distribution:

The stratigraphic range is known from Upper Visean through Bashkirian (Altıner, 1981). Our specimens were recovered from Upper Serpukhovian.

Mediocris breviscula Ganelina, 1951

Pl. XI, fig. 3

1951. *Eostaffella mediocris* Viss. *breviscula* Ganelina, pl. 3, figs. 1-3

1954. *Eostaffella breviscula* Ganelina; Grozdilova and Lebedeva, pl. 13, figs.

12, 13

1967. *Mediocris breviscula* Ganelina; Brazhnikova et al., pl. 8, fig. 15

1968. *Mediocris mediocris* Viss.var. *breviscula* Ganelina; Aisenverg et al., pl. 19, fig. 22

1969. *Mediocris mediocris* var. *breviscula* Ganelina; Manukalova-Grebeniuk et al., pl. 6, figs. 3, 4

1981. *Mediocris breviscula* Ganelina; Altıner, pl. 28, figs. 20-25

1983. *Mediocris* ex gr. *breviscula* Ganelina; Aisenverg and others, pl. 12, fig.6a

1988. *Mediocris breviscula* Ganelina; Groves, fig. 15 (1-14)

1989. *Mediocris breviscula* Ganelina; Fewtrell and others, pl. 3.4, fig. 21

1990. *Mediocris breviscula* Ganelina; Gibshman and Akhmetshina, pl. 3, figs. 26-30

1991. *Mediocris breviscula* Ganelina; Groves, pl. 1, figs. 1-17

1991. *Mediocris breviscula* Ganelina; Vachard and Beckary, pl. 5, figs.2-3

1999. *Mediocris breviscula* Ganelina; Özkan, p. 94-95, pl. 10, figs. 9-20

Description:

Test is discoidal with rounded periphery and straight sided to slightly depressed umbilici. It has three to four volutions. Coiling is planispiral. Secondary deposits occur in all volutions. Wall is thin, microgranular.

Dimensions (mm):

Diameter : 0,270

Width : 0,090

W/D Ratio : 0,434

Remarks:

This species is different from other *Mediocris* species in their very small size, rapid expansion of coiling. It differs from *M. mediocris* by strong compression of the test and smaller width to diameter ratio.

Stratigraphic Distribution:

The stratigraphic distribution is from Upper Visean through Bashkirian (Altıner, 1981). Our specimens were recovered from Upper Serpukhovian.

Mediocris sp.

Pl. XI, fig. 4

Description:

Test is composed of three to four planispiral volutions. Secondary deposits occur as lateral fills. The chamber height gradually increases. It has larger dimensions. Wall is microgranular.

Dimensions (mm):

Diameter : 0,535

Width : 0,225

W/D Ratio : 0,420

Remarks:

It differs from *M. breviscula* and *M. mediocris* in its larger dimensions.

Stratigraphic Distribution:

Our specimens were found in Upper Serpukhovian.

Genus *Millerella* Thompson, 1942

Type species: *Millerella marblensis* Thompson, 1942

Millerella umblicata Kireeva in Rauser-Chernousova et al., 1951

Pl. XI, figs. 5, 6

1951. *Millerella umblicata*, Kireeva in Rauser-Chernousova et al., pl. 2, figs. 1-2

1967. *Millerella umblicata*, Kireeva in Rauser-Chernousova et al.; Brazhnikova et al., pl. 21, figs.14, 15

1968. *Millerella umblicata*, Kireeva in Rauser-Chernousova et al.; Aisenverg et al., pl. 25, fig. 16

1969. *Millerella umblicata*, Kireeva in Rauser-Chernousova et al.; Manukalova-Grebeniuk et al., pl. 10, figs. 22, 23

1983. *Millerella* ex gr. *umblicata*, Kireeva in Rauser-Chernousova et al.; Aisenverg et al., pl. 11, fig.32

1999. *Millerella umblicata*, Kireeva in Rauser-Chernousova et al.; Özkan, p. 92-93, pl. 10, figs. 1-3

Description:

Test is lenticular with rounded periphery. It has a deep narrow umbilical area. Width of the test increases rapidly. The coiling in the initial stage is tight, later becoming loose. Discontinuous pseudochomata are present.

Dimensions (mm):

Diameter : 0,278 – 0,367

Width : 0,135 – 0,171

W/D Ratio : 0,465 – 0,485

Remarks:

It differs from other Millerellids in having well rounded periphery. The presence of well rounded periphery, deeper umbilicus and large W/D ratio is characteristic features of this form.

Stratigraphic Distribution:

The stratigraphic distribution ranges from Upper Serpukhovian through Lower Moscovian (Aisenverg et al., 1983). Our specimens have been recovered from Lower Bashkirian (Bogdanovsky Horizon).

Millerella marblensis Thompson, 1942

Pl. XI, figs. 7, 8

1942. *Millerella marblensis* Thompson; pl. 1, figs.4, 5, 7, 8, 9, 10, 11-13

1983. *Millerella marblensis* Thompson; Groves, pl. 4, fig. 13-17

1985. *Millerella marblensis* Thompson; Skipp et al., pl. 4, figs. 9,10

1988. *Millerella marblensis* Thompson; Loeblich and Tappan, pl. 254, figs. 1-3

1988. *Millerella marblensis* Thompson; Groves, figs.15.26-15.31

1991. *Millerella marblensis* Thompson, Groves; pl. 2, figs.1-21

1994. *Millerella marblensis* Thompson, Hoare and Sturgeon, fig. 3.23-3.27

1995. *Millerella marblensis* Thompson, Altıner and Savini, pl. 1, figs. 17-19

Description:

Test is narrowly discoidal with depressed umbilici. There are four to five volutions. Coiling is highly evolute. Rate of expansion of coiling is moderately rapid. Periphery is rounded to subangular. Chomata are weakly developed.

Remarks:

Millerella marblensis is distinguished from other species in the genus by its highly evolute and typically inflated final one-half volution. *Millerella marblensis* is distinguished from *Millerella extensa* in having larger dimensions and a larger width.

Dimensions (mm):

Diameter : 0,540 – 0,585

Width : 0,180 – 0,213

W/D Ratio : 0,333 – 0,364

Stratigraphic Distribution:

The stratigraphic range is Lower Bashkirian (Groves, 1988). Our specimens were also recovered from Lower Bashkirian (Bogdanovsky Horizon).

Genus *Eostaffella* Rauser-Chernousova, 1948

Type species: *Staffella (Eostaffella) parastruvei* Rauser-Chernousova, 1948

Eostaffella pseudostruvei Rauser-Chernousova and Beliaev in Rauser-Chernousova, Beliaev and Reitlinger, 1936

Pl. XII, figs. 1-6

1936. *Staffella pseudostruvei* Rauser-Chernousova and Beliaev in Rauser-Chernousova, Beliaev and Reitlinger, pl. 1, fig. 7

1960. *Eostaffella pseudostruvei* Rauser-Chernousova and Beliaev in Rauser-Chernousova, Beliaev and Reitlinger; Grozdilova and Lebedeva, pl. 13, fig. 11

1967. *Eostaffella pseudostruvei* Rauser-Chernousova and Beliaev in Rauser-Chernousova, Beliaev and Reitlinger; Brazhnikova et al., pl. 18, fig. 4; pl. 14, fig. 7; pl. 20, figs. 11-13, pl. 21, fig.9

1968. *Eostaffella pseudostruvei* Rauser-Chernousova and Beliaev in Rauser-Chernousova, Beliaev and Reitlinger; Aisenverg et al., pl. 19, fig.4; pl. 25, figs. 4-6

1979. *Eostaffella (E.) pseudostruvei* Rauser-Chernousova and Beliaev in Rauser-Chernousova, Beliaev and Reitlinger; Semichatova et al., pl. 19, fig. 9

1979. *Eostaffella (E.) pseudostruvei* Rauser-Chernousova and Beliaev in Rauser-Chernousova, Beliaev and Reitlinger; Eionor et al., pl. 13, fig. 3

1979. *Eostaffella (E.) pseudostruvei* Rauser-Chernousova and Beliaev in Rauser-Chernousova, Beliaev and Reitlinger; Aisenverg et al., pl. 5, fig. 25

1990. E*ostaffella pseudostruvei* Rauser-Chernousova and Beliaev in Rauser-Chernousova, Beliaev and Reitlinger; Nemirovskaya et al., pl. 5, fig.28

1990. E*ostaffella* ex. gr. *E. pseudostruvei* Rauser-Chernousova and Beliaev in Rauser-Chernousova, Beliaev and Reitlinger; Nemirovskaya et al., pl. 5, fig. 29-30

2003. *Eostaffella pseudostruvei* Rauser-Chernousova and Beliaev in Rauser-Chernousova, Beliaev and Reitlinger; Brenckle and Milkina, pl. 5, fig. 25

Description:

Test is discoidal, involute and umblicate on both sides. The periphery ranges from broadly rounded to bluntly pointed. The number of whorls is four to five. The last whorl expands more rapidly than inner evenly expanding ones. Chomata are weakly developed. Wall is dark calcareous.

Dimensions (mm):

Diameter : 0,307 – 0,356

Width : 0,135 – 0,150

W/D Ratio : 0,421 – 0,439

Remarks:

The bluntly pointed periphery, shallow but noticeable umbilici are distinguishing features of species.

Stratigraphic Distribution:

The specimens were recovered from Upper Serpukhovian and Lower Bashkirian.

Eostaffella postmosquensis Kireeva in Rauser-Chernousova et al., 1951

Pl. XII, figs. 7-13

1951. *Eostaffella postmosquensis* Kireeva in Rauser-Chernousova et al., pl. 1, figs. 1, 2

1954. *Eostaffella postmosquensis* Kireeva var. *postmosquensis* Kireeva in

Rauser-Chernousova et al.; Grozdilova and Lebedeva, pl. 14, figs. 9

1967. *Eostaffella (Eostaffella) postmosquensis* Kireeva in Rauser-Chernousova et al.; Brazhnikova et al., pl. 21, fig. 7

1981. *Eostaffella postmosquensis* Kireeva in Rauser-Chernousova et al.; Altıner, pl. 27, fig.21

1983. *Eostaffella postmosquensis* Kireeva in Rauser-Chernousova et al.; Aisenverg and others pl. 11, figs. 18, 19

1988. *Eostaffella postmosquensis* Kireeva in Rauser-Chernousova et al.; Groves, fig.13. 7-13

1991. *Eostaffella* ex.gr *E. postmosquensis* Kireeva in Rauser-Chernousova et al.; Groves, pl. 2, figs. 22-23

1994. *Eostaffella postmosquensis postmosquensis* Kireeva in Rauser-Chernousova et al.; Groves, pl. 1, figs. 17-20

1999. *Eostaffella postmosquensis* Kireeva in Rauser-Chernousova et al.; Özkan, p. 110-112, pl. 12, figs. 1-17

Description:

Test is plano to nautiloid in form. The number of whorls are three to four. Spire is expanding rapidly and uniformly. Wall is single layered. It has a rounded periphery and slightly depressed umbilici. Chomata are weakly developed.

Dimensions (mm):

Diameter : 0,187 – 0,320

Width : 0,128 – 0,160

W/D Ratio : 0,500 – 0,684

Remarks:

This form differs from *Eostaffella postmosquensis acutiformis* in its more rounded equatorial periphery, from *Eostaffella pinguis* in its smaller size and less rapid expansion of the coil and from *Eostaffella mosquensis* in its depressed umbilici and smaller W/D ratio.

Stratigraphic Distribution:

The stratigraphic range of *Eostaffella postmosquensis* is from uppermost Serpukhovian through Bashkirian (Groves, 1988). The specimens were recovered from the Upper Serpukhovian to Lower Bashkirian.

Eostaffella postmosquensis acutiformis Kireeva in Rauser- Chernousova et al., 1951

Pl. XII, figs. 14-17

1951. *Eostaffella postmosquensis* var. *acutiformis* Kireeva in Rauser-Chernousova et al.; Rauser-Chernousova et al., p. 49, pl. 1, figs. 3,4

1954. *Eostaffella postmosquensis* Kireeva var. *acutiformis* Kireeva in Rauser-Chernousova et al.; Grozdilova and Lebedeva, .pl. 14, fig. 10

1968. *Eostaffella postmosquensis* Kireeva var. *acutiformis* Kireeva in Rauser-Chernousova et al.; Aisenverg et al., pl. 24, fig.15

1969. *Eostaffella postmosquensis* var. *acutiformis* Kireeva in Rauser-Chernousova et al.; Manukhalova-Grebeniuk et al., pl. 6, figs. 12-18

1979. *Eostaffella postmosquensis acutiformis* Kireeva in Rauser- Chernousova et al.; Ainsenverg et al., pl. 5, fig.28

1979. *Eostaffella (Eostaffella) postmosquensis* Kireeva in Rauser- Chernousova et al.; Ainsenverg et al., pl. 3, fig.1; pl. 9, fig.8

1981. *Eostaffella postmosquensis acutiformis* Kireeva in Rauser- Chernousova et al.; Altıner, pl. 27, figs. 22-24

1983. *Eostaffella postmosquensis* var. *acutiformis* Kireeva; Aisenverg et al., pl. 24, fig. 15

1994. *Eostaffella postmosquensis acutiformis* Kireeva in Rauser- Chernousova et al.; Groves, pl. 3, figs. 1-16

1999. *Eostaffella acutiformis* Kireeva in Rauser- Chernousova et al.; Özkan, p. 112-114, pl. 12, figs. 18-32

2003. *Eostaffella postmosquensis acutiformis* Kireeva in Rauser- Chernousova et al.; Brenckle and Milkina, pl. 6, fig. 29

Description:

The test is nautiloid in form, with angular median region. Supplementary deposits are in the form of discontinuous chomata in the final whorl. Wall is microgranular.

Dimensions (mm):

Diameter : 0,297 – 0,354

Width : 0,146 – 0,159

W/D Ratio : 0,449 – 0,492

Remarks:

It differs from specimens assigned to *Eostaffella postmosquensis* by its subangular equatorial periphery, and smaller W/D ratio.

Stratigraphic Distribution:

The stratigraphic range of *Eostaffella postmosquensis acutiformis* is from Lower Bashkirian (Syuransky-Akavassky Horizon) (Groves, 1994). Our specimens were also recovered from Lower Bashkirian.

Eostaffella pinguis Thompson, 1944

Pl. XII, figs. 20, 21

1944. *Millerella pinguis* Thompson, pl. 1, figs.18-20

1951. *Paramillerella pinguis* Thompson; Thompson, pl. 13, fig. 18

1973. *Eostaffella* cf. *E. pinguis* Thompson; Brenckle, pl. 10, fig. 29

1979. *Eostaffella pinguis* Thompson; Eionor et al., pl. 11, fig. 10

1985. *Eostaffella pinguis* Thompson; Skipp et al., pl. 4, fig. 19

1988. *Eostaffella pinguis* Thompson; Groves, pl. 13. figs. 26-30

1990. *Eostaffella pinguis* Thompson; Gibshman and Akhmetshina, pl. 4, fig. 23

1995. *Eostaffella pinguis* Thompson; Altıner and Savini, pl. 1, figs.6-7

1999. *Eostaffella pinguis* Thompson; Özkan, p. 109-110, pl. 11, fig. 18

Description:

Test is dicoidal to subnautiloid with broadly rounded to subrounded periphery in axial section. Outer volution is highly inflated. Spire expands rapidly. Chomata are absent.

Dimensions (mm):

Diameter : 0,510 – 0,583

Width : 0,246 – 0,306

W/D Ratio : 0,482 – 0,524

Remarks:

Eostaffella pinguis differs from other representatives of the genus in its rounded to subrounded periphery, larger size and rapid expansion of the coil.

Stratigraphic Distribution:

The stratigraphic range of this form is from Lower Bashkirian (Syuransky-Akavassky Horizon) (Groves, 1988). Our specimens were recovered from Lower Bashkirian (Syuransky Horizon).

Eostaffella hohsienica Chang, 1962

Pl. XII, figs. 22, 23

1962. *Eostaffella hohsienica* Chang; pl.1, figs. 4-6, 12, 13, 18-21

Description:

Test is ovoid, slightly umblicate, volutions are involute. There are four to five volutions. Chomata are massive and broad. Wall is composed of three layers, lower tectorium, upper tectorium and tectum.

Dimensions (mm):

Diameter : 0,570 – 0,687

Width : 0,266 – 0,274

W/D Ratio : 0,399 – 0,456

Remarks:

This form differs from other eostaffellids in having more massive chomata and broadly rounded periphery.

Stratigraphic Distribution:

The stratigraphic range of this form is from uppermost Lower Carboniferous (Chang, 1962). Our specimens were recorded from Lower Bashkirian (Syuransky Horizon).

Eostaffella cumberlandensis, Rich, 1980

Pl. XIII, figs. 1, 2

1980. *Eostaffella cumberlandensis,* Rich, pl.17, figs. 19, 20, 21-23; pl.18, figs. 1, 2, 3.

Description:

Test is small to medium in size and discoidal to lenticular and involute. There are umbilici on both sides. Initial two volutions are coiled differently and the outer one is more or less planispiral. It has a rounded periphery in axial

sections. Whorls are gradually and evenly expanding. Chomata are asymmetrical. Wall is microgranular.

Dimensions (mm):

Diameter : 0,434

Width : 0,190

W/D Ratio : 0,437

Remarks:

This form is larger and has a greater form ratio than *E. mosquensis. E. postmosquensis* has a larger axial length and a small average width when compared with this form.

Stratigraphic Distribution:

The stratigraphic range of this form is Upper Serpukhovian (Mississippian-Chesterian) and Bashkirian (Rich, 1980). Our specimens were recovered from Lower Bashkirian.

Eostaffella postproikensis Vdovenko in Brazhnikova et al., 1967

Pl. XIII, figs. 3-6

1967. *Eostaffella (Eostaffella) postproikensis* Vdovenko in Brazhnikova et al., pl. 55, figs. 11-17.

1979. *Eostaffella (Eostaffella) postproikensis* Vdovenko in Brazhnikova et al.; Brazhnikova in Aisenverg et al., pl. 5, figs. 29-30

1980. *Eostaffella (Eostaffella) postproikensis* Vdovenko in Brazhnikova et al.; Rich, pl. 18, fig. 24

Description:

The test is small, discoidal and involute. It has a narrow rounded periphery. Coiling is initially plectogyrid and outer volutions are planispirally coiled.

Dimensions (mm):

Diameter : 0,435 – 0,522

Width : 0,207 – 0,275

W/D Ratio : 0,475 – 0,527

Thickness of wall: 10 – 13 μm

Remarks:

The small size and subrhomboidal shape in axial sections are distinguishing features of this species.

Stratigraphic Distribution:

The specimens were recovered from uppermost Serpukhovian to Lower Bashkirian (Bogdanovsky).

Eostaffella ex gr. *ikensis* Vissarionova, 1948

Pl. XIII, figs. 7-10

1948. *Eostaffella ikensis* Vissarionova, pl. 13, figs. 8-10, pl.14, fig.1

1960. *Eostaffella ikensis* Vissarionova; Grozdilova and Lebedeva, pl. 13, figs. 1,2

1967. *Eostaffella Eostaffella ikensis* Vissarionova; Brazhnikova and others, pl. 14, fig. 8

1968. *Eostaffella ikensis* Vissarionova; Aisenverg and others, pl. 19, figs.1,2

1981. *Eostaffella* sp. aff. *E. ikensis* Vissarionova; Altıner, pl. 27, fig. 8

1983. *Eostaffella* ex gr. *ikensis* Vissarionova; Aisenverg and others, pl. 11, fig.1

1990. *Eostaffella proikensis* Rauser - Chernousova; Vdovenko et al., pl. 1, fig. 23

1993. *Eostaffella ikensis* Vissarionova; Makhlina et al., pl. 21, figs. 28,31; pl. 22, figs. 1,3

1999. *Eostaffella ikensis* Vissarionova; Özkan, p. 100-102, pl. 11, figs. 4-5

Description:

Test rounded lenticular in form, with a small acute keel in outer whorl. Axial ends are slightly convex and umbilical depressions are completely absent. Spire is expanding gradually. It is composed of dark undifferentiated wall which is thin in the outer whorls. The thickness of the wall varies between 10 – 18 μm. Septa are completely straight. Chomata absent but there are well-developed pseudochomata.

Dimensions (mm):

Diameter : 0,505– 0,920

Width : 0,252 – 0,534

W/D Ratio : 0,499 – 0,580

Remarks:

This form is referred to the genus *Eostaffella* because of its dark undifferentiated wall. It is similar to *E. proikensis* in having larger size and differs from *E. tenebrosa* in having convex sides and absence of actual keel.

Stratigraphic distribution:

The stratigraphic range of *E. ikensis* is from Upper Visean through Upper Serpukhovian (Vdovenko et al., 1990). Our specimens were recovered from Upper Serpukhovian.

Eostaffella tenebrosa Vissarionova, 1948

Pl. XIII, fig. 11

1948. *Eostaffella ikensis* var. *tenebrosa* Vissarionova, pl. 13, figs. 11-13

1954. *Eostaffella ikensis* Viss. var. *tenebrosa* Vissarionova; Grozdilova and Lebedeva, pl. 13, fig. 18

1960. *Eostaffella ikensis* Viss. var. *tenebrosa* Vissarionova; Grozdilova and Lebedeva, pl. 13, fig. 3; pl.6, fig. 29

1969. *Eostaffella ikensis* var. *tenebrosa* Vissarionova; Manukhalova-Grebeniuk et al., pl. 9, figs. 13, 14

1990. *Eostaffella proikensis* Rauser - Chernousova; Vdovenko et al., pl. 1, fig. 29

1999. *Eostaffella tenebrosa* Vissarionova; Özkan, p. 102-104, pl. 11, figs. 6-9

Description:

Test is lenticular. It has sharp keel in the last two whorls. Sometimes the keel is highly acute. Spire expands rapidly. There are five whorls. Pseudochomata are well developed. The wall is 9 μm thick and microgranular.

Dimensions (mm):

Diameter : 0,731

Width : 0,304

W/D Ratio : 0,416

Remarks:

It differs from *E.* ex gr. *ikensis* in its laterally more compressed form and having a distinct keel in the last two whorls and smaller W/D ratio.

Stratigraphic distribution:

The stratigraphic range of *E. tenebrosa* is from Upper Viscan through Upper Serpukhovian (Vdovenko et al., 1990). Our specimens were recovered from Upper Serpukhovian.

Eostaffella sp.

Pl. XIII, figs. 12, 13

Description:

Test is discoidal, planispiral and involute. There are four volutions. The chamber height more rapidly expands. It has symmetrical but discontinuous chomata and angular periphery. Coiling is planispiral. Wall is thin, undifferentiated microgranular.

Dimensions (mm):

Diameter : 0,151 – 0,157

Width : 0,418 – 0,431

W/D Ratio : 0,361 – 0,364

Remarks:

Two specimens are referred here. This form differs from other eostaffellids in its small W/D ratio.

Stratigraphic Distribution:

Specimens were recovered from Lower Bashkirian (Syuransky Horizon).

Genus *Eostaffellina* Reitlinger, 1963

Type Species: *Eostaffella protvae* Rauser-Chernousova, 1948

Eostaffellina paraprotvae Rauser-Chernousova, 1948

Pl. XIII, figs. 14-16

1948. *Eostaffella paraprotvae* Rauser-Chernousova; Rauser-Chernousova and others, pl. 16, fig. 20

1954. *Eostaffella* aff. *paraprotvae* Rauser-Chernousova; Grozdilova and Lebedeva, pl. 14, figs. 5,6

1967. *Eostaffella (Eostaffellina) paraprotvae* Rauser-Chernousova; Brazhnikova and others, pl. 21, fig. 13

1968. *Eostaffellina paraprotvae* (Rauser - Chernousova); Aisenverg et al., pl. 25, figs. 13-15

1969. *Eostaffella paraprotvae* Rauser - Chernousova; Manukhalova-Grebeniuk et al., pl. 8, figs. 1-8

1979. *Eostaffella (Eostaffellina) paraprotvae* Rauser-Chernousova; Eionor et al., pl. 13, fig. 14

1979. *Eostaffella paraprotvae* Rauser-Chernousova; Aisenverg et al., pl. 2, figs. 12-13

1981. *Eostaffellina paraprotvae* Rauser - Chernousova; Altıner, pl. 28, figs. 6,7

1983. *Eostaffellina paraprotvae* Rauser - Chernousova; Aisenverg et al., pl. 10, fig. 10

1994. *Eostaffella paraprotvae* Rauser-Chernousova; Groves, pl. 2, figs. 12-13

1999. *Eostaffellina paraprotvae* Rauser - Chernousova; Özkan, p. 123-124, pl. 14, figs. 6-18

Description:

Test is oval, compressed along the axis of coiling. It has rounded periphery and shallow, broad umbilicus. Spire expands uniformly. Wall is layered. Chomata are weakly developed.

Dimensions (mm):

Diameter : 0,310 – 0,403

Width : 0,190 – 0,243

W/D Ratio : 0,602 – 0,612

Remarks:

This form is very similar to *E. protvae* from which it differs only in having more compressed test and greater size. It differs from other Lower Carboniferous *Eostaffella* in the presence of chomata even though they are weakly developed.

Stratigraphic Distribution:

The stratigraphic range of this form is from Protvinsky Horizon of Upper Serpukhovian through Lower Bashkirian (Groves, 1994). Our specimens were recovered from uppermost Serpukhovian and Lower Bashkirian.

Genus *Plectostaffella* Reitlinger, 1971

Type species: *Eostaffella? (Plectostaffella) jakhensis* Reitlinger, 1971

Plectostaffella bogdanovkensis Reitlinger, 1980

Pl. XIV, figs. 1-5

1971. *Plectostaffella* sp., Reitlinger, pl. 1, fig.6

1980. *Plectostaffella bogdanovkensis* Reitlinger, pl. 3, fig.3

1983. *Plectostaffella bogdanovkensis* Reitlinger; Aisenverg and others, pl. 13, fig.1

1983. *Plectostaffella bogdanovkensis angulata* Brazhnikova and Vdovenko; Aisenverg et al., pl. 13, fig.2

1990. *Plectostaffella bogdanovkensis* Reitlinger; Gibshman and Akhmetshina, pl. 4, figs. 12, 16

1996. *Plectostaffella bogdanovkensis* Reitlinger; Vachard and Maslo, pl. 3, fig.4

1997. *Plectostaffella bogdanovkensis* Reitlinger; Kulagina and Sinitsyna, pl. 1, figs. 7, 8

1999. *Plectostaffella bogdanovkensis* Reitlinger; Özkan, p. 129-130, pl. 14, fig. 30

Description:

Test shape varies during growth from ovoid to lenticular, widening along the axis of coiling. There are four to five whorls coiled in different planes. Wall has a discontinuous tectum in earlier whorls. Secondary deposits are rare including mound-shaped chomata.

Dimensions (mm):

Diameter : 0,234 – 0,350

Width : 0,183 – 0,208

W/D Ratio : 0,594 – 0,610

Remarks:

Plectostaffella bogdanovkensis differs from *Plectostaffella jakhensis* in the continuously changing coiling plane and from *Plectostaffella varvariensis* in the 90° rotation of the coil between whorls.

Stratigraphic Distribution:

The stratigraphic range is from Upper Serpukhovian and Lower Bashkirian (Gibshman and Akhmetshina, 1990). Our specimens were recovered from Lower Bashkirian.

Plectostaffella jakhensis Reitlinger, 1971

Pl. XIV, figs. 6-9

1971. *Eostaffella*? (Plectostaffella) jakhensis Reitlinger, pl. 1, fig.1

1988. *Plectostaffella jakhensis* Reitlinger; Groves, figs. 17(1-13)

1990. *Plectostaffella jakhensis* Reitlinger; Gibshman and Akhmetshina, pl. 4,fig.11

1994. *Plectostaffella jakhensis* Reitlinger; Groves, pl. 1, figs. 22-32

1995. *Plectostaffella jakhensis* Reitlinger; Altıner and Savini, pl. 1, figs. 12-13

1996. *Plectostaffella jakhensis* Reitlinger; Vachard and Maslo, pl. 3, fig. 5

1997. *Plectostaffella* ex gr. *jakhensis* Reitlinger; Kulagina and Sinitsyna, pl. 1, fig. 10

1999. *Plectostaffella jakhensis* Reitlinger; Özkan, p. 126-127, pl. 14, figs. 20-28

2003. *Plectostaffella jakhensis* Reitlinger; Brenckle and Milkina, pl. 6, figs. 5, 6, 7, 8

2003. *Plectostaffella jakhensis* Reitlinger; Kulagina and Sinitsyna, fig.5.8

Description:

Test shape is nautiloid in early stage, acute-ovoid later. Outline of median region is rounded to angular. There are three to four volutions. Initial coiling is planispiral, later asymmetrical. Asymmetrical chomata is weakly developed. Wall is undifferentiated.

Dimensions (mm):

Diameter : 0,270 – 0,315

Width : 0,213 – 0,219

W/D Ratio : 0,695 – 0,788

Remarks:

This species is distinguished from the other species of the genus in its ovoid shape and considerable variation in the asymmetry of coiling.

Stratigraphic Distribution:

The stratigraphic range of *P. jakhensis* is from Upper Serpukhovian through Lower Bashkirian (Gibshman and Akhmetshina, 1990). Our specimens were recovered from Lower Bashkirian.

Plectostaffella varvariensis Brazhnikova and Potievskaya, 1948

Pl. XIV, figs. 10, 11

1948. *Eostaffella varvariensis* Brazhnikova and Potievskaya, pl. 5, fig. 18

1967. *Eostaffella (Eostaffella) varvariensis* Brazhnikova and Potievskaya; Brazhnikova et al. pl. 21, figs. 12

1969. *Eostaffella varvariensis* Brazhnikova and Potievskaya; Manukalova-Grebeniuk, pl. 10, figs. 10, 11.

1983. *Plectostaffella varvariensis* Brazhnikova and Potievskaya; Aisenverg, pl. 4, fig. 14

1988. *Plectostaffella jakhensis* Reitlinger; Groves, fig.17.1, 3

1990. *Plectostaffella varvariensis* Brazhnikova and Potievskaya; Gibshman and Akhmetshina, pl. 4, figs. 4, 5, 7, 8

1994. *Plectostaffella jakhensis* Reitlinger; Groves, figs.24-27

1997. *Plectostaffella varvariensis* Brazhnikova and Potievskaya; Kulagina and Sinitsyna, pl.1, figs. 11, 12

1999. *Plectostaffella varvariensis* Brazhnikova and Potievskaya; Özkan, p. 127-128, pl. 14, fig. 29

2003. *Plectostaffella varvariensis* Brazhnikova and Potievskaya; Kulagina and Sinitsyna, fig.5. 11,12

Description:

Test is almond shaped and rounded initially and later becoming acute. Lateral sides are flat. Whorls are coiled in different planes, alternating at 45 degree angles. Lateral sides are flat. There is distinct triangular chomata or

knobs. Wall is thin, single-layered.

Dimensions (mm):

Diameter : 0,278 – 0,410

Width : 0,170 – 0,198

W/D Ratio : 0,482 – 0,611

Remarks:

This form differs from *Plectostaffella jakhensis* and *Plectostaffella bogdanovkensis* in the contact of each successive whorl near the convex part of the lateral slope of the preceding volution. The 45° of alternation in the axis of coiling is also characteristic feature of this species.

Stratigraphic distribution:

The stratigraphic range of this species is Bashkirian (Gibshman and Akhmetshina, 1990). Our specimens were found in the Bogdanovsky Horizon of Lower Bashkirian.

Genus *Semistaffella* Reitlinger, 1971

Type species: *Pseudostaffella variabilis* Reitlinger, 1961

Semistaffella sp.

Pl. XIV, figs. 12-14

Description:

Test is broadly nautiloid to subsphearical. Coiling is moderately skewed throughout entire spire. Chomata are prominent, nearly symmetrical.

Dimensions (mm):

Diameter : 0,297 – 0,389

Width : 0,180 – 0,239

W/D Ratio : 0,606 – 0,614

Remarks:

The characteristic feature of this species is the changing direction throughout the spire.

Stratigraphic Distribution:

Our specimens were recovered from the Syuransky Horizon of Lower Bashkirian.

Family Pseudoendothyridae Mamet in Mamet Mikailov and Mortelmans, 1970

Genus *Pseudoendothyra* Mikhailov, 1939

Type species: *Fusulinella struvei* Möller, 1879

Pseudoendothyra luminosa Ganelina, 1956

Pl. XV, figs. 15, 16

1956. *Parastaffella luminosa* Ganelina; pl. 12, fig. 12

1968. *Pseudoendothyra luminosa* Ganelina; Aisenverg et al., pl. 20, fig. 4

Description:

Test is lenticular. It has an acute periphery in later whorls. The final volution is evolutely coiled. Coiling is loose and height of whorl increases rapidly. The number of whorls is four to five. Wall is with a distinct diaphanotheca. Chomata is weakly developed and seen in the inner whorls.

Dimensions (mm):

Diameter : 0,599 – 0,625

Width : 0,286 – 0,307

W/D Ratio : 0,477 – 0,491

Remarks:

The distinguishing features of this species are compressed test, the sharp evolution of the final whorl and the peripheral depressions.

Stratigraphic Distribution:

The stratigraphic range is upper Visean through Lower Bashkirian (Aisenverg et al., 1968). Our specimens were recovered from Lower Bashkirian.

Pseudoendothyra spp.

Pl. XV, figs. 1-14

Description:

Several forms which are not assigned to particular species are grouped under this taxonomical rank. Because of their distinct wall structure, they are placed within the genus *Pseudoendothyra*. Tests are planispirally coiled, discoidal with a recrystallized wall.

Remarks:

The wall structure and the presence of umbilici differentiate the members of this group from *P. luminosa*.

Stratigraphic Distribution:

Specimens were recovered from uppermost Serpukhovian and Lower Bashkirian.

CHAPTER VI

DISCUSSIONS AND CONCLUSIONS

In the Hadim region, a 25.64 m thick mid-Carboniferous boundary section was measured within the Yarıcak Formation which is mainly composed of carbonates and quartz arenitic sandstone alternations. This study aimed to delineate mid-Carboniferous (Serpukhovian – Bashkirian) boundary, to determine the cyclicity of meter-scale shallowing upward cycles of the measured section and to discuss the response of calcareous foraminifera to cyclicity.

The Upper Serpukhovian was subdivided into two horizons the Protvinsky and the Zapaltyubinsky and the Lower Bashkirian substage was subdivided into the Syuransky, Akavassky and Askynbashsky Horizons. Initially defined the mid- Carboniferous boundary was placed at the base of the the Bogdanovsky Horizon which corresponds to the Voznesensky Horizon of Russian Platform (Einor et al., 1979), Semichatova et al., 1979). Ainsenverg et al. (1979) described the mid-Carboniferous boundary at the top of the Voznesensky Horizon. This was ratified in 1995 by the commission on the Carboniferous System and the mid-Carboniferous boundary was placed at the base the Bogdanovsky Horizon in Urals and the Voznesensky Horizon in Russian Platform (Groves, 1999). The contact is defined between Zapaltyubinsky-Voznesensky Horizons in the Russian Platform and the Mississippian-Pennsylvanian subsystems in North America.

In this study, the mid-Carboniferous boundary was delineated by a careful biostratigraphical study based on foraminifera. 62 species belonging to the calcareous foraminifera from Upper Serpukhovian and Lower Bashkirian have been identified and illustrated. They were grouped based on their morphological features such as, wall structure, coiling type, chamber arrangement and dimensions of test. These species were assigned to six superfamilies, Archaediscacea, Palaeotextulariacea, Tetrataxacea,

Ammodiscacea, Endothyracea and Fusulinacea. Based on these foraminiferal taxa, The Upper Serpukhovian to Lower Bashkirian interval has been divided into four biostratigraphic zones. The Upper Serpukhovian part of the section is assigned to *Eostaffella* ex gr. *ikensis* – *E. postmosquensis* zone. The age of this biostratigraphic zone corresponds to Protvinsky – Zapaltyubinsky Horizon of Russian Platform. The Lower Bashkirian within the studied section has been divided into 3 zones, namely, *Plectostaffella bogdanovkensis* – *P. jakhensis* zone, *Millerella marblensis* zone and *Semistaffella* sp. zone. The ages of these zones are assigned to respectively, Lower Bogdanovsky, Upper Bogdanovsky and Syuransky Horizons. The mid-Carboniferous boundary is delineated in this study between *Eostaffella* ex gr. *ikensis* – *E. postmosquensis* Zone (Protvinsky/Zapaltyubinsky Horizon) and *Plectostaffella jakhensis* – *P. bogdanovkensis* Zone (Bogdanovsky Horizon).

In the Hadim region, the studied section is mainly composed of subtidal shallow water carbonates. The sediment distribution and faunal characteristics are mostly affected by sea level variations. Therefore, to understand the meter-scale cyclicity a microfacies analysis was carried out and 11 different microfacies types were identified comprising bioclastic grainstone with foraminifera, coated bioclastic grainstone, crinoidal coated grain packstone, aggregate-grain grainstone, oolitic packstone, oolitic packstone-grainstone, oolitic grainstone, mudstone-wackestone, sandy oolitic grainstone, sandy pelloidal packstone, and quartz arenite facies. The vertical evolution of these microfacies delineates the subtidal shallowing upward cycles. Based on the stacking pattern, 6 different types, A – F and 12 subtypes were determined. A type cycles predominantly contain quartz arenites, characterized by relatively poor fossil content. This cycle type starts at the bottom with quartz arenitic sandstones and is capped by sandy oolitic grainstones at the top. B type cycle is characterized by aggregate-grain grainstone facies. The grain size increases towards the upper part indicating a shallowing trend. C type cycles are characterized by the presence of bioclastic grainstone facies at the bottom, rich in calcareous foraminifera, crinoid and echinid fragments. This type of cycle is capped by oolitic grainstones with lumps and the mudstone-wackestone facies. D

type cycles are composed of oolitic grainstone facies. This cycle type starts at the bottom with the oolitic grainstone facies and is capped by the aggregate grain grainstones, the oolitic grainstones with lumps and mudstone-wackestone facies. E type cycle starts with the coated grain grainstones and is capped by the oolitic grainstones. F type cycles are characterized by coated crinoidal packstone facies. This type of cycle evolves vertically into oolitic grainstones with quartz fragments.

The vertical stacking of these meter scale cycles corresponding to parasequences in sequence stratigraphy was used to identify the larger scale sequences. Two sequences are identified within the measured section. These sequences are correletable with the cycles in the Donets Basin defined by Izart et al. (2003). Following this correlation, the duration of the section was calculated as around 2 my. Based on these data, cycle periodicities were calculated as approximately 100 ky corresponding to the Milankovitch eccentricity cycles.

In addition to the microfacies changes, the abundance and distribution of fauna is another important criterion for the identification of these cycles. In this study, eight main foraminifer groups, namely, costaffellids, archaediscids, unilocular forms, irregularly coiled bilocular forms, biseriamminids, endothyrids, paleotextularids and pseudoendothyrids were counted in order to understand responses of foraminifers to carbonate cyclicity. In the measured section, cycles are mainly characterized by oolitic and bioclastic grainstone facies and consist of diverse fauna and abundant calcareous foraminifera.

The general trend obtained from the point counting studies is that the total abundance of foraminifera increases at the bottom of the cycles and as a sign of a deepening trend. However, the abundance decreases at the top of the cycles, which is probably an evidence for a shallowing trend. In addition to the abundance of the foraminifera, the volume of dark clasts and lumps also give a good response to cyclicity. Towards the upper part of the cycle, the volume of these grains increases in contrast to the abundance of foraminifera.

In A type cycles, which are capped by unfossiliferous quartz arenitic sandstones, the variations in the total abundance of whole foraminifera, the abundances of archaediscids and costaffellids seem to be significant since the

abundance generally decreases towards the upper part of the cycle. In B and D type cycles, which are mainly composed of aggregate grain grainstones and oolitic grainstones, the total abundance of foraminifera, the abundances of archaediscids and eostafellids have good response to cyclicity. On the contrary, in the other cycle types, for example E and F the response is not significant. The aggregate grain grainstones and oolitic grainstones were deposited in the same facies belt (shoal) and therefore, no significant biological changes have been observed responding to cyclicity. The point counting results of biseriamminids and paleotextularids are similar to those of archaediscids, eostaffellids, unilocular forms and irregularly coiled bilocular forms in the A type cycles however the responses of the same groups of foraminifera are not significant in the B type cycles. As for the pseudoendothyrids and endothyrids, they do not seem to display any significant response to cyclicity because these forms are not abundant and randomly distributed within the studied section.

REFERENCES

Aisenverg, D.E., Astakhova, T.V., Berchenko, O.I., Brazhnikova, N.E., Vdovenko, M.V., Dunaeva, N.N., Zernetskaya, N.V., Poletaev, V.I. and Sergeeva, M.T. 1983. Upper Serpuchovian substage in the Donetz Basin. Akademia Nauk Ukrainskoi SSR, Instituta Geolociicheskii Nauk "Dumka" 161 p. (in Russian with English summary).

Aisenverg, D.E., Brazhnikova, N.E. and Potievskaya, P.D. 1968. Biostratigraphic division of the Carboniferous deposits of the southern slope of the Voronezhsky Massif, Akademia Nauk Ukrainskoi S.S.R, Institut GeoloQicheskii Nauk " Dumka" Kiev, 151 p. (in Russian).

Aisenverg, D.E., Brazhnikova, N.E., Vassilyuk, N.P., Vdovenko, M.V., Gorak, S.V., Dunaeva, N.N., Zernetskaya, N.V., Poletaev, V.I., Potievskaya, P.D., Rotai, A.P. and Sergeeva, M.T. 1979. The Carboniferous sequence of the Donetz Basin: A standard section for the Carboniferous System. In: The Carboniferous of the USSR, Occ. Publ. Yorks. *Geol. Soc.*, **4**, 197-224.

Akçar, N., 1998. Meter-scale cyclic deposits in the Lower Cretaceous peritidal Carbonates of the Üzümlü Area (Western Taurides, Turkey). M. S. Thesis, Middle East Technical University, Ankara, Turkey, 109 p. (unpublished).

Al-Tawil A., Read J.F. 2003. Late Mississippian (Late Meramecian-Chesterian) glacio-eustatic sequence development on an active distal foreland ramp, Kentucky, U.S.A. *SEPM Special Publication,* **78**, AAPG Memoir 83, 35-55.

Al-Tawil A., Wynn T.C. and Read J.F. 2003. Sequence response of a distal to proximal foreland ramp to glacio-eustasy and tectonics: Mississippian,

Appalachian Basin, West Virginia-Virginia, U.S.A., *SEPM Special Publication,* **78**, AAPG Memoir 83, 11-34.

Altıner D. 1981. Recherches stratigraphiques et micropaleontologiques dans le Taurus Oriental au NW'de Pınarbaşı (Turquie). These Universite de Geneve, No. 2005, Geneve, 450 p.

Altıner, D. 1984. Upper Permian foraminiferal biostratigraphy in some localities of the Taurus Belt. In: Tekeli O. and Göncüoğlu M.C. (ed.), Geology of the Taurus Belt, Mineral Research and Exploration Institude of Turkey Publication, 255 – 268.

Altıner, D. and Özgül, N. 2001. Paleoforams 2001; International Conference on Paleozoic Benthic Foraminifera; Carboniferous and Permian of the allochthonous terranes of the Central Tauride Belt, Southern Turkey. *Guide Book*. 35 p.

Altıner, D., Özkan-Altıner, S. and Koçyiğit, A. 2000. Late Permian foraminiferal biofacies in Turkey. In: E. Bozkurt, J.A., Winchester and J.D.A., Piper (eds.), Tectonics and magmatism in Turkey and the surrounding area, *Geological Society*, London, Special publication, **173**, 83-96.

Altıner, and Savini, R. 1995. Pennsylvanian foraminifera and biostratigraphy of the Amazonas and Solimoes basins (North Brazil). *Revue de Paleobioloqie*, **14 (2)**, 417-453.

Altıner, D., Yılmaz, İ.Ö., Özgül, N., Bayazıtoğlu, M. and Gaziulusoy, Z. E. 1999. High resolution sequence stratigraphic correlation in the Upper Jurassic (Kimmeridgian) – Upper Cretaceous (Cenomanian) peritidal carbonate deposits, Western Taurides, Turkey. *Geological Journal*, **34**, 139 – 150.

Altiner, D. and Zaninetti, L. 1980. Les Archaediscidae (foraminiferes): Analyse taxonomique et proportionspour une nouvelle subdivision. *Arch. Sc. Ceneve.*, **32**, (**2**), 163-175.

Bayazıtoğlu, M. 1998. Short distance sequence stratigraphic correlation in a carbonate succession of Fele area (North of Beyşehir Lake), Western Taurides, Turkey. M. S. Thesis, M.E.T.U., Ankara, Turkey, 125 p. (unpublished).

Blumenthal, M. M. 1944. Bozkır güneyinde Toros sıradağlarının serisi ve yapısı. *İstanbul Üniversitesi Fen Fakültesi Mec.,* V. B. **9**, 95-125.

Blumenthal, M. M. 1947. Beyşehir-Seydişehir hinterlandındaki Toros dağlarının jeolojisi. *Maden Tetkik Arama Enst. Ankara, seri D*, **2**, 242 p.

Blumenthal, M. M. 1951. Batı Toroslarda Antalya ardı ülkesinde jeolojik araştırmalar. *Maden Tetkik Arama Enst. Ankara, seri D,* **5**, 194 p.

Blumenthal, M.M. 1956. Karaman Konya Havzası Güney batısında Toros Kenar Silsileleri ve Şist Radyolarit Formasyonu Stratigrafi Meselesi. *Maden Tetkik Arama Enst. Derg.*, **48**, 1-36.

Brady, H.B. 1873. On *Archaediscus karreri*, a new type of Carboniferous foraminifera. *Annals and Magazine of Natural History*, series 4, **12**, 286-290.

Brady, H.B. 1876. A monograph of Carboniferous and Permian foraminifera, *Paleont. Soc. Pub.*, **30**, 166 p., London.

Brand, U. and Brenckle, P. 2001. Chemostratigraphy of the Mid-Carboniferous boundary global stratotype section and point (GSSP), Bird Spring Formation, Arrow Canyon, Nevada, U.S.A. *Palaeogeogr. Palaeoclimatol. Palaeoecol.*, **165**, 321-347.

Brand, U., and Bruckschen, P. 2002. Correlation of the Askyn River section, Southern Urals, Russia, with the mid-Carboniferous Boundary GSSP, Bird Spring Formation, Arrow Canyon, Nevada, USA: implications for global paleoceanography. *Palaeogeogr. Palaeoclimatol. Palaeoecol.*, **184**, 177-193.

Brazhnikova, N.E. and Potievskaya, P.D. 1948. Results of studying foraminifera in material from wells at the western boundary of Donets Basin, Academia Nauk Ukrainskoi SSR, Institut Geolociicheskikh Nauk. *Seriya Stratic i Paleontolo.*, **1**, 76-103 (in Russian).

Brazhnikova, N.E., Vakarchuk, G.I., Vdovenko, M.V., Vinnichenko, L.V., Karpova, M.A., Kolomiets, Ya. I., Potievskaya, P.D., Rostovtseva, L.F., and Shevchenko, G.D. 1967. Microfaunal reference horizons of the Carboniferous and Permian deposits of the Dniepr Donets Depression, Akademia Nauk Ukrainskoi SSR, Institut GeoloQicheskii Nauk "Dumka" Kiev, 224 p. (In Russian with English, French and Germany summaries).

Brazhnikova, N.E. and Yartseva, M.V. 1956. K voprosu ob evolyutsii roda *Monotaxis* (On the Quaestion of evolution of the genus *Monotaxis)*, *Voprosy Mikropaleontologii,* **1**, 62-68.

Brenckle, P.L. 1973. Smaller Mississippian and Lower Pennsylvanian calcerous foraminifers from Nevada. *Cushman Foundation for Foraminiferal Research.* Special Publication. **11**, 82 p.

Brenckle, P.L., Baesemann, J.F., Lane, H.R., West, R.R., Webster, G.D., Langenheim, R.L., Brand, U. Richards, B.C. 1997. Arrow Canyon, the mid-Carboniferous boundary stratotype. In: P.L., Brenckle and W.R., Page (eds.), Paleoforams'97 Guidebook: Post-Conference Field Trip to the Arrow Canyon Range, Southern Nevada, U.S.A., *Cushman Foundation Foraminiferal Research Supplement to Special Publication,* No. 36, 13-32.

Brenckle, P.L. and Grelecki, C.J., 1993. Type Archaediscacean Foraminifers (Carboniferous) from the former Soviet Union and Great Britain, With a description of computer modeling of Archaediscacean coiling, *Cushman Foundation for Foramineral Research,* Special Publication. no.**30**, 1-59.

Brenckle, P., Groves, J.R. and Skipp, B., 1982. A Mississippian/Pennsylvanian (mid-Carboniferous) Boundary in North America based on Calcareous Foraminifera. In: W.H.C., Ramsbottom, W.B., Saunders, B., Owens, (eds.), Biostratigraphic data for a mid-Carboniferous boundary, Subcommission on Carboniferous Stratigraphy. Subcommission on Carboniferous Stratigraphy, 42-51.

Brenckle, P.L., Lane, H.R., Manger, W.L., Saunders, W.B. 1977. The Mississippian–Pennsylvanian boundary as an international biostratigraphic datum. *Newslett. Stratigr.*, **6**, 106–116.

Brenckle, P.L., and Marchant, T.R. 1987. Calcerous microfossils, depositional environments and correlation of the Lower Carboniferous Um Bogma formation at Gebel Nukhul, Sinai, Egypt. *Journal of Foraminiferal Research,* **17**, 74-91.

Brenckle, P.L. and Milkina, N.V. 2003. Foraminiferal timing of carbonate deposition on the Late Devonian (Famennian) – Middle Pennsylvanian (Bashkirian) Tengiz platform, Kazakhstan. *Rivista Italiana di Paleontologia e Stratigrafia*, **109**, 2, 131-158.

Bruckschen, P., Oesmann, S., Veizer, J. 1999. Isotope stratigraphy of the European Carboniferous: proxy signals for ocean chemistry, climate and tectonics. Chem. Geol., **161**, 127-163.

Bykova, E.V. 1955. Foraminifery i radiolyarii Devona Volgo-Ural'skoi oblasti i tsentral'nogo Devonskogo polya i ikh znachenie dlya stratigrafii,

(Devonian foraminifera and radiolaria of the Volga-Ural district and Central Devonian field, and their significance for stratigraphy). *Trudy Vsesoyuznogo Neftyanogo Nauchno-isseledovatel'skogo Geologorazvedochnogo Instituta (VNIGRI),* ser. **87**, 5-190.

Catuneanu, O. 2002. Sequence stratigraphy of clastic systems: concepts, merits, and pitfalls. *Journal of African Earth Sciences.*, **35**, 1, 1-43.

Chang, L.S. 1962. Fusulinids from the Hockow limestone, Hohsien, Anhui. *Acad. Sinica.*, no. 4, **10**, 439-441.

Chernysheva, N.E., 1948. Some new species of foraminifera from the Visean of the Makarov District. Academia Nauk SSSR, Trudy Geologicheskii Institute 62. 246-250 (in Russian).

Collier, R.E.LL., Leeder, M.R., Maynard, J.R. 1990. Transgressions and regressions: a model for the influence of subsidence, deposition and eustasy, with application to Quaternary and Carboniferous examples. Geol. Mag., **127 (2)**, 117-128.

Dain, L.G. and Grozdilova, L. 1953. Iskopaemye Foraminifery S.S.S.R.: Turneyellidy: Archedistsidy (Fossil foraminifera of the U.S.S.R.: Tournayellidae and Archaediscidae, Trudy Vsesesoyuznogo Neftyanogo Nauchno-issledovatel'skogo Geologorazvedochnogo Instituta (VNIGRI), ser. **74**, 1-115.

Dean, W. T. ve Monod, O. 1970. The lower Paleozoic stratigraphy and faunas of the Taurus Mountains near Beyşehir, Turkey. *I. Stratigraphy: Bull. Brit. Mus. (nat. His.), Geol.*, **19 (8)**, 411-426.

Demirtaşlı, E., 1984. Stratigraphy and tectonic of the area between Silifke and Anamur, Central Taurus Mountains: In.Tekeli O. and Göncüoğlu M. C.

(eds), Geology of the Taurus Belt. Mineral Research and Exploration Institute of Tukey Publication, 101-123.

Derville, P.H. 1931. Les Marbres du Calcaire carbonifere en Bas-Boulonnais. Imprimerie O. Boehm., Strasbourg, 322 p.

Derville, P.H. 1952. A propos de Calcispheres (rectification). *Soc. Geol. France Compte Rendue Sommaire*, 236-237.

Dunham, R.J. 1962. Classification of carbonate rocks according to depositional texture. In: Ham, W.E. (eds.): Classification of carbonate rocks. A symposium. *Amer. Ass. Petrol. Geol. Mem.*, **1**, 108-171.

Ehrenberg, C.G. 1854. Beitrag zur Kentniss der Natur und Entstehung des Grünsandes; weitere Mittheilungen über die Natur und Entstehung des Grünsandes. *Bericht über die zu Bekanntmachung geeigneten Verhandlungen der Königlichen Preussischen Akademie der Wissenschaften zu Berlin,* **1854**, 374-377.

Einor, O.L., Brazhnikova, N.E., Vassilyuk, N.P., Gorak, S.V., Dunaeva, N.N., Kireeva, G.D., Kotchetkova, N.M., Popov, A.B., Potievskaya, P.D., Reitlinger, E.A., Rotai, A.P., Sergeeva, M.T., Teteryuk, V.K., Fissunenko, O.P. and Furduy, R.S. 1979. The Lower-Middle Carboniferous Boundary. In: The Carboniferous of the USSR, Occ. Publ. Yorks. *Geol. Soc.,* **4**, 61-80.

Einsele, G., Ricken W. and Seilacher, A. 1991. Cycles and Events in Stratigraphy - basic concepts and terms. In: W. R. G. Einsele, W. Ricken & A. Seilacher (eds.), Cycles and Events in Stratigraphy, Berlin, Heidelberg, New York, Springer Verlag, 1-19.

Etheridge, R., Jr. 1873. Notes on certain genera and species mentioned in the foregoing lists. *Scotland Geological Survey Memoir*, Explanation of Sheet 23, 93-107.

Eyles, C.H., Eyles, N. and França, A.B. 1993. Late Paleozoic glaciation in anctive cratonic basin. Itararé Group, Parana Basin, Brazil. *Sedimentology*, **40**, 1-25.

Fewtrell, M.D, Ramsbottom, W.H.C, and Strank, A.R.E. 1989. Carboniferous. In Stratigraphical Atlas of fossil foraminifera, D.G., Jenkins and J.W., Murray (eds.), Ellis Norwood Limited. England, 32-86.

Fisher, A.G. 1984. The two Phanerozoic supercycles. In: Catastropes in Earth History; The Uniformitarianism, W.A. Berggren and J.A. Van Couvering, (eds.), Princeton University Press, 129 pp.

Flügel E. 2004. Microfacies of carbonate rocks: analysis, interpretation and application. Springer, 976 p.

Frakes, L.A., Francis, J.E., and Syktus, J.I. 1992. Climate modes of the Phanerozoic. Cambridge University Press, 274 pp.

Galloway, J.J. and Harlton, B.H. 1928. Some Pennsylvanian foraminifera of Oklahoma with special reference to the genus *Orobias*. *Journal of Paleontology*, **2**, 338-357.

Galloway, J.J. and Ryniker, C. 1930. Foraminifera from the Atoka formation of Oklahoma. *Oklahoma Geological Survey Circular*, **21**, 1-36.

Ganelina, R.A. 1951. Eostaffellidae and Millerellidae of Visean and Namurian (stages of Lower Carboniferous) of western part of the Moscow basin. Trudy Vsesesoyuznogo Neftyanogo Nauchno-issledovatel'skogo.

Geologorazvedochnogo Instituta (VNIGRI). Microfauna SSSR, **56**, 179-210 (in Russian).

Ganelina, R.A. 1956. Foraminifera of the Visean sediments of the northwest region of the Moscow syncline, Trudy Vsesesoyuznogo Neftyanogo Nauchno-issledovatel'skogo Geologorazvedochnogo Instituta (VNIGRI). *Microfauna SSSR*, Sonic 8, **98**, 61–159 (in Russian).

Garzanti, E. and Sciunnach, D. 1997. Complpilation of stable isotope fractionation factors of geochemical interest, in Data of geochemistry (sixth edition): *U.S. Geological Survey Professional Paper*, **440**, 109 pp.

Gaziulusoy, Z. E. 1999. A sequence stratigraphical approach from microfacies analysis to the Aptian-Albian peritidal carbonates of Polat Limestone (Seydişehir), Western Taurides, Turkey. M. S. Thesis, M.E.T.U., Ankara, Turkey, 97 p. (unpublished).

Gibshman, N., and Akhmetshina, L.Z. 1990. Micropaleontological basis for determination of the mid-Carboniferous boundary in the North Caspian Syneclise, USSR. *Cuorier Forschungs Institute Senckenberg*, **130**, 273 – 296.

Goldhammer, R. K., Dunn, P. A. and Hardie, L. A. 1987. High frequency glacio-eustatic sea-level oscillations with Milankovitch characteristics recorded in Middle Triassic platform carbonates in northern Italy. *Am. J. Sci.*, **287**, 853-892.

Goldhammer, R. K., Dunn, P. A. and Hardie, L. A. 1990. Depositional cycles, composite sea-level changes, cycle stacking patterns, and their hierarchy of stratigraphic forcing: examples from Alpine Triassic platform carbonates. *Geol. Soc. of Am. Bull.*, **102**, 663.

Goldhammer, R. K., Harris, M. T., Dunn, P. A., and Hardie, L. A. 1993, Chapter 14: Sequence stratigraphy and systems tract development of the Latemar Platform, Middle Triassic of the dolomites (northern Italy): Outcrop calibration keyed by cycle stacking patterns, *in* R. G. Loucks, and J. F. Sarg, eds., Carbonate Sequence Stratigraphy: Recent Developments and Applications, *American Association of Petroleum Geologists Memoir,* **57**, 353-387.

Gonzalez, C.R. 1990. Development of the Paleozoic glaciations of the South American Gondwana in western Argentina. *Paleogeography, Paleoclimatology, Paleoecology*, **79**, 275-287.

Göncüoğlu, M.C. 1997. Distribution of Lower Paleozoic units in the Alpine Terranes of Turkey: paleogeographic constraints. In: M.C, Göncüoğlu, and A.S., Derman, (eds.), Lower Paleozoic Evolution in northwest Gondwana, Turkish Assoc. Petrol. *Geol., Spec. Publ.*, No: **3**, 13-24.

Göncüoğlu, M.C., Dirik, K. and Kozlu, H. 1997. Pre-Alpine and Alpine terranes in Turkey: Explanatory Notes to the Terrane map of Turkey. D. Papanikolaou and F.P. Sass (eds.). IGCP Project No: 276 Final Volume: Terrane Maps and Terrane Descriptions. Annales. géol. Pays Helléniques, **37**, 515-536.

Grozdilova, L.P. 1953. Arkhedistsidy (Archaediscidae). In: L.G., Dain and L.P., Grozdilova, Iskopaemye foraminifery S.S.S.R., turneiellidy i arkhedistsidy (Fossil foraminifers of the U.S.S.R., Tournayellidae and Archaediscidae). Trudy Vsesoyuznogo Neftyanogo Nauchno-Issle-dovatel'skogo Geologorazvedochnogo Instituta (VNIGRI), Novaya Seriya, publication **74**, 65-123.

Grozdilova, L.P. and Lebedeva, N.S. 1954. Foraminifers from the Lower Carboniferous and Bashkirian stage of the Middle Carboniferous of the Kolvo-Vishera area. Trudy Vsesesoyuznogo Neftyanogo Nauchno-issledovatel'skogo

Geologorazvedochnogo Instituta (VNIGRI), *Microfauna S.S.S.R.*, sbornik 7, **81**, 4-236 (in Russian).

Grozdilova, L.P. and Lebedeva, N.S. 1960. Foraminifera from the Carboniferous deposits of the western slope of the Urals and Timan, Trudy Vsesesoyuznogo Neftyanogo Nauchno-issledovatel'skogo Geologorazvedochnogo Istituta (VNIGRI). *Microfauna S.S.S.R.*, **150**, 1-264 (in Russian).

Groves, J.R. 1983. Calcareous foraminifers and algae from the type Morrowan (Lower Pennsylvanian) region of northeastern Oklahoma and northwestern Arkansas. *Bulletin of the Oklahoma Geological Survey,* **133**, 1-65.

Groves, J.-R. 1988. Calcerous foraminifers from the Bashkirian stratotype (Middle Carboniferous, south Urals) and their significance for intercontinental correlation and the evolution of fusulinidae. *Journal of Paleontology*, **62**, 368-399.

Groves, J.R. 1991. Fusulinacean biostratigraphy of the Marble Falls Limestone (Pennsylvanian), western Llano region, central Texas. *Journal of Foraminiferal Research*, **21**, 67-95.

Groves, J.R., 1992. Stratigraphic distribution of non-fusulinacean foraminifers in the Marble Falls Limestone (Lower-Middle Pennsylvanian), Western Liona region, Central Texas, Oklahoma Geological Survey Circular, 94.

Groves, J.R. 1994. Middle Carboniferous fusulinacean biostratigraphy, northern Ellesmere Island (Sverdrup Basin. Canadian Arctic Archipelago). *Geological Survey of Canada Bulletin*, **469**, 55 p.

Groves, J.R. 1999. Correlation of the type Bashkirian stage (Middle Carboniferous, South Urals) with the Morrowan and Atokan series of the Midcontinental and western United States. *J. Paleont.,* **73** (**3**), 529-539.

Gutnic M., Monod O., Poisson A. and Dumont J. F. 1979. Géologie des Taurides Occidentales (Turquie). *Mémoires dela Sociéte geologique de France*, **137**, 1-112.

Hoare, R.D. and Sturgeon, M.T. 1994. Small fusulinids from the Pennsylvanian of Ohio. The Paleontological Society, Memoir **38**, 1-21.

House, M.R. 1995. Orbital Forcing Timescales: an introduction. In: M.R., House and A.S. (eds.), Gale, Orbital Forcing Timescales and Cyclostratigraphy, Geological Society, Special Publication, **85**, 1-18.

Izart, A., Stephenson, R., Vai, G. B., Vachard, D., Nindre, Y. L., Vaslet, D., Fauvel, P. J., Süss, P., Kossovaya, O., Chen, Z., Maslo, A., Stovba, S. 2003. Sequence stratigraphy and correlation of late Carboniferous and Permian in the CIS, Europe, Tethyan area, North Africa, Arabia, China, Gondwanaland and the USA. *Palaeogeogr. Palaeoclimatol. Palaeoecol.*, **196**, 59-84.

Khalifa M.A. 2005. Lithofacies, diagenesis and cyclicity of the 'Lower Member' of the Khuff Formation (Late Permian), Al Quasim Province, Saudi Arabia. *Journal of Asian Earth Sciences*, **25**, **5**, 719-734.

Krestovnikov, V.N. and Teodorovich, G.I. 1936. A new species of foraminifera of the genus *Archaediscus* from the middle Urals. Moskovskoye Obshchestva Ispytatelei Prirody Bulletin, Otdelenie Geologii, **44**, Geologicheskaya Seria No. **14** (**1**), 86-90 (in Russian).

Kulagina E.I. and Sinitsyna Z.A. 1997. Foraminiferal zonation of the Lower Bashkirian in the Askyn section, South Urals, Russia. In C.A. Ross, and

P.L. Brenckle (eds), Late Paleozoic Foraminifera; their biostratigraphy, evolution, and paleoecology and the mid-Carboniferous boundary, *Cushman Foundation for Foraminiferal Research, Special Publication,* **36**, p. 83-88

Kulagina, E.I. and Sinitsyna, Z.A. 2003. Evolution of the Pseudostaffellidae in the Bashkirian Stage (Middle Carboniferous). *Rivista Italiana di Paleontologica e Stratigrafia*, **109 (2)**, 213-223.

Lane, H.R., Brenckle, P.L., Baesemann, J.F., Richards, B. 1999. The IUGS boundary in the middle of the Carboniferous: Arrow Canyon, Nevada, USA. *Episodes,* **22**, 272-283.

Lane, H.R., and Manger, W.L. 1985. The Basis for a Mid-Carboniferous Boundary. *Episodes*, **8 (2)**, 112-115.

Lehrmann, D.J. and Goldhammer, R.K. 1999. Secular variation in facies and parasequence stacking patterns of platform carbonates: a guide to application of the stacking patterns technique in strata of diverse ages and settings. In: D.M., Harris, A.H., Saller, J.A., Simo (eds.), Recent Advances in Carbonate Sequence Stratigraphy, Application to Reservoirs, Outcrops and Models, Soc. Econ. Paleontol. Mineral., Spec. publ. **62**, 187-226.

Lever, H. 2004. cyclic sedimentation in the shallow marine Upper Permian Kenndy Group, Carnarvon Basin,Western Australia. *Sedimentary Geology*, **172**, 187-209.

Loeblich, A.R. Jr. and Tappan, H. 1988. Foraminiferal genera and their classification. Von Nostrand Reinhold Company, New York, 2v, 970 p.

Makhlina, M.K., Vdovenko, M.V., Alekseev, A.S., Byrsheva, T.V., Donakova, L.M., Zhulitova, V.E., Kononova, L.I., Umnova, N.J. and Chik, E.M.

1993. Lower Carboniferous of Moscow syncline ans Voronezh anticline, Akademia Nauk S.S.S.R., Moscow, 219 p. (in Russian).

Mamet, B.L. 1974. Taxonomic note on Carboniferous Endothyracea. *Journal of Foraminiferal Research*, **4**, 200-204.

Mamet, BL. 1996. Late Paleozoic small foraminifers (endothyrids) from South America (Ecuador and Bolivia). *Can. J. Earth Sci.*, **33,** 452-459.

Manukalova-Grebeniuk, M.F., Ilina, M.T., and Serezhnikova, T.D. 1969, An Atlas of foraminifers from the Middle Carboniferous of the Dneiper-Donetz basin. Ministerstvo Geologii SSSR, Trudy Ukrainskii nauchro Issledovatel'skii Geologo-Razvedochii Institut Ukranigril, **20**, 287 p. (in Russian).

Mii, H., Grossman, E.L., Yancey, T.E. 1999. Carboniferous isotope stratigraphies of North America: Implications for Carboniferous paleoceanography and Missippian glaciation. *GSA Bulletin*, **111**, 960-973.

Mikhailov, A.V. 1939. K kharakterististike rodov Nizhnkamennougol'nykh foraminifer territorii S.S.S.R. (On characteristic genera of lower Carboniferous foraminifera in territories of the U.S.S.R.). Sbonik Leningradskogo Geologicheskogo Upravleniya, Glvnoe Geologicheskoe Upravlenei, **3**, 47-62.

Miklukho-Maklai, A.D. 1956. Biostratigraficheskoe razdelenie verkhnego Paleozoya Khr. Kara-Chartyr (Yuzhnaya Fergana), (Biostratigraphic subdivision of the Upper Paleozoic in the Kara-Chartyr Mountain range (southern Fergana)). *Doklady AkademiiNauk S.S.S.R.,* **108**, 1152-1155.

Mithchum, R. M., Vail, P. R. and Thomson, S. 1977. Seismic stratigraphy and global changes of sea level, part 2: The depositional sequences

as a basic unit of for stratigraphic analysis. Applications to Hydrocarbon Exploration: *Association of Petroleum Geologist Memoir,* **26**, 53-62.

Möller, V.V. 1878. Die spiral-gewundenen foraminiferen des russichen Kohlenkalks. *Memories de I'Akademie Imperiale des Sciences de St. Petersbourg*, **7** (**25**), 1-147.

Monod, O. 1967. Presence d'une faune Ordovicienne dans les schistes de Seydişehir ala base des calcaries du Taurus occidental. *MTA Bul.*, **69**, 79-89.

Monod O. 1977. Recherches géologiques dans le Taurus occidental au Sud de Beysehir (Turquie). *Université de Paris-Sud, Centre d'Orsay*, 442 p.

Monod, O. and Akay, E. 1984. Evidence for a late Triassic-Early Jurassic orogenic event in the Taurides. In the Geological evolution of the Eastern Mediterranean, Dixon, J.E. and Robertson, A. H.F. (eds.), *Geol. Soc. Spec. Publ.*, 824 p.

Möller, V.V. 1879. Die Foraminiferen des Russischen Kohlenlaks. *Memories de I'Akademie Imperiale des Sciences de St. Petersbourg,* **7** (**27**), 1-131.

Nemirovskaya, T.I., Poletaev, V.I., and Vdovenko, M.V. 1990. The kai'mius section, Donbass, Ukraine, CIS: A soviet proposal for the Mid-Carboniferous boundary stratotype. *Cuorier Forschungs Institut Senckenberg*, **130**, 247 – 272.

Okan, Y. and Hoşgör, İ. 2005. Nohutluk Tepe (Aladağlar, Dogu Toroslar) istifinde bulunan Başkiriyen (erken Geç Karbonifer) yaşlı Bivalbia türü *Astartella consentrica* (Conrad)'nın tanımı ve paleocoğrafik dağılımı. *Yerbilimleri*, **26** (3), 13-23.

Okuyucu, C. 1999. A new multidiscus? species (Foraminifera) from a Fusulinacean-rich succession encompassing the Carboniferous – Permian boundary in the Hadim Nappe (Central Taurus, Turkey) . *Rivista Italiana di Paleontologia E Stratigrafia*, **105(3),** 439 – 444.

Orlova, I.N. 1955. Novyi rod semeistva Archaediscidae E. Tchern. Akademia Nauk S.S.S.R. Doklady, **102**, 621-622.

Osleger, D. and Read, J. F. 1991. Relation of eustacy to stacking patterns of meter-scale Carbonate cycles, late Cambrian, U.S.A. *Journal of Sed. Pet.*, **61 (7)**, 1225-1252.

Özgül, N. 1971. Orta Torosların kuzey kesiminin yapısal gelişiminde blok hareketlerinin önemi. *Türkiye Jeol. Kur. Bült.*, **14**, 75-87.

Özgül, N. 1976. Some geological aspects of the Taurus orogenic belt-Turkey. *Society of Turkey Bulletin*, **19**, 65-78 (in Turkish with English abstract).

Özgül, N. 1984. Stratigraphy and tectonic evolution of the Central Taurides. In.Tekeli O. and Göncüoğlu M. C. (eds), Geology of the Taurus Belt. Mineral Research and Exploration Institute of Tukey Publication, 77-90.

Özgül, N. 1997. Stratigraphy of the tectono-stratigraphic units in the region Bozkır-Hadim-Taşkent (northern central Taurides). *Mineral Research and Exploration Institute of Turkey (MTA) Bulletin*, **119**, 113-174 (in Turkish with English abstract).

Özgül, N., Bölükbaşı S., Alkan, H., Öztaş, Y., and Korucu, M., 1991. Tectono-stratigraphic units of lake district, Western Taurides, *In Ozan Sungurlu Symposium*, 213-238.

Özgül ve Gedik İ. 1973. Orta Toroslar'da Alt Paleozoyik yaşta Çaltepe Kireçtaşı ve Seydişehir Formasyonu'nun stratigrafisi ve konodont faunası hakkında yeni bilgiler. *Türkiye Jeoloji Kurumu Bülteni*, **16**, 39-52.

Özgül ve Metin, S. Erdogan, B., Göğer, E.; Bingöl, I. Ve Bayar, O., 1973. Tufanbeyli dolayının (Doğu Toroslar, Adana) Kambriyen-Tersiyer kayaları. *Türkiye Jeol. Kur. Bült.*, **16**, 39-52.

Özgül, N., and Turşucu, A. 1984. Stratigraphy of the Mesozoic carbonate sequence of the Munzur Mountains (Eastern Taurides). In.Tekeli O. and Göncüoğlu M. C. (eds.), Geology of the Taurus Belt. Mineral Research and Exploration Institute of Tukey Publication, 173-180.

Özkan, R. 1999. Lower and middle Carboniferous micropaleontology and biostratigraphy of eastern part of pre-Caspian depression, western Kazakhstan. M. S. Thesis, Middle East Technical University, Ankara, Turkey (unpublished) 246 pp.

Phillips, J. 1846. On the remains of microscopic animals in the rocks of Yorkshire. *Geol. Polytech. Soc.,* West Riding, Yorkshire, **2**, 274-285.

Posamentier, H. W., Jervey, M. T. and Vail, P. R. 1988. Eustatic controls on clastic Deposition I-Conceptual framework. Sea-Level Changes-An Integrated Approach. *The Society of Economic Paleontologist and Minaralogist,* Special Publication , **42**, 109-124.

Potievskaya, P.D. 1958. Foraminiferi verkhn'obashkirs'kikh vidkladiv zakhnidnoi chastini Donets'kogo baseinu. *Akad. Nauk Ukrains'koi RSR, Kiev, Inst. Geol. Nauk Trudy, Ser. Strat. i Paleontol.*, **31**, 91 p.

Pütürgeli, E. 2002. Meter-scale shallowing upward cycles in the Midian (Upper Permian) strata (Central Taurides, Turkey). M. S. Thesis, Middle East Technical University, Ankara, Turkey, 103 p. (unpublished).

Rankey, E.C. 1999. Relations between relative changes in sea level and climate shifts: Pennsylvanian – Permian mixed carbonate-siliciclastic strata, western U.S.A.: Reply, *Geological Society of America Bulletin*, 469-472.

Rauser-Chernousova, D.M. 1948. Materials and foraminiferal fauna from the Carboniferous deposits of central Kazakhstan, Akademiva Nauk SSSR, Trudy Institut Geologicheskii Nauk, 66. *Geologicheskaya Seriva*, **21**, 1-243 (in Russian).

Rauser-Chernousova, D.M., Beliaev, G.M. and Reitlinger, E.A. 1936. Verkhnepaleozoyskie foraminifery Pechorskogo kraya, (Upper Paleozoic foraminifera from the Pechora territory). *Trudy Polyarnoy Komissii, Akademia Nauk,* S.S.S.R., **28**, 159-232.

Rauser-Chernousova, D.M., Gryslova, N.D., Kireeva, G.D., Leontovich, G.E., Safonova, T.P., and Chernova, E.I. 1951. Middle Carboniferous fusulinids of the Russian Platform and adjacent regions. Akademiya Nauk SSSR, Trudy Institut Geologicheskii Nauk. Ministerstvo Neftvanoi Promyshleeosti SSSR, 380 p. (in Russian).

Rauser-Chernousova, D.M. and Fursenko, A.V. 1937. Determination of foraminifera from the oil-producing regions of the USSR. Glavnova Redaktsya Gorno-Toplivnoi Literatury Leningrad, Moskova, 315 p. (in Russian).

Rauser-Chernousova, D.M. and Fursenko, A.V. 1959. Principles of Paleontology, part 1, Protozoa. Akad. Nauk S.S.S.R., Moscow, 482 p. (in Russian).

Read, J. F. 1995. Overview of carbonate platform sequences, cycle stratigraphy and reservoirs in greenhouse and icehouse worlds. In J. F. Read, C. Kerans, and L. J. Weber, eds., Milankovitch Sea Level Changes, Cycles and Reservoirs on Carbonate Platforms in Greenhouse and Ice-house Worlds, SEPM Short Course Notes, **35**, 1, 1-102.

Reitlinger, E.A. 1949. An account of the smaller foraminifera in the lower part of Middle Carboniferous in the central Ural and Kama regions, Akademia Nauk SSSR. Isvestia Seria Geologii, **6**, 149-164, (in Russian).

Reitlinger, E.A. 1950. Foraminifera from the Middle Carboniferous deposits of the central part of the Russian Platform (excluding family Fusulinidae). Akademia Nauk SSSR. Trudy Institut Geologicheskii Nauk, **126 (47)**, 1 - 127 (in Russian).

Reitlinger, E.A. 1961. Nekotorye voprosy sistematiki kvaziendotir. Akad Nauk S.S.S.R., Moskva, Otdel, Geol. Geogr. Nauk, Geol. Inst., Voprosy Mikropaleontologii, **5**, 31-68 (in Russian).

Reitlinger, E.A. 1963. On the micropaleontological criteria for determining the boundaries of the Lower Carboniferous on the basis of foraminifera. Akademia Nauk S.S.S.R., Voprosy Mikropaleontologii, No. **7**, 22-56 (in Russian).

Reitlinger, E.A. 1971. Some problems of systematics in the light of evolutionary, stages of upper Paleozoic foraminifers. Akademiya Nauk SSSR, Voprosy Micropaleontologii, **14**, 3-16 (in Russian).

Reitlinger, E.A. 1980. The problem of the boundary between the Bogdanovsky and Krasnopalyansky horizons. Akademiya Nauk SSSR, Trudy Paleontologicheskogo Institut, **97**, 128 p. (in Russian).

Rich, M. 1980. Carboniferous calcareous foraminifera from northeastern Alabama, South-Central Tennessee, and Northwestern Georgia, *Cushman Foundation for Foraminiferal Research*, **18**, 1-84.

Rich, M. 1982. Foraminiferal zonation of the Floyd formation (Mississippian) in the type area near Rome, Floyd County, Georgia. *Journal of Foraminiferal Research,* **12** (3), 242-260.

Ross, C.A. and Ross, J.R.P. 1987. Late Paleozoic Sea Levels and Depositional Sequences. *Cushman Foundation for Foraminiferal Researc.,* Special Publication, **24**, 137-149.

Rozovskaya, S.E. 1961. On the systematics of the families Endothyridae and Ozawainellidae. *Paleontologicheskii Zhurnal,* No. **3**, 19-21 (in Russian).

Sarg, J. F. 1988. Carbonate sequence stratigraphy In Sea Level Changes: An integrated approach. In: Wilgus, C. K., Hastings, B. S. et al. (eds.), *The Society of Economic Paleontologist and Mineralogist,* Special Publication, **42**, 155-181.

Schubert, R.J. 1921. Paleontologische daten zur Stammesgeschichte der Protozoen. *Palaontogische Zeitschrift* (1920), **3**, 129-188.

Semichatova, S.V., Einor, O.L., Kireeva, G.D., Vassilyuk, N.P., Gubareva, V.S. and Potievskaya, P.D. 1979. The Bashkirian stage as a global stratigraphic unit. In: R.H., Wagner, A.G., Higgins and S.V. Meyen, The Carboniferous of U.S.S.R., Yorkshire Geological Society, **4**, 99-116.

Shcherbakov, O.A. 1997, Biostratigraphy of the Carboniferous system of the Urals. In C.A. Ross, and P.L. Brenckle (eds.) Late Paleozoic Foraminifera; their biostratigraphy, evolution, and paleoecology; and the mid-Carboniferous

boundary, *Cushman Foundation for Foraminiferal Research*, Special Publication **36**, 129-134.

Sinitsyna, Z.A. and Sinitsyn, I.I. 1987. Biostratigraphy of the stratotype of the Bashkirian stage. Akademiya Nauk S.S.S.R. Bashkirskii Filial, Institut Geologii, 71 p.

Skipp, B., Baesemann, J.F. and Brenckle, P.L. 1985. A reference area for the Mississippian/Pennsylvanian (mid-Carboniferous) boundary in East-Central Idaho, U.S.A. Xth International Congress, Carboniferous Stratigraphy and Geology, Madrid (1983), **4**, 403-428.

Sloss, L. L. 1963. Sequences in the cratonic interior of North America. *Geological Society of America Bull.,* **74**, 93-114.

Smith, L.B. Jr., Read, J.F. 2000. Rapid onset of late Paleozoic glaciation on Gondwana: Evidence from Upper Mississippian strata of the Midcontinent, United States. *Geology*, **28**, 279-282.

Steenwinkel, M.V. 1990. Sequence stratigraphy from 'stop' outcrops-example for carbonate-dominated setting: Devonian-Carboniferous transition Dinant synclinarium (Belgium), Sedimentary Geology, **69**, 256-280.

Strasser, A. 1988. Shallowing-upward sequence in Purbeckian peritidal carbonates (Lowermost Creataceous, Swiss and French Jura mountains). *Sedimentology*, **35**, 369-383.

Şen, A., 2002, Meter-scale subtidal cycles in the Middle Carboniferous of Central Taurides, Southern Turkey and response of fusulinacean foraminifers to sedimentary cyclicity, M. Sc. Thesis, Middle East Technical University, Ankara, Turkey, 121 p.

Şenel, M. 1999. Stratigraphic and tectonic features of the tecnostratigraphic units in the Taurus Belt, and the redefinition of these units. Proceeding of the 52nd Geological Congress of Turkey, 376-378

Tekeli, O., Aksay, A., Ürgün, B. M. and Işık, A. 1984. Geology of the Aladağ Mountains. In Geology of the Taurus Belt, Tekeli O. and Göncüoğlu M. C. (eds.), Mineral Research and exploration Institute of Turkey Publications, 143-158.

Thompson, M.L. 1942. New genera of Pennsylvanian fusulinids. *American Journal of Science,* **240**, 403-420.

Thompson, M.L. 1944. Pennsylvanian rocks and fusulinids of east Utah and northwest Coloroda correlated with Kansas section. *State geological Survey of Kansas Bulletin*, **60**, 17-84.

Thompson, M.L. 1951. New genera of fusulinid foraminifera. *Contributions from the Cushman Foundation for Foraminiferal Research,* **2**, 115-119.

Ueno, K., Maruyama, K.H., Hisada, I. 1994. Carboniferous fossils from limestone pebbles in a conglomerate of the Early Cretaceous Yuna Formation, Okayama Prefecture, southwest Japan. *Jour. Geol. Soc. Japan*, **100 (2)** , 181-184.

Ueno, K. and Nakazawa, T. 1993. Carboniferous foraminifers from the lowermost part of the Omi Limestone Group, Niigata Prefecture, central Japan. Science Reports of the Institute of Geoscience, University of Tsukuba, section B, Geological Sciences, **14**, 1-51.

Ünal, E. 2002. Cyclic sedimentation across the Permian-Triassic boundary (Central Taurides, Turkey). M. S. Thesis, Middle East Technical University, Ankara, Turkey (unpublished).

Ünal, E., Altıner, D., Yılmaz, İ. Ö., and Özkan-Altıner, S. 2003. Cyclic sedimentation across the Permian-Triassic boundary (Central Taurides, Turkey). *Rivista Italiana di Paleontologia e Stratigrafia*, **109**, N. 2, 359-376.

Vachard, D. and Beckary, S. 1991. Algues et foraminiferes Bashkirien des coal balls de la Mine Rosario (Truebano, Leon, Espagne). *Revue de Paleobiologie*, **10 (2)**, 315-357.

Vachard, D. and Maslo, A. 1996. Precisions biostratigraphiques et micropaleontologiques sur Ie Bashkirien D'Ukraine (Carboniferemoyen). *Revue de Paleobiologie*, **15 (2)**, 357-383.

Vail, P. R., and Mitchum, JR. 1977. Seismic stratigraphy and global changes of sea level, Part 1: Overview-Applications to Hydrocarbon Exploration. *Am.Association of Petroleum Geologists. Memoir,* **26**, 63-81.

Vail, P. R., Mitchum, R. M. and Thompson, S. 1977. Seismic stratigraphy and global changes of sea level, Part 4: Global cycles of relative changes of the sea level, in payton, C. E., eds., seismic stratigraphy. Application to Hydrocarbon Exploration. *Am. Association of Petroleum Geologist Memoir,* **26**, 83-97.

Van Wagoner, J. C., Posamentier, H. W., Mithchum, R. M., Vail, P. R., Sarg, J. F. Loutit, T. S. and Hardenbol, J. 1988. An overview of the fundamentals of sequence stratigraphy and key definitions. Sea-Level Changes-An Integrated Approach, *The Society of Economic Paleontologist and Mineralogist*. Special Publication, **42**, 40-44.

Vdovenko, M.V., Aisenverg, D.Y.E., Nemirovskaya, T.I. and Poletaev, V.I. 1990. An overview of Lower Carboniferous biozones of the Russian Platform. *Journal of Foraminiferal Research*, **20**, 184-194.

Vdovenko, M.V., Solovieva, M.N. and Bensh, F.R. 1986. A Carboniferous zonation by foraminifers. In: D.M., Rauser-Chernousova, M.N., Solovieva, Zhamoida, A.I. and others (eds.), Zonal stratigraphy by microorganisms and modes of development, Abstracts, 10th all-Union Micropaleontological meeting, Leningrad, Izdatelstvo-Vseoyuznogo nauchvo-issledova telskogo Geologo-Rasuedochnogo Instituta (VNIGRI), 52-54 (in Russian).

Veevers, J.J., Powell, C.McA. 1987. Late Paleozoic glacial episodes in Gondwanaland reflected in transgressive-regressive depositional sequences in Euramerica, Geological Society of America Bulletin, **98**, p.475-487.

Villa, E. 1982. Observaciones sobre la edad de la formacion Valdeteja (Carbonifero de la Cordillera Cantabrica) en su Area-Tipo. *Revista Espanola de Micropaleontologia,* **14**, 63-72.

Vissarionova, A.Y. 1948. Primitive Fusulinidae from the Lower Carboniferous of the European part of the SSSR. Akademiya Nauk SSSR. Trudy Institut Geologicheskii Nauk. 62. *Geologicheskaya Seriva.*, **19**, 216-226 (in Russian).

Weber, M.E., Fenner, J., Thies, A. and Cepek, P. 2001. Biological response to Milankovitch forcing during the Late Albian (Kirchrode I borehole, northwest Germany). *Paleogeography, Paleoclimatology, Palaeoecology*, **174**, 269-286.

Weedon, G. 2003. Time-Series Analysis and Cyclostratigraphy: Examining stratigraphic records of environmental cycles. Cambridge University Press, 259 p.

Wilson, J. L. 1975. Carbonate facies in geologic history. Springer-Verlag, New York, 469 p.

Yang, W., Kominz, M.A., Major, R.P. 1998. Distinguishing the roles of autogenic versus allogenic processes in cyclic sedimentation, Cisco Group (Virgilian and Wolfcampanian), north-central Texas. *GSA Bulletin*, **110**, 10, p.1333-1353.

Yılmaz, İ. Ö. 1997. Sequence stratigraphy and dasyclad algal taxonomy in the Upper Jurrasic (Kimmeridgian) – Upper Cretaceous (Cenomanian) peritidal carbonates of the Fele area, Western Taurides, Turkey. M. S. Thesis, M.E.T.U., Ankara, Turkey, 223 p. (unpublished).

Yılmaz, İ. Ö. and Altıner, D. 2001. Use of sedimentary structures in the recognition of sequence boundaries in the Upper Jurassic (Kimmeridgian) – Upper Cretaceous (Cenomanian) peritidal carbonates of the Fele (Yassıbel) area (Western Taurides, Turkey). *International Geology Review* (Published in association with the International Division of the Geological Society of America and Economic Geology, ISSN 0020-6814), **43 (8)**, 736-754.

Young, J. and Armstrong, J. 1871. On the Carboniferous fossils of the west of Scotland. *Geological Society of Glasgow Transactions*, **3**, supplement, 1-103.

APPENDIX A

EXPLANATION OF PLATES

PLATE I

Figure 1: *Diplosphearina inequalis*, sample no: HB04-12, X200

Figure 2: *Diplosphearina inequalis*, sample no: HB04-27, X200

Figure 3: *Diplosphearina inequalis*, sample no: HB04-51, X200

Figure 4: *Diplosphearina inequalis*, sample no: HB04-52, X200

Figure 5: *Tuberitina* sp., sample no: HB04-45, X200

Figure 6: *Tuberitina* sp., sample no: HB04-43, X200

Figure 7: *Tuberitina* sp., sample no: HB04-52, X200

Figure 8: Parathuramminacean foraminifera, sample no: HB04-48, X200

Figure 9: Parathuramminacean foraminifera, sample no: HB04-33, X200

Figure 10: Parathuramminacean foraminifera, sample no: HB04-54, X200

Figure 11: Parathuramminacean foraminifera, sample no: HB04-50, X200

Figure 12: Parathuramminacean foraminifera, sample no: HB04-50, X200

Figure 13:*Pseudoglomospira subquadrata,* sample no: HB04-51, X100

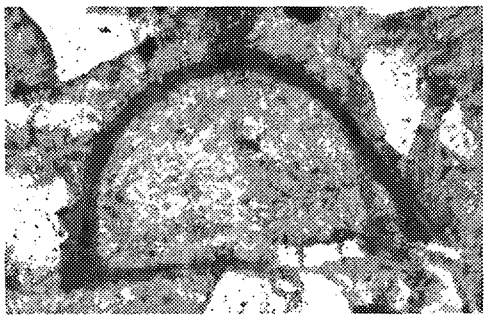
Figure 14: *Pseudoglomospira subquadrata,* sample no: HB04-33, X100

Figure 15: *Pseudoglomospira subquadrata,* sample no: HB04-51, X100

Figure 16: *Pseudoglomospira subquadrata,* sample no: HB04-43, X100

Figure 17: *Pseudoglomospira subquadrata,* sample no: HB04-48, X100

PLATE I



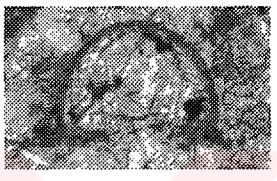
1



2



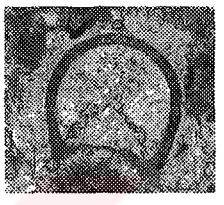
3



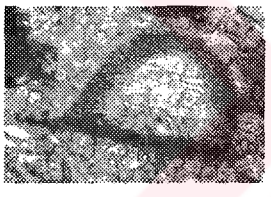
4



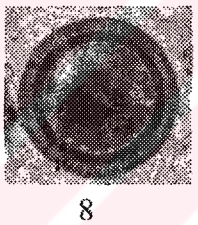
5



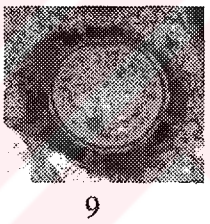
6



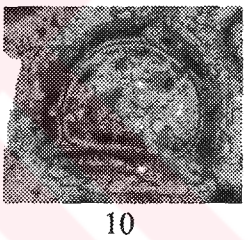
7



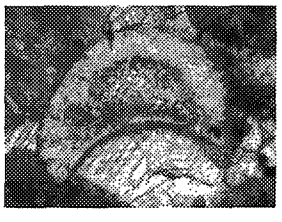
8



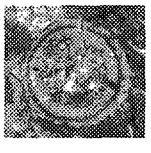
9



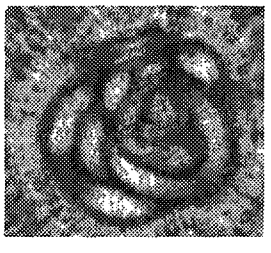
10



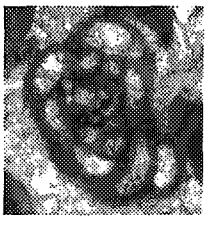
11



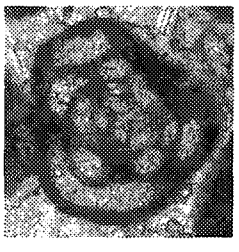
12



13



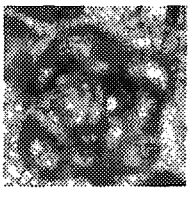
14



15



16



17

PLATE II

Figure 1: *Pseudoglomospira subquadrata,* sample no: HB04-51, X100

Figure 2: *Pseudoglomospira subquadrata,* sample no: HB04-44, X100

Figure 3: *Pseudoglomospira subquadrata,* sample no: HB04-45, X100

Figure 4: *Pseudoglomospira subquadrata,* sample no: HB04-33, X100

Figure 5: *Pseudoglomospira* sp. A, sample no: HB04-51, X100

Figure 6: *Pseudoglomospira* sp. A, sample no: HB04-47, X100

Figure 7: *Pseudoglomospira* sp. B, sample no: HB04-51, X100

Figure 8: *Pseudoglomospira* sp. B, sample no: HB04-50, X100

Figure 9: *Paleonubecularia* sp., sample no: HB04-43, X80

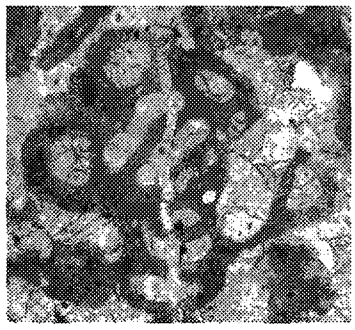
Figure 10: *Paleonubecularia* sp., sample no: HB04-11, X80

Figure 11: *Paleonubecularia* sp., sample no: HB04-02, X80

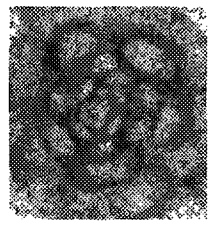
PLATE II



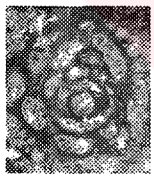
1



2



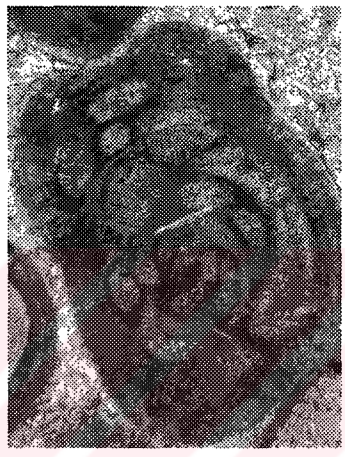
3



4



5



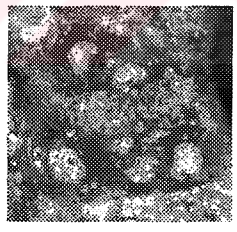
6



7



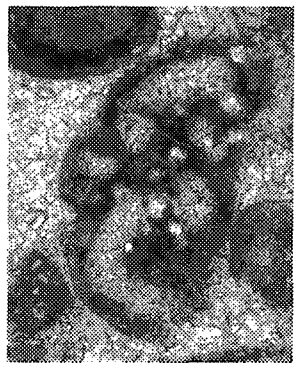
8



9



10



11

PLATE III

Figure 1: *Archaediscus postmoelleri*, sample no: HB04-04, X110

Figure 2: *Archaediscus postmoelleri*, sample no: HB04-26, X110

Figure 3: *Archaediscus postmoelleri*, sample no: HB04-40, X110

Figure 4: *Archaediscus longus*, sample no: HB04-04, X170

Figure 5: *Archaediscus longus*, sample no: HB04-05, X160

Figure 6: *Archaediscus krestovnikovi*, sample no: HB04-28, X110

Figure 7: *Archaediscus krestovnikovi*, sample no: HB04-26, X180

Figure 8: *Archaediscus karreri*, sample no: HB04-46, X75

Figure 9: *Archaediscus moelleri*, sample no: HB04-59, X100

Figure 10: *Eosigmoilina* sp., sample no: HB04-29, X150

Figure 11: *Archaediscus* sp., sample no: HB04-18, X100

Figure 12: *Archaediscus* sp., sample no: HB04-27, X100

Figure 13: *Archaediscus* sp., sample no: HB04-26, X100

Figure 14: *Archaediscus* sp., sample no: HB04-26, X100

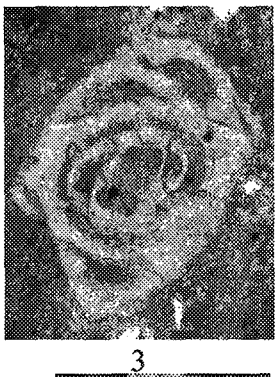
PLATE III



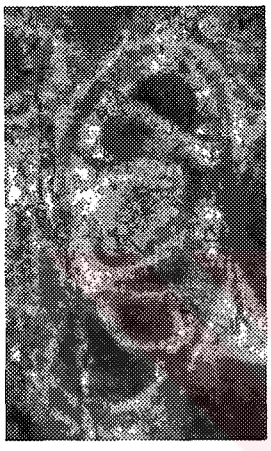
1



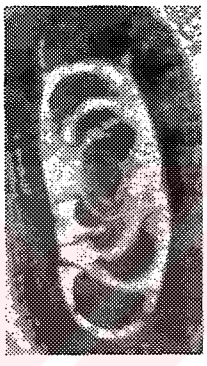
2



3



4



5



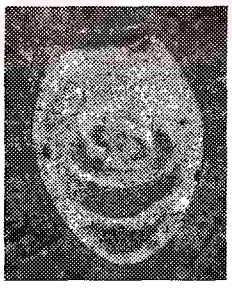
6



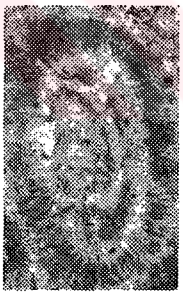
7



8



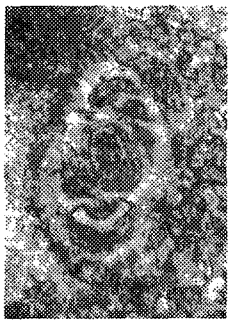
9



10



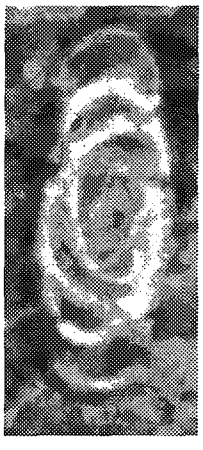
11



12



13



14

PLATE IV

Figure 1: *Paraarchaediscus koktjubensis*, sample no: HB04-54, X100

Figure 2: *Paraarchaediscus koktjubensis*, sample no: HB04-44, X100

Figure 3: *Paraarchaediscus koktjubensis*, sample no: HB04-50, X100

Figure 4: *Paraarchaediscus koktjubensis*, sample no: HB04-36, X100

Figure 5: *Paraarchaediscus koktjubensis*, sample no: HB04-24, X100

Figure 6: *Paraarchaediscus koktjubensis*, sample no: HB04-40, X100

Figure 7: *Paraarchaediscus koktjubensis*, sample no: HB04-50, X100

Figure 8: *Paraarchaediscus koktjubensis*, sample no: HB04-43, X100

Figure 9: *Paraarchaediscus koktjubensis*, sample no: HB04-41, X100

Figure 10: *Paraarchaediscus koktjubensis*, sample no: HB04-43, X100

Figure 11: *Paraarchaediscus koktjubensis*, sample no: HB04-45, X100

Figure 12: *Paraarchaediscus stilus*, sample no: HB04-50, X170

Figure 13: *Paraarchaediscus stilus*, sample no: HB04-50, X170

Figure 14: *Paraarchaediscus stilus*, sample no: HB04-51, X170

Figure 15: *Paraarchaediscus stilus*, sample no: HB04-54, X170

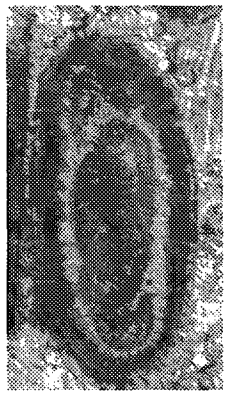
PLATE IV



1



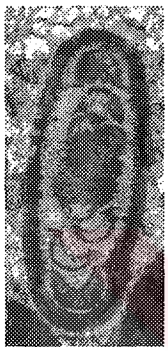
2



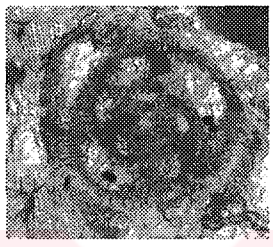
3



4



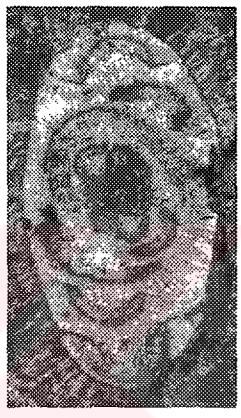
5



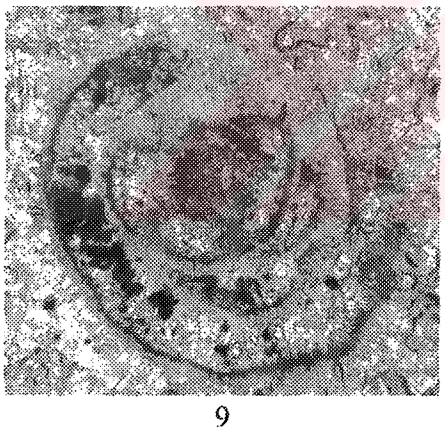
6



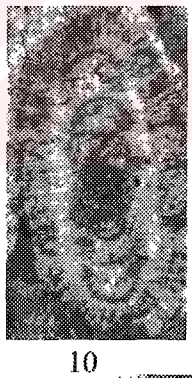
7



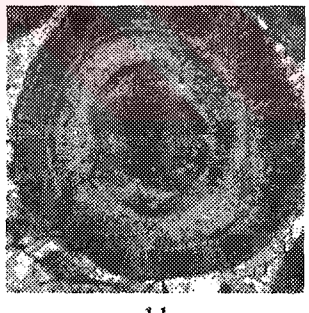
8



9



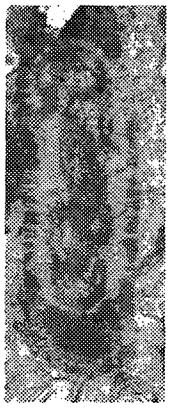
10



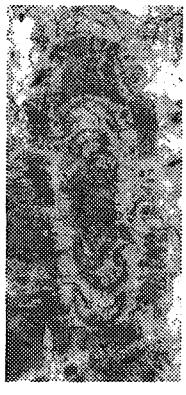
11



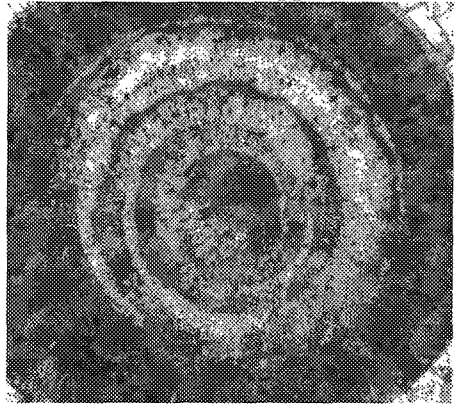
12



13



14



15

PLATE V

Figure 1: *Paraarchaediscus ninae*, sample no: HB04-46, X150

Figure 2: *Paraarchaediscus ninae*, sample no: HB04-48, X150

Figure 3: *Paraarchaediscus ninae*, sample no: HB04-43, X150

Figure 4: *Paraarchaediscus ninae*, sample no: HB04-51, X150

Figure 5: *Paraarchaediscus ninae*, sample no: HB04-51, X150

Figure 6: *Paraarchaediscus ninae*, sample no: HB04-43, X150

Figure 7: *Paraarchaediscus ninae*, sample no: HB04-43, X150

Figure 8: *Paraarchaediscus ninae*, sample no: HB04-50, X150

Figure 9: *Paraarchaediscus ninae*, sample no: HB04-43, X150

Figure 10: *Paraarchaediscus* sp., sample no: HB04-50, X150

Figure 11: *Paraarchaediscus* sp., sample no: HB04-30, X150

Figure 12: *Neoarchaediscus timanicus*, sample no: HB04-24, X150

Figure 13: *Neoarchaediscus timanicus*, sample no: HB04-24, X150

Figure 14: *Neoarchaediscus timanicus*, sample no: HB04-27, X150

PLATE V



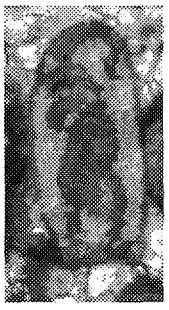
1



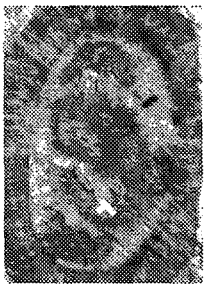
2



3



4



5



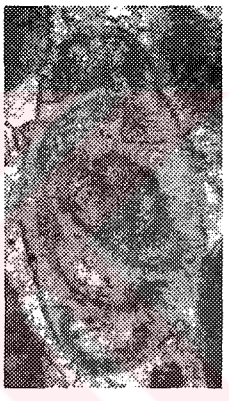
6



7



8



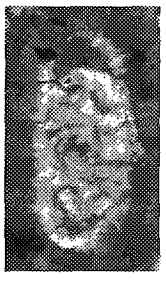
9



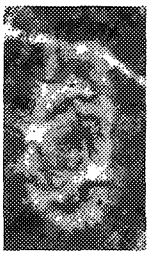
10



11



12



13



14

PLATE VI

Figure 1: *Neoarchaediscus probatus,* sample no: HB04-19, X150

Figure 2: *Neoarchaediscus probatus,* sample no: HB04-27, X150

Figure 3: *Neoarchaediscus probatus,* sample no: HB04-29, X150

Figure 4: *Neoarchaediscus probatus,* sample no: HB04-52, X150

Figure 5: *Neoarchaediscus probatus,* sample no: HB04-11, X150

Figure 6: *Neoarchaediscus probatus,* sample no: HB04-11, X150

Figure 7: *Neoarchaediscus probatus,* sample no: HB04-25, X150

Figure 8: *Neoarchaediscus subbaschkiricus*, sample no: HB04-07, X150

Figure 9: *Neoarchaediscus subbaschkiricus*, sample no: HB04-09, X150

Figure 10: *Neoarchaediscus subbaschkiricus*, sample no: HB04-26, X150

Figure 11: *Neoarchaediscus subbaschkiricus*, sample no: HB04-26, X150

Figure 12: *Neoarchaediscus subbaschkiricus*, sample no: HB04-09, X150

Figure 13: *Neoarchaediscus subbaschkiricus*, sample no: HB04-25, X150

Figure 14: *Neoarchaediscus subbaschkiricus*, sample no: HB04-21, X150

Figure 15: *Neoarchaediscus subbaschkiricus*, sample no: HB04-26, X150

Figure 16: *Neoarchaediscus subbaschkiricus*, sample no: HB04-07, X150

Figure 17: *Neoarchaediscus subbaschkiricus*, sample no: HB04-27, X150

Figure 18: *Neoarchaediscus subbaschkiricus*, sample no: HB04-52, X150

PLATE VI

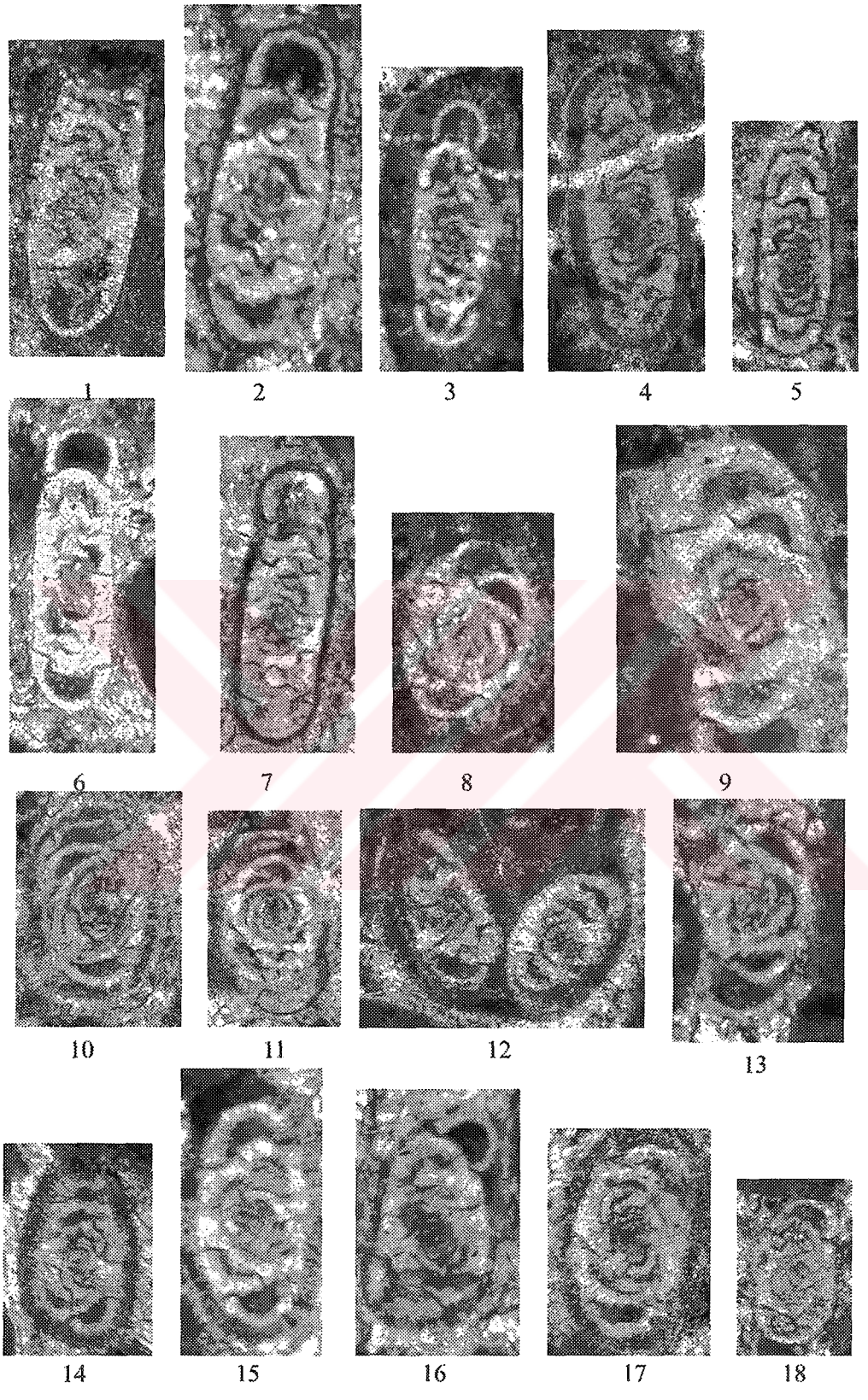


PLATE VII

Figure 1: *Neoarchaediscus parvus*, sample no: HB04-63, X150

Figure 2: *Neoarchaediscus parvus*, sample no: HB04-49, X150

Figure 3: *Neoarchaediscus achimensis*, sample no: HB04-47, X80

Figure 4: *Neoarchaediscus achimensis*, sample no: HB04-32, X80

Figure 5: *Neoarchaediscus achimensis*, sample no: HB04-32, X80

Figure 6: *Neoarchaediscus achimensis*, sample no: HB04-54, X80

Figure 7: *Neoarchaediscus* spp., sample no: HB04-63, X150

Figure 8: *Neoarchaediscus* spp., sample no: HB04-54, X150

Figure 9: *Neoarchaediscus* spp., sample no: HB04-06, X150

Figure 10: *Neoarchaediscus* spp., sample no: HB04-04, X150

Figure 11: *Neoarchaediscus* spp., sample no: HB04-27, X150

Figure 12: *Neoarchaediscus* spp., sample no: HB04-54, X150

Figure 13: *Neoarchaediscus* spp., sample no: HB04-33, X150

Figure 14: *Asteroarchaediscus rugosus*, sample no: HB04-54, X150

Figure 15: *Asteroarchaediscus rugosus*, sample no: HB04-30, X150

Figure 16: *Asteroarchaediscus rugosus*, sample no: HB04-33, X150

Figure 17: *Asteroarchaediscus rugosus*, sample no: HB04-54, X150

Figure 18: *Asteroarchaediscus baschkiricus*, sample no: HB04-51, X150

Figure 19: *Asteroarchaediscus baschkiricus*, sample no: HB04-37, X150

Figure 20: *Asteroarchaediscus baschkiricus*, sample no: HB04-37, X150

Figure 21: *Asteroarchaediscus baschkiricus*, sample no: HB04-52, X150

Figure 22: *Asteroarchaediscus* sp., sample no: HB04-57, X80

Figure 23: *Asteroarchaediscus* sp., sample no: HB04-06, X80

PLATE VII

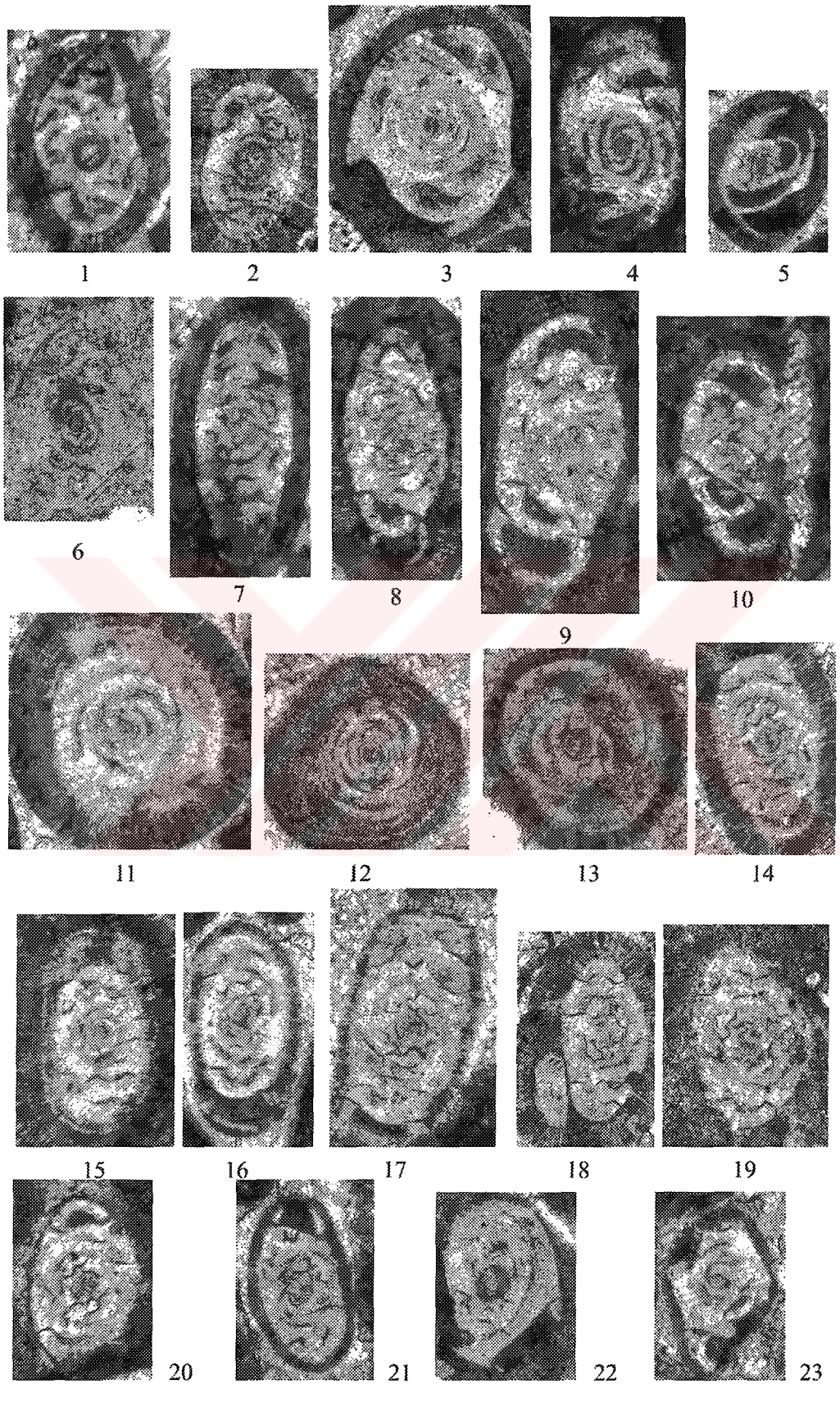


PLATE VIII

Figure 1: *Monotaxinoides* sp., sample no: HB04-16, X200

Figure 2: *Paleotextularia* sp., sample no: HB04-43, X40

Figure 3: *Paleotextularia* sp., sample no: HB04-39, X40

Figure 4: *Paleotextularia* sp., sample no: HB04-44, X40

Figure 5: *Cribrostomum* sp., sample no: HB04-45, X40

Figure 6: *Climacammina* sp., sample no: HB04-11, X40

Figure 7: *Climacammina* sp., sample no: HB04-08, X40

Figure 8: *Biseriella parva*, sample no: HB04-43, X120

Figure 9: *Biseriella parva*, sample no: HB04-37, X120

Figure 10: *Biseriella parva*, sample no: HB04-39, X120

Figure 11: *Biseriella parva*, sample no: HB04-52, X120

Figure 12: *Biseriella parva*, sample no: HB04-43, X120

Figure 13: *Biseriella parva*, sample no: HB04-43, X120

Figure 14: *Biseriella parva*, sample no: HB04-43, X120

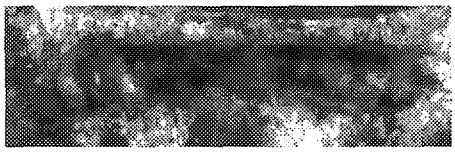
Figure 15: *Biseriella parva*, sample no: HB04-43, X120

Figure 16: *Biseriella parva*, sample no: HB04-44, X120

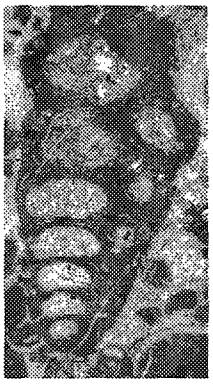
Figure 17: *Biseriella parva*, sample no: HB04-44, X120

Figure 18: *Globivalvulina bulloides*, sample no: HB04-41, X80

PLATE VIII



1



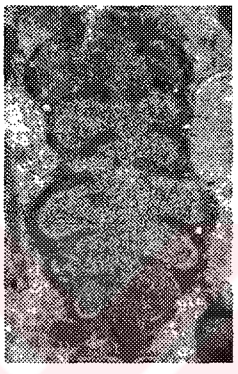


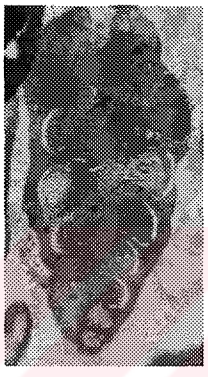


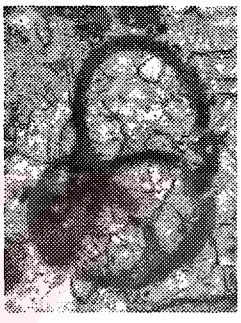
2 3 4



5



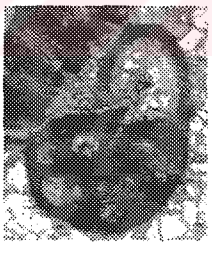


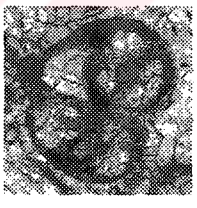




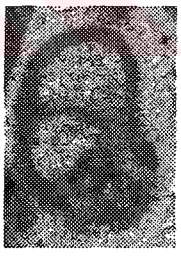
6 7 8 9











10 11 12 13 14









15 16 17 18

PLATE IX

Figure 1: *Globivalvulina bulloides*, sample no: HB04-54, X120

Figure 2: *Globivalvulina bulloides*, sample no: HB04-44, X120

Figure 3: *Globivalvulina bulloides*, sample no: HB04-51, X120

Figure 4: *Globivalvulina bulloides*, sample no: HB04-47, X120

Figure 5: *Globivalvulina bulloides*, sample no: HB04-47, X120

Figure 6: *Globivalvulina bulloides*, sample no: HB04-52, X120

Figure 7: *Globivalvulina bulloides*, sample no: HB04-45, X120

Figure 8: *Globivalvulina bulloides*, sample no: HB04-50, X120

Figure 9: *Globivalvulina bulloides*, sample no: HB04-07, X120

Figure 10: *Globivalvulina bulloides*, sample no: HB04-45, X80

Figure 11: *Globivalvulina bulloides*, sample no: HB04-05, X80

Figure 12: *Globivalvulina granulosa*, sample no: HB04-44, X120

Figure 13: *Globivalvulina granulosa*, sample no: HB04-43, X120

Figure 14: *Globivalvulina granulosa*, sample no: HB04-44, X120

Figure 15: *Globivalvulina granulosa*, sample no: HB04-44, X120

Figure 16: *Globivalvulina scaphoidea*, sample no: HB04-11, X120

PLATE IX

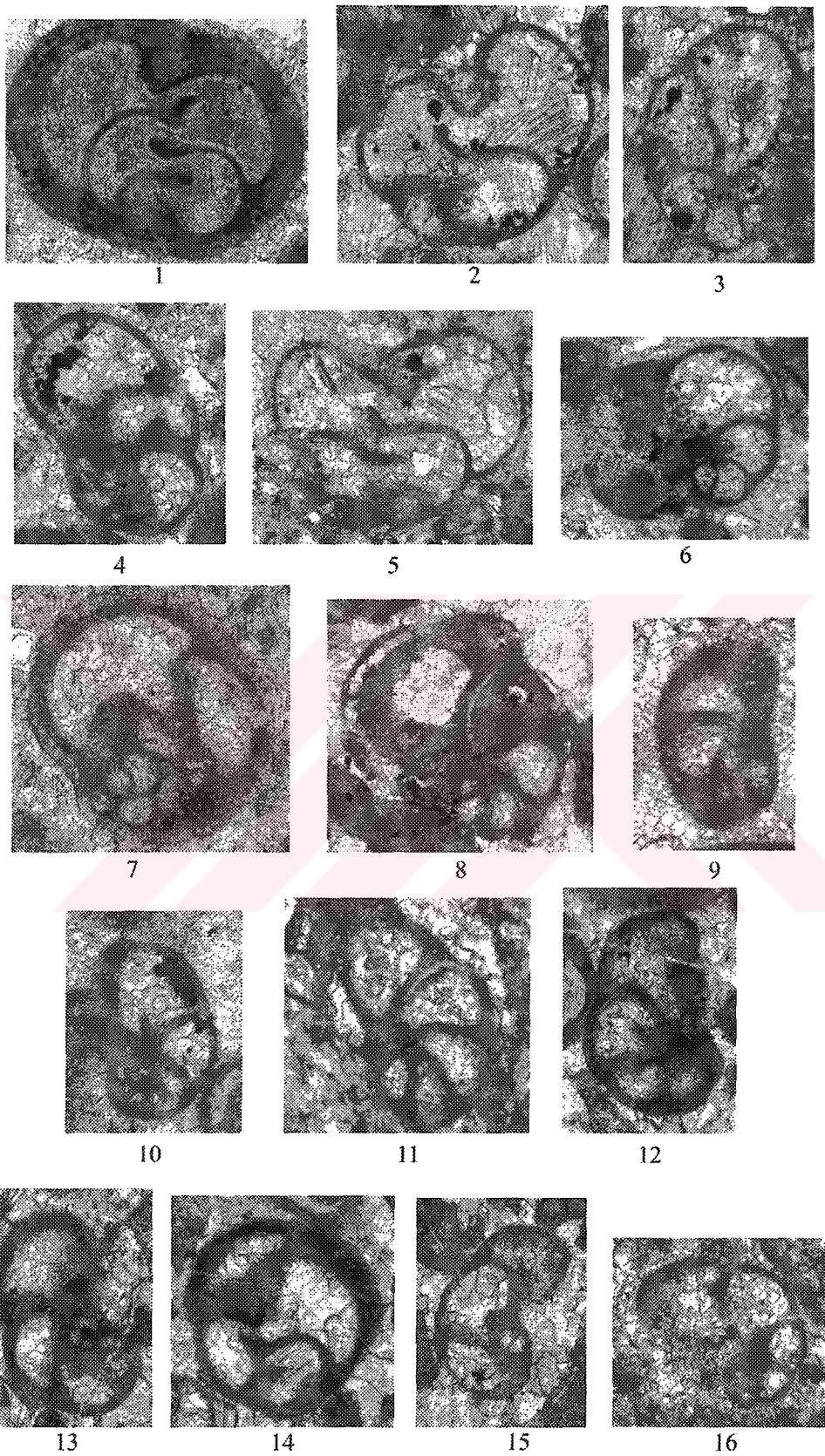


PLATE X

Figure 1: *Globivalvulina* sp., sample no: HB04-50, X80

Figure 2: *Globivalvulina* sp., sample no: HB04-43, X80

Figure 3: *Globivalvulina* sp., sample no: HB04-45, X80

Figure 4: *Globivalvulina* sp., sample no: HB04-36, X80

Figure 5: *Endothyra* spp., sample no: HB04-05, X80

Figure 6: *Endothyra* spp., sample no: HB04-11, X80

Figure 7: *Endothyra* spp., sample no: HB04-16, X80

Figure 8: *Endothyra* spp., sample no: HB04-48, X80

Figure 9: *Endothyra* spp., sample no: HB04-20, X80

Figure 10: *Endothyra* spp., sample no: HB04-26, X60

Figure 11: *Endothyra* spp., sample no: HB04-39, X60

Figure 12: *Endothyra* spp., sample no: HB04-43, X60

Figure 13: *Planoendothyra* spp., sample no: HB04-20, X80

Figure 14: *Bradyina cribrostomata.*, sample no: HB04-4, X40

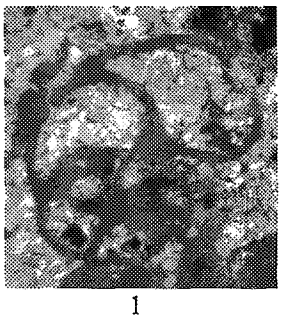
Figure 15: *Bradyina cribrostomata.*, sample no: HB04-33, X40

Figure 16: *Bradyina cribrostomata.*, sample no: HB04-41, X40

Figure 17: *Bradyina cribrostomata.*, sample no: HB04-30, X40

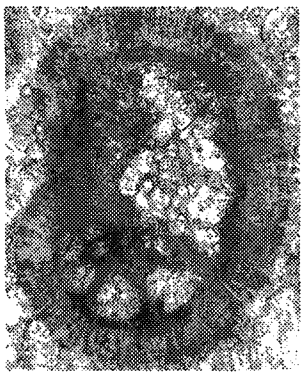
Figure 18: *Bradyina* sp., sample no: HB04-44, X40

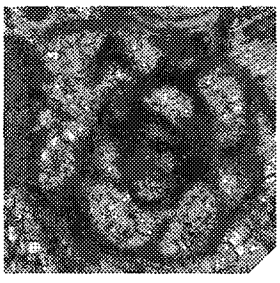
PLATE X

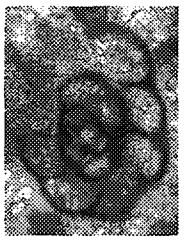

1


2


3


4

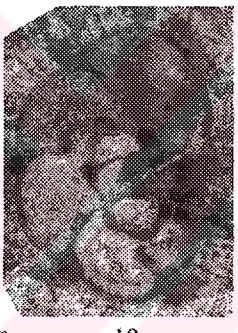

5

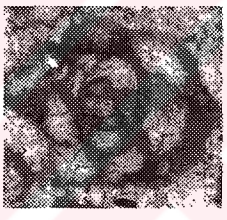

6

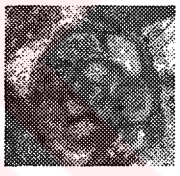

7


8


9

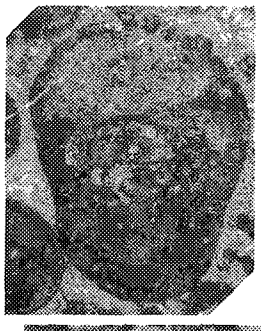

10

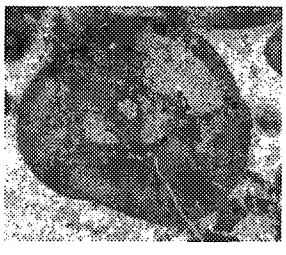

11

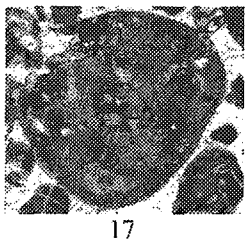

12


13


14


15


16


17

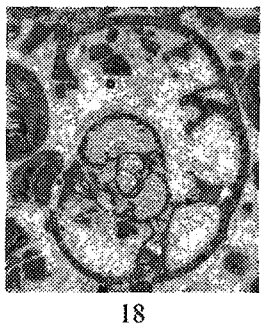

18

PLATE XI

Figure 1: *Tetrataxis* sp., sample no: HB04-30, X60

Figure 2: *Mediocris mediocris,* sample no: HB04-51, X100

Figure 3: *Mediocris breviscula*, sample no: HB04-44, X100

Figure 4: *Mediocris* sp., sample no: HB04-44, X100

Figure 5: *Millerella umblicata,* sample no: HB04-08, X100

Figure 6: *Millerella umblicata,* sample no: HB04-16, X100

Figure 7: *Millerella marblensis,* sample no: HB04-11, X80

Figure 8: *Millerella marblensis,* sample no: HB04-10, X80

Figure 9: *Syzgial cyst,* sample no: HB04-01, X100

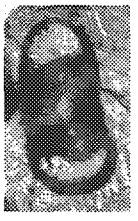
PLATE XI



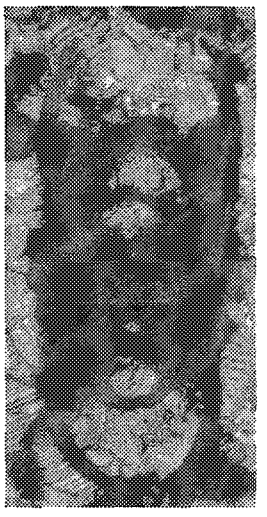
1



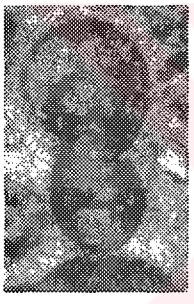
2



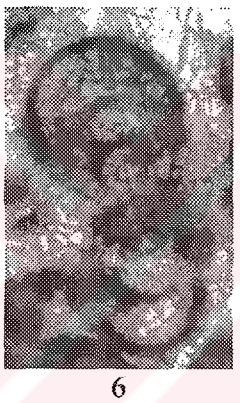
3



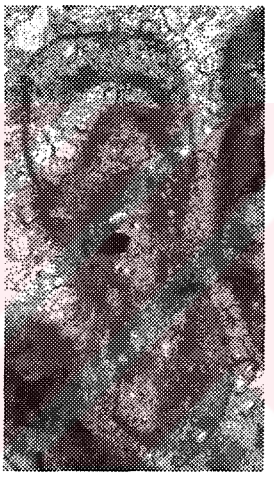
4



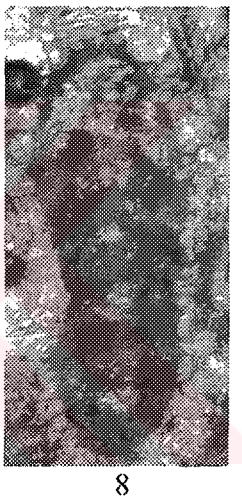
5



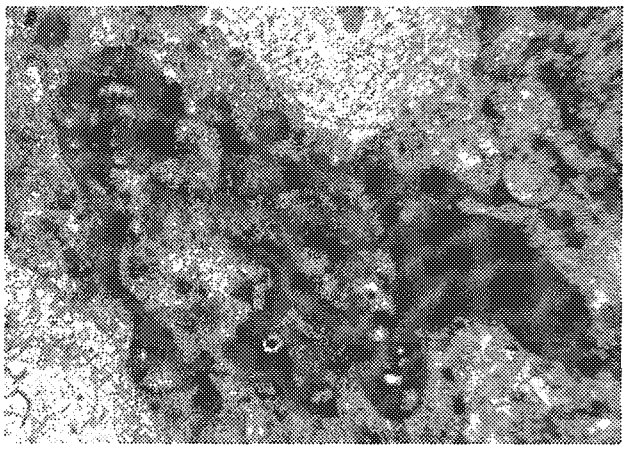
6



7



8



9

PLATE XII

Figure 1: *Eostaffella pseudostruvei*, sample no: HB04-06, X100

Figure 2: *Eostaffella pseudostruvei*, sample no: HB04-19, X80

Figure 3: *Eostaffella pseudostruvei*, sample no: HB04-04, X80

Figure 4: *Eostaffella pseudostruvei*, sample no: HB04-04, X80

Figure 5: *Eostaffella pseudostruvei*, sample no: HB04-63, X80

Figure 6: *Eostaffella pseudostruvei*, sample no: HB04-07, X80

Figure 7: *Eostaffella postmosquensis*, sample no: HB04-16, X100

Figure 8: *Eostaffella postmosquensis*, sample no: HB04-11, X100

Figure 9: *Eostaffella postmosquensis*, sample no: HB04-11, X100

Figure 10: *Eostaffella postmosquensis*, sample no: HB04-51, X100

Figure 11: *Eostaffella postmosquensis*, sample no: HB04-51, X100

Figure 12: *Eostaffella postmosquensis*, sample no: HB04-63, X100

Figure 13: *Eostaffella postmosquensis*, sample no: HB04-41, X100

Figure 14: *Eostaffella postmosquensis acutiformis*, sample no: HB04-19, X100

Figure 15: *Eostaffella postmosquensis acutiformis*, sample no: HB04-21, X100

Figure 16: *Eostaffella postmosquensis acutiformis*, sample no: HB04-14, X100

Figure 17: *Eostaffella postmosquensis acutiformis*, sample no: HB04-32, X100

Figure 18: *Eostaffella sp.*, sample no: HB04-52, X100

Figure 19: *Eostaffella sp.*, sample no: HB04-36, X100

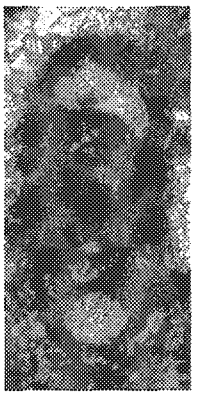
Figure 20: *Eostaffella pinguis*, sample no: HB04-05, X100

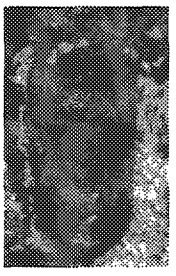
Figure 21: *Eostaffella pinguis*, sample no: HB04-04, X100

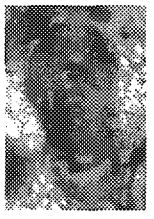
Figure 22: *Eostaffella hohsienica*, sample no: HB04-19, X100

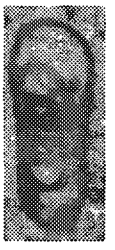
Figure 23: *Eostaffella hohsienica*, sample no: HB04-33, X100

PLATE XII


1


2

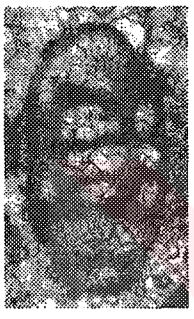

3

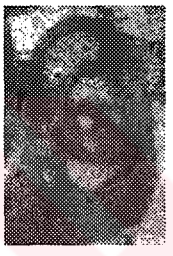

4

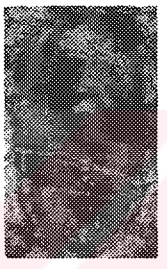

5


6

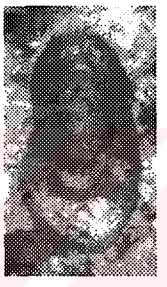

7


8


9

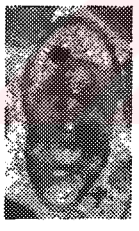

10


11

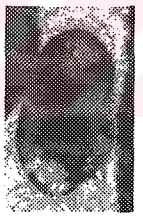

12

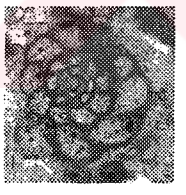

13

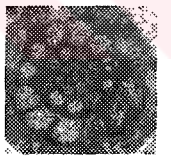

14

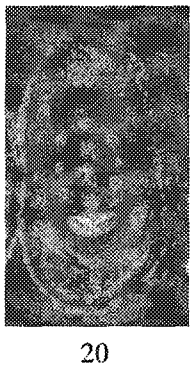

15

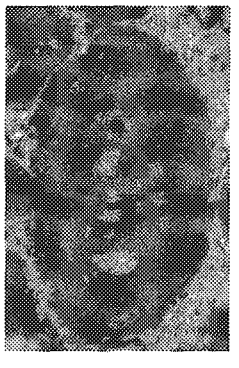

16


17


18


19


20


21


22


23

PLATE XIII

Figure 1: *Eostaffella cumberlandensis*, sample no: HB04-19, X110

Figure 2: *Eostaffella cumberlandensis*, sample no: HB04-18, X110

Figure 3: *Eostaffella postproikensis*, sample no: HB04-32, X120

Figure 4: *Eostaffella postproikensis*, sample no: HB04-33, X120

Figure 5: *Eostaffella postproikensis*, sample no: HB04-33, X120

Figure 6: *Eostaffella postproikensis*, sample no: HB04-33, X120

Figure 7: *Eostaffella* ex gr. *ikensis*, sample no: HB04-31, X80

Figure 8: *Eostaffella* ex gr. *ikensis*, sample no: HB04-32, X100

Figure 9: *Eostaffella* ex gr. *ikensis*, sample no: HB04-48, X100

Figure 10: *Eostaffella* ex gr. *ikensis*, sample no: HB04-50, X80

Figure 11: *Eostaffella tenebrosa*, sample no: HB04-31, X80

Figure 12: *Eostaffella* sp., sample no: HB04-08, X100

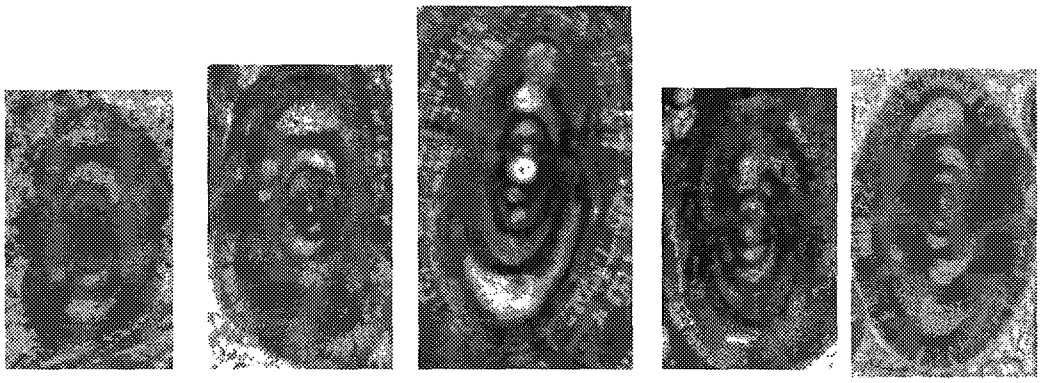
Figure 13: *Eostaffella* sp., sample no: HB04-63, X100

Figure 14: *Eostaffellina paraprotvae*, sample no: HB04-21, X100

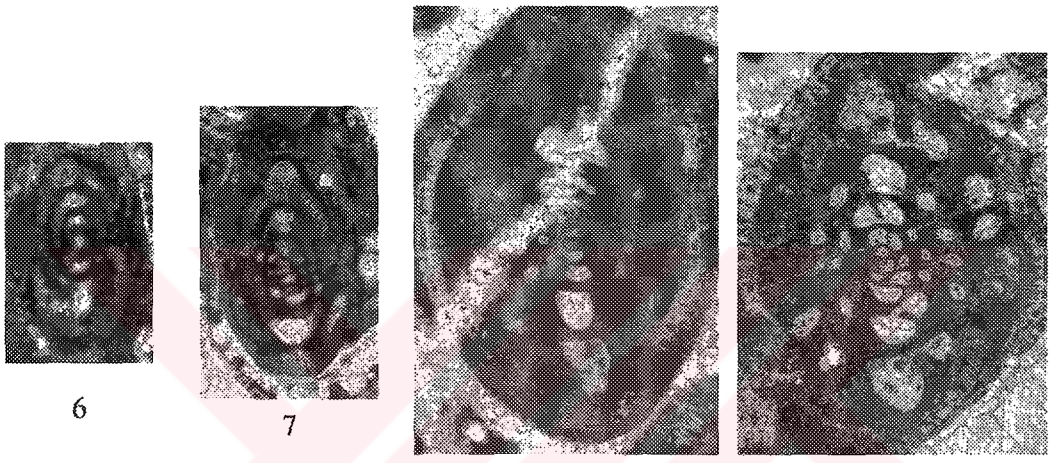
Figure 15: *Eostaffella paraprotvae*, sample no: HB04-14, X100

Figure 16: *Eostaffella paraprotvae*, sample no: HB04-04, X100

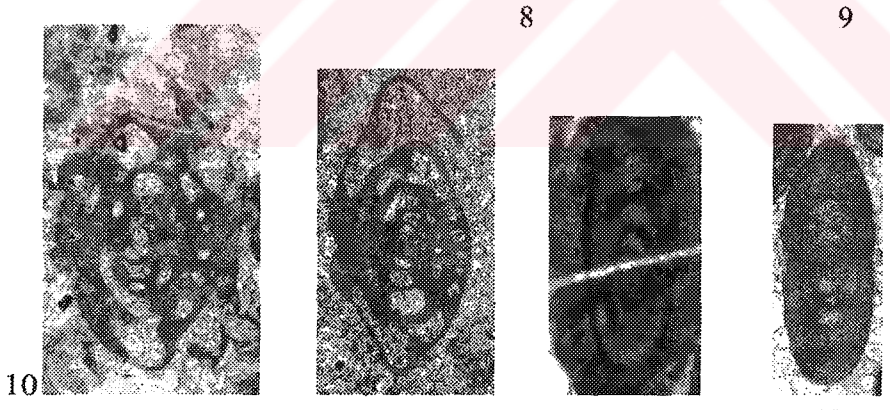
PLATE XIII



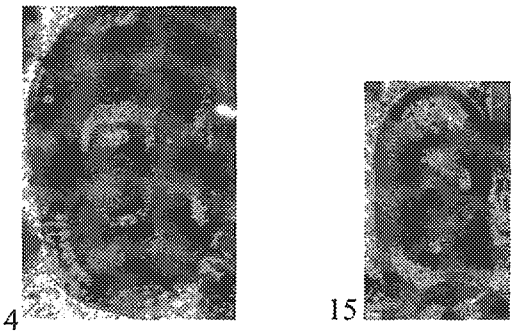
1 2 3 4 5



6 7 8 9



10 11 12 13



14 15 16

PLATE XIV

Figure 1: *Plectostaffella bogdanovkensis*, sample no: HB04-06, X100

Figure 2: *Plectostaffella bogdanovkensis*, sample no: HB04-07, X100

Figure 3: *Plectostaffella bogdanovkensis*, sample no: HB04-14, X100

Figure 4: *Plectostaffella bogdanovkensis*, sample no: HB04-16, X100

Figure 5: *Plectostaffella bogdanovkensis*, sample no: HB04-17, X100

Figure 6: *Plectostaffella jakhensis*, sample no: HB04-07, X100

Figure 7: *Plectostaffella jakhensis*, sample no: HB04-51, X100

Figure 8: *Plectostaffella jakhensis*, sample no: HB04-46, X100

Figure 9: *Plectostaffella jakhensis*, sample no: HB04-10, X100

Figure 10: *Plectostaffella varvariensis*, sample no: HB04-05, X150

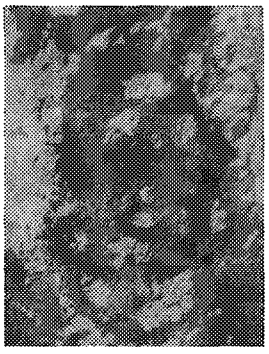
Figure 11: *Plectostaffella varvariensis*, sample no: HB04-27, X100

Figure 12: *Semistaffella* sp., sample no: HB04-10, X100

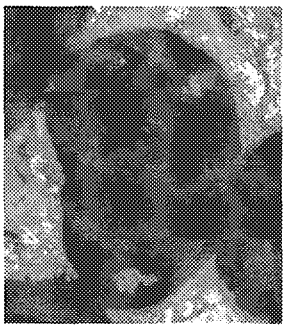
Figure 13: *Semistaffella* sp., sample no: HB04-10, X150

Figure 14: *Semistaffella* sp., sample no: HB04-10, X100

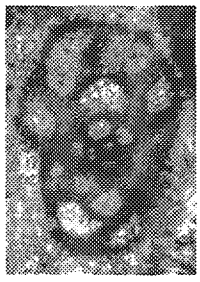
PLATE XIV



1



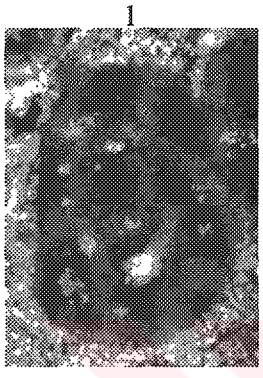
2



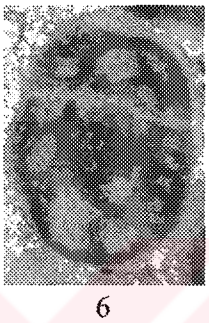
3



4



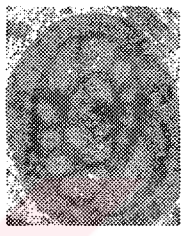
5



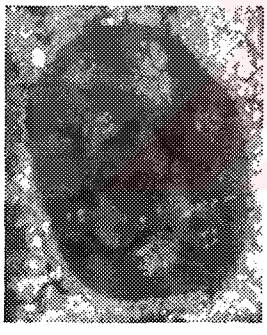
6



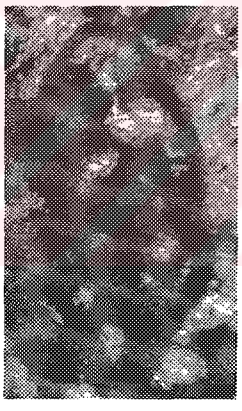
7



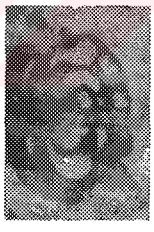
8



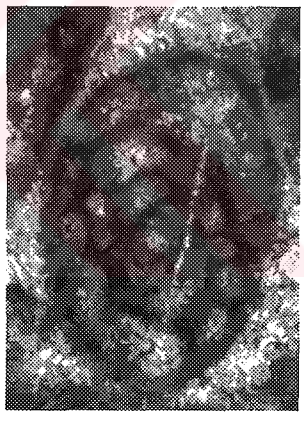
9



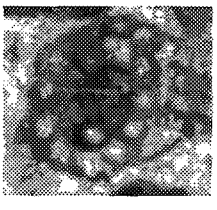
10



11



12



13



14

PLATE XV

Figure 1: *Pseudoendothyra* spp., sample no: HB04-45,X40

Figure 2: *Pseudoendothyra* spp., sample no: HB04-08,X40

Figure 3: *Pseudoendothyra* spp., sample no: HB04-08,X40

Figure 4: *Pseudoendothyra* spp., sample no: HB04-13,X40

Figure 5: *Pseudoendothyra* spp., sample no: HB04-08,X40

Figure 6: *Pseudoendothyra* spp., sample no: HB04-59,X40

Figure 7: *Pseudoendothyra* spp., sample no: HB04-38,X40

Figure 8: *Pseudoendothyra* spp., sample no: HB04-30,X40

Figure 9: *Pseudoendothyra* spp., sample no: HB04-51,X40

Figure 10: *Pseudoendothyra* spp., sample no: HB04-53,X40

Figure 11: *Pseudoendothyra* spp., sample no: HB04-06,X40

Figure 12: *Pseudoendothyra* spp., sample no: HB04-11,X40

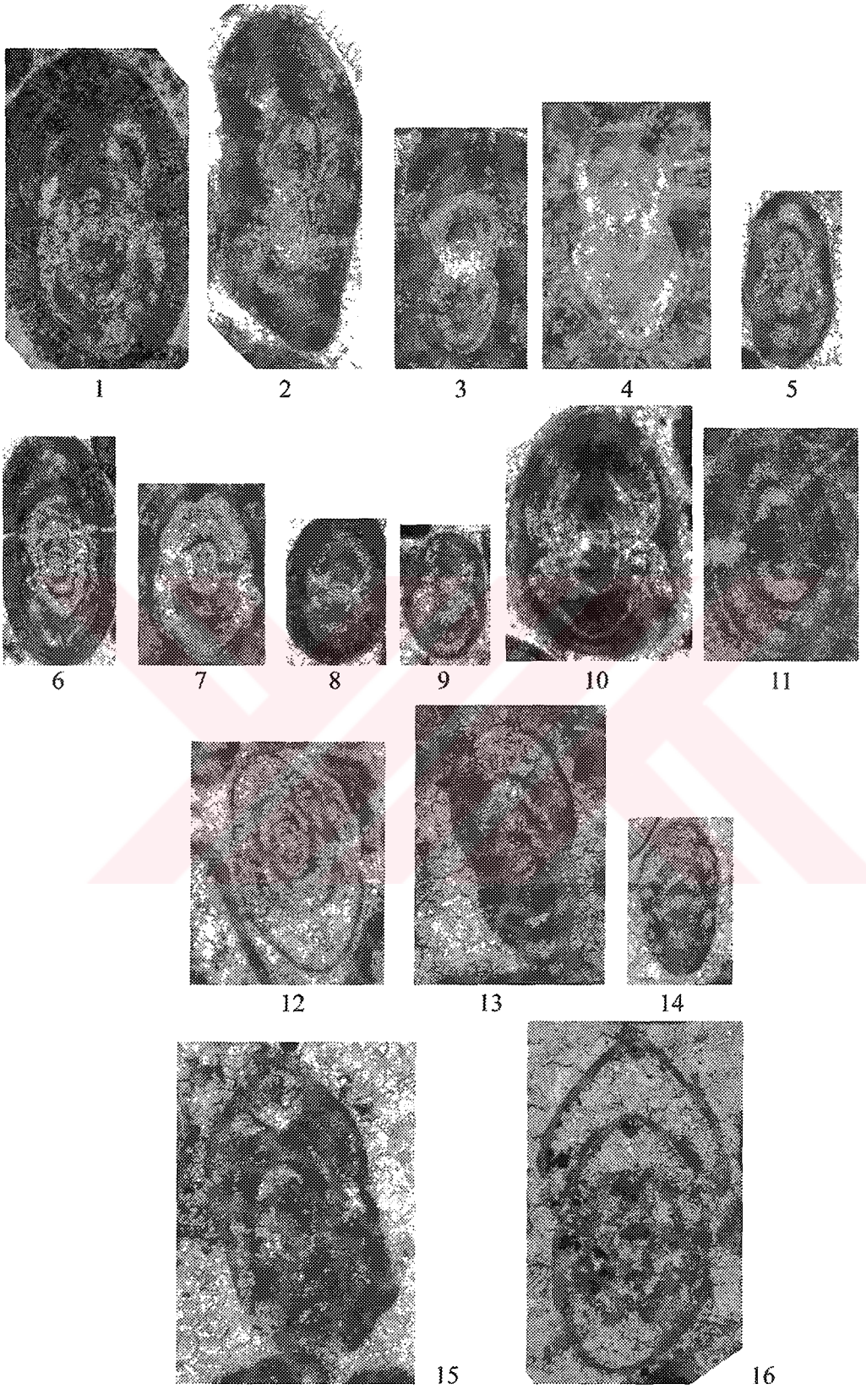
Figure 13: *Pseudoendothyra* spp., sample no: HB04-11,X40

Figure 14: *Pseudoendothyra* spp., sample no: HB04-46,X40

Figure 15: *Pseudoendothyra luminosa.,* sample no: HB04-49,X40

Figure 16: *Pseudoendothyra luminosa*, sample no: HB04-41,X40

PLATE XV



APPENDIX – B

Faunal distribution of limestones in the measured section

(Arc: Archaediscids; EO: Eostaffellids; IC: Irregularly coiled bilocular forms; UF: Unilocular forms; P: Paleotextularids; Endo: Endothyrids; Bis: Biseriamminids; Pseudo: Pseudoendothyrids)

	1 (Arc)	2 (EO)	3 (IC)	4 (UF)	5 (P)	6 (Endo)	7 (Bis)	8 (Pseudo)	Total
Sample 1	2	26	26	30	6	2	8	0	100
Sample 2	13	9	38	48	0	1	10	0	119
Sample 3	0	0	0	0	0	0	0	0	0
Sample 4-1	39	67	32	26	4	5	14	29	216
Sample 4-2	47	89	51	23	4	13	5	67	299
Sample 5	24	90	33	50	7	26	19	16	265
Sample 6	45	100	25	45	9	13	10	52	299
Sample 7	43	89	41	42	36	6	20	71	348
Sample 8	54	181	59	28	46	24	17	110	519
Sample 9	30	58	13	14	46	2	2	30	195
Sample 10	14	80	16	22	12	12	5	22	183
Sample 11	49	286	98	48	22	41	30	15	589
Sample 12	0	0	0	0	0	0	0	0	0
Sample 13	1	47	16	11	7	2	0	16	100
Sample 14	16	292	16	38	6	31	29	45	473
Sample 15	2	31	20	12	10	3	3	15	96
Sample 16	11	16	4	8	4	3	4	10	60
Sample 17	32	73	4	21	3	3	3	18	157
Sample 18-1	12	125	7	15	25	5	8	36	233
Sample 18-2	13	169	14	17	13	23	21	45	315
Sample 19	30	164	21	28	29	12	12	21	317
Sample 20	0	33	21	40	7	6	9	12	128
Sample 21	7	17	12	23	11	6	9	49	134
Sample 22-1	9	53	4	18	13	7	1	18	123
Sample 22-2	2	57	6	6	10	3	4	26	114
Sample 23	10	57	5	23	13	4	0	13	125
Sample 24	95	55	33	42	0	6	3	10	244
Sample 25	72	44	33	55	3	8	6	6	227
Sample 26	161	79	20	43	0	7	7	8	325
Sample 27	65	35	16	51	0	6	7	5	185
Sample 28	33	19	17	25	0	3	3	1	101

	1	2	3	4	5	6	7	8	Total
Sample 29	56	24	10	35	0	5	3	1	134
Sample 30	15	34	34	30	4	6	5	16	144
Sample 31	5	17	36	12	8	2	0	4	84
Sample 32	21	42	75	34	6	5	5	17	205
Sample 33	67	66	112	61	7	7	16	13	349
Sample 34	7	6	1	12	0	0	0	0	26
Sample 35	15	34	61	13	16	4	18	9	170
Sample 36	36	29	73	21	11	6	20	9	205
Sample 37	7	10	38	14	5	3	5	6	88
Sample 38	9	7	31	23	8	3	0	4	85
Sample 39	11	25	51	9	16	6	18	7	143
Sample 40	9	13	63	19	9	1	14	5	133
Sample 41	7	23	62	12	13	1	22	1	141
Sample 42	8	19	31	7	12	7	7	4	95
Sample 43	38	53	68	65	34	18	36	8	320
Sample 44	29	74	54	44	17	20	50	7	295
Sample 45	37	40	84	54	14	5	33	3	270
Sample 46	41	39	117	38	25	4	34	17	315
Sample 47	20	39	42	24	37	9	9	21	201
Sample 48	14	43	71	14	22	4	24	5	197
Sample 49	29	33	46	9	16	3	10	8	154
Sample 50	54	49	53	20	32	17	15	9	249
Sample 51	114	84	78	19	12	6	29	6	348
Sample 52	95	61	67	25	18	5	25	3	299
Sample 53	34	21	19	10	4	5	7	7	107
Sample 54	47	26	33	14	5	5	11	12	153
Sample 55	19	13	7	6	0	0	2	0	47
Sample 56	11	13	32	4	3	1	11	7	82
Sample 57	13	5	25	10	15	3	7	3	81
Sample 58	5	6	8	3	1	0	1	5	29
Sample 59	14	18	32	18	19	1	7	5	114
Sample 60	14	13	12	15	0	2	9	1	66
Sample 61	0	5	0	2	0	1	1	0	9
Sample 62	0	3	0	2	0	0	3	0	8
Sample 63	66	49	26	7	6	6	4	7	171
Sample 64	0	0	0	0	0	0	0	0	0